



**THESIS APPROVAL**  
**GRADUATE SCHOOL, KASETSART UNIVERSITY**

Doctor of Philosophy (Chemistry)

**DEGREE**

Chemistry

Chemistry

**FIELD**

**DEPARTMENT**

**TITLE:** Investigation on Electronic Structures and Properties of Poly  
(fluorenevinylene) Derivatives: Theoretical Studies

**NAME:** Miss Wichanee Meeto

**THIS THESIS HAS BEEN ACCEPTED BY**

**THESIS ADVISOR**

( Associate Professor Supa Hannongbua, Dr.rer.nat. )

**THESIS CO-ADVISOR**

( Mr. Chak Sangma, Ph.D. )

**THESIS CO-ADVISOR**

( Mr. Sornthep Vannarat, Ph.D. )

**THESIS CO-ADVISOR**

( Professor Peter Wolschann, Dr.rer.nat. )

**DEPARTMENT HEAD**

( Associate Professor Supa Hannongbua, Dr.rer.nat. )

**APPROVED BY THE GRADUATE SCHOOL ON**

**DEAN**

( Associate Professor Gunjana Theeragool, D.Agr. )

# THESIS

## INVESTIGATION ON ELECTRONIC STRUCTURES AND PROPERTIES OF POLY(FLUORENEVINYLENE) DERIVATIVES: THEORETICAL STUDIES

WICHANEE MEETO

A Thesis Submitted in Partial Fulfillment of  
the Requirements for the Degree of  
Doctor of Philosophy (Chemistry)  
Graduate School, Kasetsart University  
2010

Wichanee Meeto 2010: Investigation on Electronic Structures and Properties of Poly(fluorenevinylene) Derivatives: Theoretical Studies. Doctor of Philosophy (Chemistry), Major Field: Chemistry, Department of Chemistry. Thesis Advisor: Associate Professor Supa Hannongbua, Dr.rer.nat. 136 pages.

A systematic study on the structural and photo-physical properties of model bifluorene-vinylene compounds based on the density functional theory (DFT) and its time-dependent version was presented (TD-DFT). The main aim of this work was the investigation of the direct influence of substitution using electron acceptor (CN) or electron donor (NH<sub>2</sub>, OCH<sub>3</sub>, OH) groups on the optimal geometry, torsional potentials and photo-physical properties. The ground state and the lowest singlet excited-state geometries of poly-(9,9-dialkylfluorene-2,7-vinylene) copolymer or PFV and its derivatives PFV-NH<sub>2</sub>, PFV-CN, PFV-OCH<sub>3</sub> and PFV-OH were investigated based on density functional theory (DFT) and time-dependent DFT using B3LYP functional. The ground state and the lowest singlet excited-state geometries of the oligomers were optimized at the B3LYP/6-31G(d) and TD-B3LYP/SVP levels, respectively. The calculated ground state geometries favor the aromatic type structure, while the electronic excitations lead to quinoid type distortion, which exhibited a shortening of the inter-ring bonds (about 0.03 Å). Substitution on vinylene bridge, from the structural point of view, leads to the twisting of molecular fragment on the side of added group. Absorption and fluorescence energies were extrapolated to infinite chain length making use of their good linearity with respect to 1/n. The predicted energy gaps of the copolymer derivatives were calculated and compared to available experimental data. Fluorescence energies are 1.78, 1.77, 1.74, 2.00 and 1.73 eV and the predicted radiative lifetime are 0.6, 0.6, 1.0, 0.8 and 1.0 ns for PFV, PFV-NH<sub>2</sub>, PFV-CN, PFV-OCH<sub>3</sub> and PFV-OH, respectively. The presented fundamental structural and electronic information can be useful in designing of novel optical materials as well as understanding of excitation-relaxation phenomena.

---

Student's signature

---

Thesis Advisor's signature

## ACKNOWLEDGEMENTS

I would like to grateful thank and deeply indebted to Assoc. Prof. Dr. Supa Hannongbua my thesis advisor for advice, encouragement, kindness throughout the course of my graduate and valuable suggestion for completely doing research and writing of thesis. Special thanks are due to my graduate committees, Dr. Chak Sangma, Dr. Sornthep Vannarat for their helpful comments and suggestions. I would sincerely like to thank Prof. Dr. Peter Wolschann for kindly providing a helpful Guidance and valuable suggestions when I did the research at University of Vienna. Furthermore, this thesis should be credited to Prof. Dr. Harald-Friedrich Kauffmann who offers me a grant from University of Vienna during my research doing time at Institute of Theoretical Chemistry, University of Vienna. Prof. Dr. Vladimir Lukes is also appreciated for his kindly support, valuable guidance and suggestions.

Thailand Graduated Institute of Science and Technology (TGIST) is acknowledged for financial support. Supporting from the Thailand Research Fund TRF (**RTA5080005**), Kasetsart University Research and Development Institute (KURDI) and the Postgraduate Education and Research Programs in Petroleum, Petrochemical Technology and Advanced Materials (ADB-MUA) are also gratefully acknowledged. Large scale simulations center: ITANIUM of the National Electronics and Computer Technology Center (NECTEC), LCAC and computing center of KU for computing resources and research facilities.

Finally, I would like to dedicate this thesis to my parents and my colleagues at Laboratory for Computational and Applied Chemistry (LCAC) for their encouragement. They also support me with love and sincerity throughout the entire study.

Wichanee Meeto

May, 2010



## TABLE OF CONTENTS

	<b>Page</b>
TABLE OF CONTENTS	i
LIST OF TABLES	iii
LIST OF FIGURES	v
ABBREVIATIONS	viii
INTRODUCTION	1
OBJECTIVES	8
LITERATURE REVIEW	9
METHODS	20
Quantum chemical calculation	20
Ground state calculation	20
Models of calculation	20
Conformational analysis	21
Ground state geometry optimization	23
Excited state calculation	24
Excited state structure	24
Electronic property	24
HOMO-LUMO energy	24
Vertical excitation energy	24
Ionization potential and electron affinity	25
Fluorescent energy and lifetime	25
RESULTS AND DISCUSSION	27
Ground state calculation	27
Conformational analysis	27
Ground stated geometry optimization	31
Bond length alternation (BLA)	39
Excited state calculation	41
Excited state structure	41

## TABLE OF CONTENTS (Continued)

	<b>Page</b>
HOMO-LUMO and vertical excitation energy	50
Ionization potential and electron affinity	60
Fluorescence energy and lifetime	62
CONCLUSION	64
LITERATURE CITED	66
APPENDICES	78
Appendix A Theoretical background	79
Appendix B Oral presentation and poster contributions to conferences	102
Appendix C Publications	107
CURRICULUM VITAE	135

## LIST OF TABLES

Table	Page
1 Optimal bond lengths (in Å) for asymmetric substitution systems, obtained from B3LYP/6-31G(d) calculations	33
2 Optimal bond lengths (in Å) for symmetric substitution systems, obtained from B3LYP/6-31G(d) calculations	34
3 Optimal dihedral angles, $\Theta_1$ (between the bonds 12, 14 and 15) and $\Theta_2$ (between the bonds 15, 16 and 17), (in degrees) and BLA parameters (in Å) for <i>all-trans</i> conformations, obtained by B3-LYP/6-31G(d) calculations	40
4 Relative energies $\Delta E$ and dihedral angles $\Theta_1$ and $\Theta_2$ of external points for torsional dependencies with respect to the most stable structure. The angles are in degrees and energies in eV or kcal/mol (values in parentheses)	48
5 Optimized inter-ring torsion angles, $\phi$ (degrees) of $F_nV_m$ ( $n=2-5$ , $m=1-4$ ) in the ground state ( $S_0$ ) and the lowest excited state ( $S_1$ ), obtained from B3LYP/6-31G* and TD-B3LYP/SVP calculations	49
6 The lowest excitation energies in eV and oscillator strengths (values in parentheses) for the optimal all-trans geometries. The values written in italics stand for the excitation contributions in percentage involved in each calculated transition (H denotes HOMO and L is LUMO)	51
7 Extrapolated excitation energy ( $E_{exc}$ ), oscillator strength ( $f$ ), HOMO energy, and absorption wavelength ( $\lambda_{abs}$ ) of the derivatives calculated from TD-B3LYP/SVP and TD-B3LYP/TZVP methods, the values in parenthesis are experimental results. Column 1 indicates the oligomers and polymers ( $n, m = \infty$ ) for different copolymers	55

**LIST OF TABLES (Continued)**

<b>Table</b>		<b>Page</b>
8	Ionization Potential (IP), Electron Affinity (EA), Highest Occupied Molecular Orbital (HOMO) and Lowest Unoccupied Molecular Orbital (LUMO) of FV based oligomers calculated by B3LYP/6-31G(d)	61
9	Calculated fluorescence energies ( $E_{flu}$ ) and radiative lifetimes of FV oligomers as obtained from TD-B3LYP/SVP calculations. Geometries were optimized at TD-B3LYP/SVP level	63

## LIST OF FIGURES

Figure		Page
1	Structures of conjugated polymers	3
2	Structures of (a) poly(9,9-di-noctylfluorenyl-2,7-vinylene) (PFV), (b) CN-poly(dihexylfluorenevinylene) (CN-PFV) and (c) poly[9,9-bis(4 octyloxyphenyl)fluorenyl-2,7-vinylene] (PBOPFV)	4
3	Schematic structure, bond and dihedral angle numbering of studied systems in all-trans conformation	21
4	Schematic diagram of dihedral angle used in this calculation	22
5	Potential energy curves of torsional angle $\theta_1$ ( $\angle C14-C15-C22-C23$ ) obtained for F2V. The curves were calculated by AM1, HF/3-21G(d), HF/6-31G(d) and B3LYP/6-31G(d) methods	23
6	Potential energy surface (PES) of torsional angle $\theta_1$ ( $\angle C14-C15-C22-C23$ ) and $\theta_2$ ( $\angle C29-C28-C23-C22$ ) obtained for F2V. The curves were calculated by B3LYP/6-31G(d) methods	28
7	One-dimensional dependence of the electronic ground state and vertically excited energies of studied symmetric systems on the torsion calculated at the B3LYP/6-31G(d) theoretical level.	29
8	One-dimensional dependence of the electronic ground state and vertically excited energies of studied asymmetric systems on the torsion calculated at the B3LYP/6-31G(d) theoretical level.	30
9	Optimized bond lengths (in Å ) of F <sub>2</sub> V obtained from RI-CC2/SVP, RI-PBE/SVP and B3LYP/6-31G(d) methods	32
10	Computed B3LYP/6-31G(d) bond lengths of the asymmetric substitution molecules under study	36
11	Computed B3LYP/6-31G(d) bond lengths of the symmetric substitution molecules under study	37
12	Optimized bond distances of F <sub>n</sub> V <sub>m</sub> (n=2-5 and m=1-4) as obtained from B3LYP/6-31G(d), bond distances are given in Å unit (Y axis)	38

## LIST OF FIGURES (Continued)

Figure		Page
13	One-dimensional dependence of the electronic ground state and vertically excited energies of studied asymmetric systems on the torsion calculated at the B3LYP/6-31G(d) theoretical level. The ground-state energy minimum is taken as energy reference (see also Table 4). The open squares denote electronic ground state and the next symbols indicate the first six excited states (S <sub>1</sub> : ○; S <sub>2</sub> : Δ; S <sub>3</sub> : ∇; S <sub>4</sub> :+; S <sub>5</sub> : ×; S <sub>6</sub> :~ )	43
14	One-dimensional dependence of the electronic ground state and vertically excited energies of the studied symmetric systems on the torsion calculated at the B3LYP/6-31G(d) theoretical level. The ground-state energy minimum is taken as energy reference (see also Table 4). The open square denote electronic ground state and the next symbols indicate the first six excited states (S <sub>1</sub> : ○; S <sub>2</sub> : Δ; S <sub>3</sub> : ∇; S <sub>4</sub> :+; S <sub>5</sub> :×; S <sub>6</sub> : -)	44
15	Relative ground state and the first lowest excitation state bond lengths (in angstrom), calculated by B3LYP/6-31G(d) and TD-B3LYP/SVP methods, respectively, of the copolymer derivatives as compared to fluorene-vinylene dimer	45
16	Ground (S <sub>0</sub> ) and excited (S <sub>1</sub> ) states torsional angle changes (in degrees) of FV-derivatives. Optimized ground state geometries, calculated from B3LYP/6-31G(d) method and excited state geometries, by TD-B3LYP/SVP method. F <sub>3</sub> V <sub>2</sub> -NH <sub>2</sub> is represented by solid circles, F <sub>3</sub> V <sub>2</sub> -CN by open circles, F <sub>3</sub> V <sub>2</sub> -OCH <sub>3</sub> by solid triangles, F <sub>3</sub> V <sub>2</sub> -OH by open triangles	47



## LIST OF FIGURES (Continued)

Figure		Page
17	Plots of the B3LYP/6-31G(d) molecular orbitals contributing significantly to the lowest energy transitions of studied molecules in <i>all-trans</i> conformation. H denotes HOMO and L is LUMO	52
18	Calculate excitation energies of PFV, PFV-CN, PFV-NH <sub>2</sub> , PFV-OCH <sub>3</sub> and PFV-OH by TDB3LYP method with SVP and TZVP basis sets based on ground state geometries optimized by B3LYP/6-31G(d) method	57
19	Correlation of the excitation energies of fluorene-vinylene oligomers with the inverse chain units (dimer to heptamer). The energies are calculated by B3LYP/6-31G(d) method	59
<b>Appendix Figure</b>		
A1	Generalized Jablonski Diagram	93
A2	Idealized Absorption Spectrum	96
A3	Schematic representations of the origins of UV-Vis absorption (bottom) and fluorescence (top) spectra	99
A4	Illustration of the Franck-Condon principle for vertical electronic transitions	100
A5	Relationship between the broad electronic absorption and fluorescence bands of liquids and solids	101

## LIST OF ABBREVIATIONS

$\Delta E$	=	Energy gap, Excitation energy
$f$	=	Oscillator strength
AM1	=	Austin Model 1
AOs	=	Atomic Orbitals
BLYP	=	Beck-Lee-Yang-Parr functional
B3LYP	=	Becke's three parameter hybrid functional using the LYP correlation functional
CC2	=	Second-Order Approximate Coupled-Cluster
DFT	=	Density Functional Theory
EA	=	Electron affinity
$E_g$	=	Energy gap
EL	=	Electroluminescence
eV	=	Electron Volt
GTO	=	Gaussian-Type Orbital
HF	=	Hartree-Fock
HOMO	=	Highest Occupied Molecular Orbital
IP	=	Ionization potential
KS	=	Kohn-Sham
LCAO	=	Linear Combination of Atomic Orbitals
LCAO-MO	=	Linear combination of atomic orbitals to molecular orbitals
LDA	=	Local Density Approximation
LEDs	=	Light Emitting Diodes
LEPs	=	Light-emitting polymers
LUMO	=	Lowest Unoccupied Molecular Orbital
LYP	=	Lee-Yang-Parr functional
MNDO	=	Modified Neglect of Diatomic Overlap
MOs	=	Molecular Orbitals
MP2	=	Second-order Møller–Plesset perturbation theory
OLED	=	Organic light emitting diode

## LIST OF ABBREVIATIONS (Continued)

PES	=	Potential Energy Surface
PF	=	Polyfluorene
PFV	=	Poly(fluorenevinylene)
PFV-CN	=	Cyano-substituted poly(fluorenevinylene)
PFV-(CN) <sub>2</sub>	=	Di-cyano-substituted poly(fluorenevinylene)
PFV-NH <sub>2</sub>	=	Amino-substituted poly(fluorenevinylene)
PFV-(NH <sub>2</sub> ) <sub>2</sub>	=	Di-amino-substituted poly(fluorenevinylene)
PFV-OCH <sub>3</sub>	=	Methoxy-substituted poly(fluorenevinylene)
PFV-(OCH <sub>3</sub> ) <sub>2</sub>	=	Di-methoxy-substituted poly(fluorenevinylene)
PFV-OH	=	Hydroxy-substituted poly(fluorenevinylene)
PFV-(OH) <sub>2</sub>	=	Di-hydroxy-substituted poly(fluorenevinylene)
PL	=	Photoluminescence
PPV	=	Poly(p-fluorenevinylene)
QM	=	Quantum Mechanics
RI	=	Resolution of Identity approximation
S <sub>0</sub>	=	Ground state
S <sub>1</sub>	=	First excited state
S <sub>2</sub>	=	Second excited state
S <sub>3</sub>	=	Third excited state
SCF	=	Self-Consistent Field
STO	=	Slater Type orbital
STO-3G	=	Slater Type orbital approximated by 3 Gaussian Type prbitals
TDDFT	=	Time-Dependent DFT
TDHF	=	Time-Dependent HF
UV-VIS	=	Ultraviolet-Visible Spectroscopy
ZINDO	=	Zerner's Intermediat Neglect of Differential Overlap

# INVESTIGATION ON ELECTRONIC STRUCTURES AND PROPERTIES OF POLY(FLUORENEVINYLENE) DERIVATIVES: THEORETICAL STUDIES

## INTRODUCTION

In 1976, Alan MacDiarmid, Hideki Shirakawa, and Alan Jay Heeger, together with their groups, discovered conducting polymers and the ability to dope these polymers over the full range from insulator to metal (Heeger, 2001). Polyacetylene, which consists of alternate single and double carbon-carbon bonds, is the simplest model of this kind of materials (Heeger *et al.*, 1977; Chiang *et al.*, 1977). This was particularly exciting because it created a new field of research on the boundary between chemistry and condensed matter physics. In a conjugated polymer, the chemical bonding leads to one unpaired electron (the  $\pi$ -electron) per carbon atom. Moreover,  $\pi$ -bonding, in which the carbon orbitals are in the  $sp^2pz$  configuration and in which the orbitals of carbon atoms along the backbone are overlapping, leads to electron delocalization along the backbone of the polymer. This electronic delocalization provides the way for charge mobility along the backbone of the polymer chain.

In the past two decades, a large number of studies has been performed both experimentally and theoretically by introducing fused ring systems, ladder type structure or electron acceptor units, and so forth into  $\pi$ -conjugated backbone, aiming at the decreasing the energy gap value to present a true organic conductor without dopants. Many novel polymers have been synthesized to obtain materials with optimum physicochemical characteristics. There are three routes to design and synthesize small band gap polymers. The first way to design small band gap polymer is the constructing fully fused-ring hydrocarbon structure in order to obtain system corresponding more or less to a one-dimensional graphite (Bredas, 1986). A second route, small band gap polymers can be obtained by modifying the geometric and/or electronic structure of known and well-characterized conjugated polymers that can be

easily derivatized (Karpfen *et al.*, 1997; Loegdlund *et al.*, 1994). A third route to initiate narrow band gap conjugated polymers was obtained by building a conjugated backbone consisting of regularly alternating strong donor and acceptor like units. Among these approaches, side chain modification is one of the useful and practical routes to optimize polymers. In this way, polymers can be made processable. More importantly, the optical properties can be tuned by different substituents.

Nowadays, conjugated polymers have been widely studied as conducting materials due to their potential use in wide range of practical application (Li and Meng, 2007) such as laser (Kallinger *et al.*, 1998), transistor (Babel and Jenekhe, 2002; Scott *et al.*, 2006), batteries (Mermillod *et al.*, 1986; Bittihn *et al.*, 1987), photovoltaic devices (Sailor *et al.*, 1990) and light-emitting diodes (LEDs) (Heeger, 2001). The advantages of these polymers are that their solubility properties and HOMO and LUMO energy levels can be adjusted by varying the molecular structure of the polymer. Many conjugated polymers, such as poly(*p*-phenylene)s, poly(*p*-phenylenevinylene)s, poly[2,7-(9,9-dialkylfluorene)]s, poly(carbazole)s, poly(thiophene)s and poly(pyrrole)s are shown in Figure 1.

The particular application of the conjugated polymers in organic light-emitting diodes (OLEDs) was initiated since poly(*p*-phenylene vinylene) (PPV) was found to emit electroluminescence (EL) in 1990 (Burroughes *et al.*, 1990). PPVs are well known as the first class of electroluminescent polymers and large number of studies has been reported. This kind of light-emitting materials is famous because it can be fabricated on a flexible substrate and easily processed for specific purposes (Chiang *et al.*, 1977; Becker *et al.*, 1999). Compared with single molecules, polymers have longer  $\pi$ -conjugation lengths, higher glass-transition temperatures, better film-forming properties, and stable film morphologies; there are further advantages on device fabrication such as higher quantum efficiencies, longer lifetime, and simplified processing by spin-coating. Until now, efficient and stable polymer blue light-emitting LEDs have been still developed. Therefore, the design and synthesis of new green or blue light-emitting polymer are of primary importance for the realization of full-color polymer LEDs.



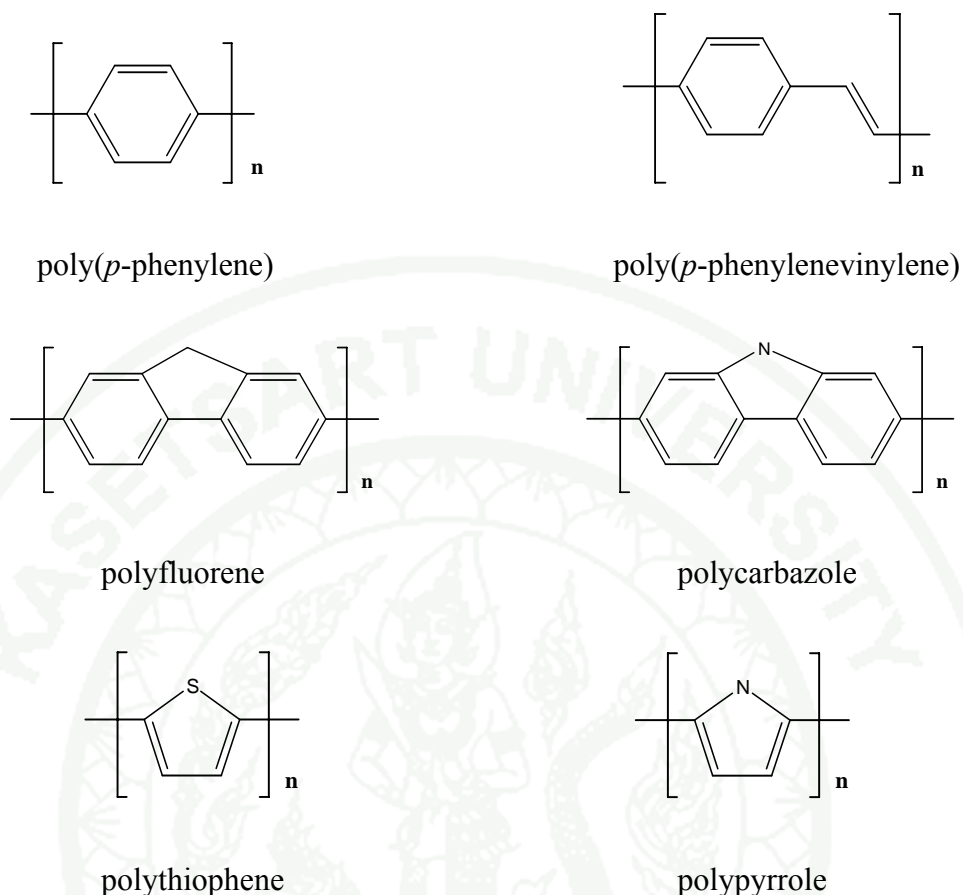


**Figure 1** Structures of conjugated polymers

Polyfluorenes (PFs) (Pei *et al.*, 1996; Ranger *et al.*, 1997) and their analogous derivatives are getting much application in the LEDs due to their high efficient blue emission in both photoluminescence (PL) and electroluminescence (EL). By structural modification at 9-position of fluorene ring, the different polyfluorene derivatives can be synthesized and possessed good thermal stability. However, polyfluorene tends to aggregate in solid state and has the high energy barrier for hole injection, lead to poor efficiency of LEDs. It was found that copolymerization of fluorene with various aryls allows for tuning of electronic properties and enhanced thermal stability. A new series, various fluorene-based copolymers have been synthesized, aiming at achieving color tuning over the visible spectrum and minimizing the injection barriers of LED device. Poly(9,9-dialkylfluorene-2,7-vinylene)s or PFVs (Figure 2) is another class of conjugated polymers that combine the structural characteristics of PPVs and PFs. This polymer emits greenish-blue light color and shows other good characteristics such as



high thermal stability, high molecular weight, low dispersion, facile purification and also high PL quantum yield. PFVs have been synthesized by means of acyclic diene metathesis (ADMET) polymerization (Nomura *et al.*, 2001), the Heck reaction (Cho, *et al.*, 1997), Horner-Emmons reaction (Anuragudom *et al.*, 2006), Suzuki coupling reaction (Lopez, *et al.*, 2002) and Gilch polymerization (Jin *et al.*, 2002; Hwang *et al.*, 2009). The derivatives, CN-poly(dihexylfluorenevinylene) (PFV-CN), was synthesized by condensation polymerization utilizing the Knoevenagel reaction (Jin *et al.*, 2003). The resulting polymer exhibits good solubility in common organic solvents and emits green light.

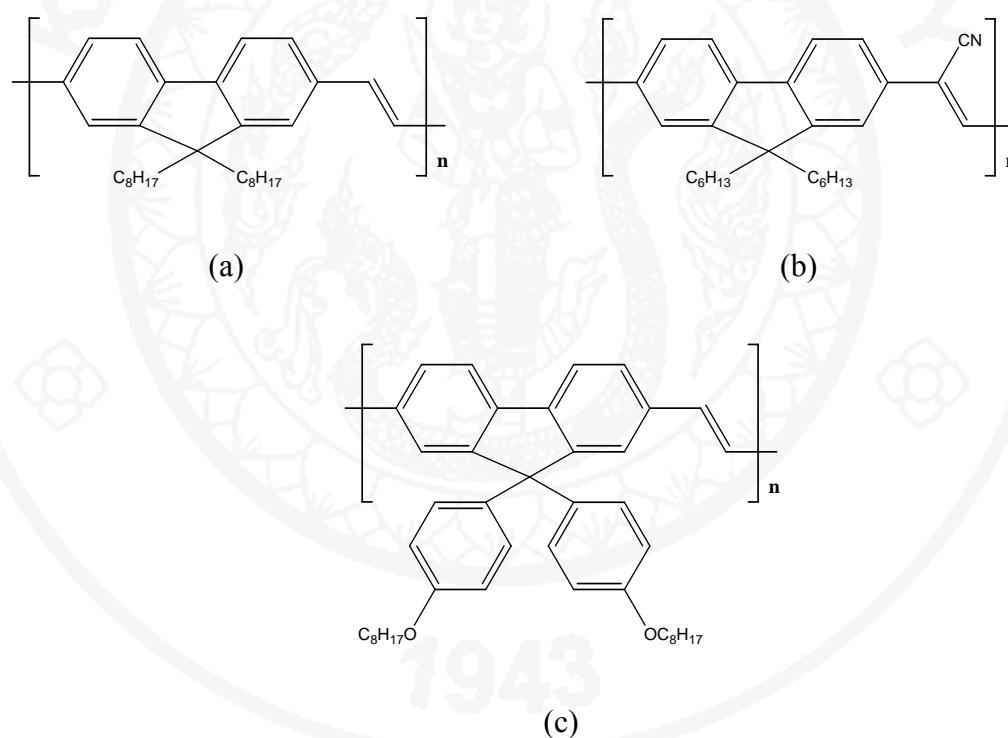


**Figure 2** Structures of (a) poly(9,9-di-noctylfluorenyl-2,7-vinylene) (PFV), (b) CN-poly(dihexylfluorenevinylene) (PFV-CN) and (c) poly[9,9-bis(4 octyloxyphenyl)fluorenyl-2,7-vinylene] (PBOPFV)

Quantum chemical calculations have been proven to be an important tool for investigation of the relationships between electronic structures and optical properties of the  $\pi$ -conjugated materials. Theoretical studies on the electronic studies of polymers have contributed a lot to rationalize the properties of known polymers and to predict those of yet unknown ones. Conformational analysis has been successfully used in various cases to predict the equilibrium torsion angles and energy barriers, which are useful to evaluate substituent effects (Pan *et al.*, 2000, 2001). There are two different theoretical approaches to evaluate the band gaps of polymers. One is the polymer approach in which the periodic structures are assumed for infinite polymers. Another one, the oligomer extrapolation technique (Salzner *et al.*, 1998), has acquired the increasing popularity in this field, however. In this approach a sequence of increasing longer oligomers is calculated, and extrapolation to infinite chain length is followed. A distinct advantage of this approach is that it can provide the convergence behavior of the structural and electronic properties of oligomers. In practice both the oligomer extrapolation and the polymer approaches are generally considered to be complementary to each other in our understanding of the properties of polymers.

The theoretical quantity for direct comparison with experimental band gap should be the transition (or excitation) energy from the ground state to the first dipole-allowed excited state. There exist a variety of theoretical approaches for evaluating this quantity for oligomers as well as infinite polymers. The crudest estimate is the orbital energy difference between the highest occupied molecular orbital (HOMO) and the lowest unoccupied molecular orbital (LUMO), obtained from Hatree-Fock (HF) or density functional theory (DFT) calculations (Salzner *et al.*, 1998; Delaere *et al.*, 2003). The implicit assumption underlying this approximation is that the lowest singlet excited state can be describe by only one singly excited configuration in which an electron is promoted from HOMO to LUMO. In addition, the orbital energy difference between HOMO and LUMO is still an approximate estimate to the transition energy since the transition energy also contains significant contributions from some two electron integrals. However, the real situation is that an accurate description of the lowest singlet excited state requires a linear combination of a number of excited configurations, although the one mentioned above often plays a

dominant role. The calculated HOMO-LUMO gap in many cases (Salzner *et al.*, 1998); it may probably due to the error of cancellations. Hence, it is desirable to obtain more rigorous information on the nature of the lowest singlet excited state by employing other elaborate theoretical methods. Among those theories, Hartree-Fock (HF)-based methods such as configuration interaction singles (CIS) and the random phase approximation (RPA), which is equivalent to the time-dependent HF (TDHF), usually only provide the qualitative or semi quantitative descriptions for the low-lying excited states. Time-dependent density functional theory (TDDFT) is recently developed tool for calculating excitation energies (Runge *et al.*, 1984; Hsu *et al.*, 2001; Appel *et al.*, 2003).

Major methodological progress has been achieved by the variational formulation of the TDDFT method by Furche and Ahlrichs (2002) facilitating the calculation of analytic TDDFT gradients, thus allowing geometry optimizations in excited states. For the theoretical investigation on both the ground and excited states, several theoretical methods have been applied to different conjugated polymer systems (Van Gisbergen *et al.*, 1999; Aouchiche *et al.*, 2004; Yang *et al.*, 2005; Poolmee *et al.*, 2005; Suramitr *et al.*, 2007). In particular, the time-dependence density functional theory (TDDFT) method was developed and used as a powerful tool for the excited state investigation. Many research groups employed TDDFT to calculate energy gaps and used the extrapolating technique to predict the energy gaps of infinite chain length of various conducting polymers (Salzner, *et al.*, 1998; Yang, *et al.*, 2005; Lukes *et al.*, 2007). Many publications focus on TDDFT electronic properties related to ground state geometry of conducting polymers, while the properties based on the excited state are not widely investigated. Therefore, calculation of electronic of excited states is still a very challenging task, especially in the calculation of geometry relaxation effects in excited states. However, Saha *et al.* (2007) point out that conventional TDDFT with the B3LYP functional should be used carefully, because it can provide inaccurate estimates of the chain length dependence of  $\pi \rightarrow \pi^*$  excitation energies for these molecules with long  $\pi$ -conjugated chains. From the work of Lukes *et al.* (2007) excited state properties of *p*-phenylene oligomers were investigated by using time-dependence DFT. The computed vertical excitation

energy and fluorescence energy are underestimated when compared with experimental results. They also suggested that the limitation of the current approximate exchanges functionals in correctly describing the exchange-correlation potential in the asymptotic region. Even though TDDFT still has some limitations, it can be helpful in understanding fundamentals of the electronic and optical characteristics of conjugated polymers and guiding the experimental efforts toward novel compounds with enhanced characteristics.

There are many experimental studies of fluorene-vinylene like system available in literatures. On the other hands, from our knowledge, there is no theoretical research study on fluorene-vinylene copolymer and/or the derivatives. Therefore, this is our challenging to perform fundamental understanding on structural and energetic properties of fluorene-vinylene copolymer.

Thus, the main objective of this work are to investigate structural, electronic and optical properties of poly(fluorene-vinylene) copolymer and its derivatives by using density functional theory method. Fluorescence energies and radiative lifetimes were analyzed and predicted. The effect of substituents on oligomeric structures and electronic energies was also studied, since a novel conducting polymer will be further synthesized by substituting the electron donating and withdrawing groups on the vinyl position.

## OBJECTIVES

1. To study the ground and excited state structures of fluorene-vinylene derivatives by using quantum chemical calculations.
2. To understand the relationship between the structure and electronic properties of fluorene-vinylene derivatives by quantum chemical calculations.
3. To investigate the excitation energies, fluorescence energies and radiative lifetimes of fluorene-vinylene derivatives by quantum chemical approach and compare with the experimental results.
4. To study the substitution effects of fluorene-vinylene based model on structure and electronic properties.



## LITERATURE REVIEW

Twenty years after the discovery by Alan J. Heeger, Alan G. MacDiarmid, Hideki Shirakawa and co-worker (1977), the doping effect on polyacetylene which was doped by using halogen materials, the conductivity of doped-polymer increase  $10^9$  times when compare to undoped one. There are a lot of works focused on conjugated polymers. These studied have let to achievement of high conductivity in other conjugated polymers and their application.

From 1990s and till now, LEDs is probably the most important application maintaining the researchers' interest towards conjugated (conducting) polymers, although in recent years, a growing interest towards other applications such as sensors and photovoltaics. Hundreds of academic research groups around the worlds have contributed to the development of electroluminescent polymers. Large commercial interests are in the possibility of solution fabrication of EL devices, and particularly, flat and/or flexible displays.

Light-emitting polymers (LEPs) have been a subject of many review articles, which dealt with various aspects of the design, the synthesis and the applications of different classes of LEPs. Many types of LEPs were discovered in order to improve physical and chemical properties. Extensive studies of conjugated polymers in the early and middle 1980s focused on searching and developing new materials with solution processibility. One of popular system was a polythiophene derivative studied by the University of California at Santa Barbara in 1987 (Tomozawa *et al.*). The first demonstration of light-emitting device with unsubstituted poly(p-phenylenevinylene) (PPV) by R.H. Friend's group at Cambridge University (1990), a high efficient polymer light-emitting diode (PLED) device was made with a solution processible polymer, poly[2-methoxy-5-(2'-ethyl-hexyloxy)-1,4-phenylenevinylene] (MEH-PPV), by Heeger's group in Santa Barbara, California (1991). Most importantly, these materials have intrinsically low charged impurity (typically below  $10^{14}$  per  $\text{cm}^3$ ) and high photoluminescent efficiency (typically in the range of 20–60%) (Becker *et al.*, 1999). However, the energy gap of PPV is not large enough to produce the blue color



which is need for full-color displayed application. Then, Searching and developing wide energy gap polymers are the significant tasks.

Blue emitters being studied include poly(p-phenylene) (PPP) (Yang *et al.*, 1996), ladder-type poly(p-phenylene) (LPPP) (Tasch *et al.*, 1996), polyfluorene (PF) (Bernius *et al.*, 2000), and their derivatives. Different routes of syntheses, properties, and LED applications of fluorene-based conjugated polymers and copolymers have been highlighted in several recent reviews (Scherf and List, 2002; Kim *et al.*, 2000). However, the drawbacks of PFs, such as aggregation and/or excimers formation in the solid state, insufficient stability, and high energy barrier for hole injection, limit their application in polymers LEDs. In fact, PFs are the only class of conjugated polymers that can emit a whole range of visible colors with relatively high Quantum Efficiency (QE).

Fluorene (Fl) is a polycyclic aromatic compound. Due to strong violet fluorescence arising from its highly conjugated planar p-electron system, it was named as “fluorene”. Positions 2 and 7 in Fl are the most reactive sites toward electrophilic attack, whereas the methylene bridge (at the 9 position) provides an opportunity to modify the processability of the polymer by substituents without perturbing the electronic structure of the backbone. The varieties, optical and electronic properties, and high thermal and chemical stability of PFs make them an attractive class of materials for PLEDs. Parent (unsubstituted) PF was first synthesized electrochemically in 1985 (Bernius and Inbasekaran, 2000). Generally, fluorene homo- and copolymers show excellent thermal stability: the  $T_{dec}$  of many PF exceeds 400°C (according to thermogravimetric analysis (TGA) analysis under inert atmosphere) (Wu *et al.*, 2004). Grell and coworkers (1998) also show the solvent effect on morphology of poly(9,9-dioctylfluorene) (PFO). Dramatic changes in the absorption spectra of PFO resulting from the dissolution in moderately poor solvent such as cyclohexane, toluene and THF. This result demonstrates that the choice of the solvent and casting, drying, and annealing techniques are very important for the device performance. Inbasekaran *et al.* (2000) have developed a number of fluorene based homopolymers and copolymers utilizing an improved Suzuki reaction. Presence

of carbon-9 in fluorene enhances the effective conjugation and the alkyl groups at C-9 impart solubility to the polymers. Polyfluorenes are highly fluorescent and LEDs based on these polymers appear to have electrons as the majority carrier. Accordingly, the device performance is enhanced considerably when modified with a suitable hole-transporting layer. An optimized green-emitting device exhibits very high luminance at very low drive voltage, attributable in part to the high hole mobility of fluorene-based polymers. Good lifetimes have been achieved with red and green LEDs based on fluorine copolymers as emitters.

The major problem in the application of PFs films in blue PLEDs is color instability. The initial hypotheses explained by the formation of aggregates (a charge transfer (CT)  $\pi$ - $\pi^*$  transition of keto-defects located onto the conjugated chain) or excimers (Lemmer *et al.*, 1995 and Lee *et al.*, 1999), resulted in the emission in the long wavelength region. Indeed, the green emission increased during the thermal annealing and was not observed in polymer solution. Although the exact mechanism of the defect formation is not known, it is believed that the monoalkyl fluorene moieties, present as impurities in poly(dialkylfluorenes), are the sites most sensitive to oxidation.

### **Synthesis of poly(fluorene-vinylene) and its derivatives**

The modifications of the chemical structure of PF can be done by introducing of side-chain substituents and end-capping units, copolymerization with other conjugated units and polymer blends. Among them, copolymerization of fluorene with other highly luminescent materials offers a possibility of fine-tuning the emitting and charge-transport properties of PF. Thus various fluorene-based copolymers were synthesized. Poly(9,9-dialkylfluorene-2,7-vinylene)s (PFVs) is another class of conjugated polymers that combine the structural characteristics of PPVs and PFs and show high thermal stability and PL quantum yield. PFVs have recently been synthesized by several methods. The first synthesis of PFV was done by Heck reaction (Cho *et al.*, 1997). The energy gap of polydialkylfluorene was reduced by introducing a vinyl unit in the main chain. Then high molecular weight trans-poly(9,9-

di-n-octylfluorene-2,7-vinylene) was prepared under acyclic diene metathesis (ADMET) polymerization (Nomura *et al.*, 2001). A UV-vis spectrum of PFV displays two absorption bands at 428 and 455 nm. Fluorescence spectra of polymer 4b with excitation at either 428 or 455 nm are comparable to two characteristic peaks at 465 and 497 nm. Jin and coworker (2002) prepared poly(9,9-di-n-octylfluorene-2,7-vinylene) (PFV) via Gilch polymerization together with its characterization and purification using membrane technology. The drawback of Gilch polymerization is the difficulty in controlling the polymerization rate and formation of the insoluble gel portion during the reaction. This might cause of head to head defect formation in the polymer chain. The absorption of PFV is approximately 40 nm red-shifted relative to that of poly(9,9-dialkylfluorene) derivatives. The maximum emission peak is at 507 nm, which corresponds to greenish-blue light. The energy gap and HOMO level of PFV film are 2.6 and 5.3 eV obtained from the cyclic voltammogram. The optical efficiency of PFV obtained by Gilch polymerization was compared to that of PPV derivative by Hwang and coworker (2003). Poly[(9,9-di-n-octylfluorenyl-2,7-vinylene)-co-(1,4-phenylenevinylene)]s [poly(FV-co-PV)s] were synthesized through Gilch polymerization, and their light-emitting properties were investigated. The copolymers showed almost the same optical properties as the PFV homopolymer, regardless of copolymer composition. The PFV and poly(FV-co-PV)s all showed PL emission maxima at approximately 465 nm. Interestingly, the EL spectra of these devices were similar to the PL spectra of the corresponding polymer film. However, the EL devices constructed from the poly(FV-co-PV)s showed 10 times higher efficiency than the devices constructed from the PFV. They suggest that this higher efficiency is possibly a result of better charge carrier balance in the copolymer systems due to the lower HOMO level (~5.5 eV) of the poly(FV-co-PV)s in comparison to that of PFV (~5.7 eV). Gilch polymerization is regarded as a useful synthetic method for obtaining high molecular weight PPV derivatives suitable for practical applications. A popular selected synthetic method is Gilch polymerization regarded as a useful synthetic method for obtaining high molecular weight polymers. Hwang and coworkers (2009) synthesized the poly[9,9-bis(4-octyloxyphenyl)fluorenyl-2,7-vinylene] (PBOPFV) via the Gilch polymerization route and its light-emission properties were characterized and compared with those of

poly(9,9-di-n-octylfluorenyl-2,7-vinylene) (PFV). The results show that introduction of alkoxy phenyl groups onto the 9-position of PFV prevents or retards the formation of additional emission and also during operation of the EL devices. There was no change in the PL spectrum of the PBOPFV polymer films, even after thermal annealing in air. It is clear that the introduction of the alkoxyphenyl groups at the 9-position of fluorene in PFV successfully suppresses the long-wavelength emission in its PL and EL. Another synthetic route, Horner-Emmons reaction, is proposed by Anuragudom and coworker (2006). The absence of saturated defects was confirmed by  $^1\text{H}$  NMR spectroscopy. The Horner-Emmons PFVs exhibited a greenish fluorescence ( $\lambda_{\text{max}}$  emission ) 466 nm with shoulder at 496 nm) in THF, which was red-shifted compared to the Gilch PFVs ( $\lambda_{\text{max}}$  emission ) 453 nm with shoulder at 488 nm).

Moreover, the electrosynthesis of a soluble poly(fluorenylene vinylene) derivative, namely poly(9,9-dioctyl-2,7-fluorenylene vinylene) (PFV), and its complete photophysical and electrochemical characterization was reported by Gruber and coworker (2006). The advantages of this route are its inherent mild conditions and high yield leading to a polymer with high molecular weight, good thermal and optical properties. The shape of the absorption spectra of electrochemically prepared PFV differs significantly from the described for the same polymer prepared by acyclic diene metathesis or via Gilch route. This reflects the fact that the optical properties of poly(fluorenylene vinylene)s are very sensitive to synthesis details and thermal conversion process, influencing the chain length distribution, degree of interchain order and isomeric properties. The solid-state emission spectrum shows three characteristic peaks at 478, 507 and 543 nm, in agreement with other PFV synthesis methods. In this work, the fluorescence lifetime of PFV was investigated by using mathematical fitting of the photoluminescence decay time. The decay time shows two time constants, 0.68 and 1.31 ns. The presence of two lifetimes can be assigned to an excited state deactivation process of the main chain, induced by the vinylene moiety. Because of the freely rotation ability of vinyl group to find an optimal conformation, the decay time during charge distribution in the excited state was affected.



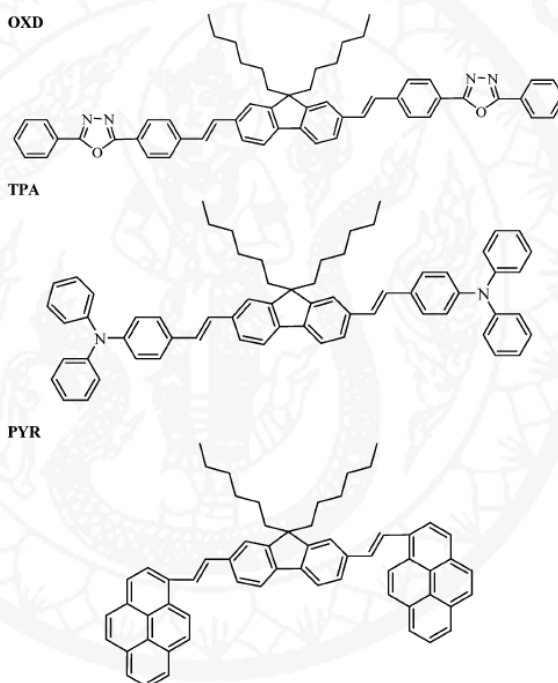
The design and synthesis the new green electroluminescent polymer by modifying the side chain of PFV was proposed by Jin and coworker (2003). The electron affinity, cyano substituent, was introduced in order to reduce the electron injection barrier. CN-poly(dihexylfluorenevinylene) (CN-PFV), which denotes poly[(9,9-dihexyl-9H-fluorene-2,7-diyl)(1-cyanoethene-1,2-diyl)(9,9-dihexyl-9H-fluorene-2,7-diyl)(2-cyanoethene-1,2-diyl)], was synthesized by condensation polymerization utilizing the Knoevenagel reaction. The resulting polymer exhibits good solubility in common organic solvents such as chloroform, THF, and ODCB. The HOMO and LUMO energy levels of CN-PDHFV are lower than that of PDHFV, which can be attributed to the introduction of the electron-withdrawing cyano group. This polymer emits the green electroluminescence ( $\lambda_{\text{max}} = 530 \text{ nm.}$ ) and shows higher EL efficiency than that of PFV. Their experiment is supported by Souza *et al.* (2000). A theoretical and experimental investigation of methoxy- and cyano-substituted *p*-phenylenevinylene model compounds were performed. The emission spectrum loses structure and shifts to the red. From the theoretical studies, there is no stabilization energy in the interaction between the cyano and methoxy groups in the geometry optimization. The ab-initio first excited state calculations show that the methoxy-substituted model compound consists of a HOMO to LUMO transition, which is delocalized across the whole molecule.

Zeng *et al.* (2003) have investigated the influence of electron acceptors and donors on the geometric and electronic properties of the poly(9,9-dihexylfluorene-1,4-phenylene) unit cell. They have shown that sizable effects can be obtained. In particular, the use of diamino or dicyano substituents on the phenylene ring allows the bandgaps to decrease significantly. This information is of prime importance in the design of new chemical structures aimed at a fine-tuning of the emitted color and at a significant improvement in quantum efficiency.

The attempt to design a novel polymer to improve the physical and chemical properties is reported by various groups of researchers. Copolymerization with other conjugated units is one of popular ways to modify the new polymers. Mikroyanidis and coworker (2006) synthesize and characterize three new 2,7-fluorenevinylene-

based trimers by Heck coupling reaction. They contained a central 2,7-fluorene-vinylene segment to which a substituent (CHART 1: trimer structures are identified by the respective substituent, OXD, TPA, or PYR) This substituent was a derivative of 2,5-diphenyl-1,3,4-oxadiazole, triphenylamine, or pyrene. These units are expected to improve the electron- and hole-transport properties of the trimers. Their light emission was bluegreen in both solution and solid state with PL maximum at the range of 455-565 nm and quantum yields of 0.65-0.74 in THF solution. All samples were fluorescent and showed nanosecond lifetime with two components in the films.

**CHART 1**  
**OXD**



The organic light-emitting diodes (OLEDs) with OXD and TPA showed green emission with electroluminescence (EL) quantum efficiencies of  $\eta_{EL} \sim 10^{-2}\%$ , while very weak EL efficiency of  $\eta_{EL} \sim 10^{-5}\%$ , was observed with PYR.

The insertion of fluoro groups in vinylene units was done by Jin and coworkers (2007) in order to increase the efficiency of copolymers. poly(9,9-dihexylfluorene-2,7-vinylene-co-p-phenylenedifluorovinylene) (PFVPDFV), have been synthesized by the Gilch polymerization. The fluoro groups were introduced on



vinylene units to increase the electron affinities of the copolymers. The maximum absorption peak at 413 nm of PFVPDFV was blue-shifted with more amount of the PDFV. This is originated from the decrease of the electron density along the  $\pi$ -conjugated polymer backbone by incorporation of the PDFV segment and decrease of the effective conjugation length of the copolymers. The increasing of luminescence efficiencies of the copolymers at room temperature was reported caused by the high electron injection ability which was originated by the presence of fluoro group on vinylene unit, but low solubility is still a problem.

Nomura and coworkers (2008) performed an exclusive end functionalization of all-trans-poly(fluorene vinylene)s by grafting poly(ethylene glycol) using ADMET condensation proceeds. The resultant copolymers possessed uniform molecular weight distributions; the copolymers were identified by  $^1\text{H}$  and  $^{13}\text{C}$  NMR spectra<sup>14</sup> and confirmed that no residual PEG was seen in GPC traces for the isolated polymer(s). Thus, they believe that the present approach should offer unique, important methodology for precise synthesis of end-functionalized conjugated polymers (PPVs, PFVs) for targeted device materials as well as synthesis of various block copolymers containing conjugated polymer fragments. Since the studies of 3,6-carbazole (Cz) containing PAVs are motivated by the strong hole-transporting ability of such systems in optoelectronic devices (due to the electron-donating properties of the nitrogen atom). Grisorio and coworkers (2007) describe the synthesis and properties of new random PFVs containing 3,6-N-octylcarbazole at various compositions. The poly(FV-co-Cz)s copolymers at different mole percent of carbazole compositions are achieved by Suzuki-Heck cascade reaction. The PL emission of the copolymers, which were found to be similar both in solution and in the solid state, whereas, their UV-vis features evidenced a slight blue shift of the absorption maxima as a function of the carbazole amount. The electroluminescence properties of the polymers were tested by constructing suitable OLED devices of configuration ITO/PEDOT-PSS/(polymers)/Ca/Al. The results show that the incorporation of carbazole unit can improve the device performance because of the better hole transportation in the materials. Moreover, HOMO-LUMO energy level of

a  $\pi$ -conjugated arylene-vinylene copolymer can be tuned by control the carbazole composition.

Beside the optical properties and applications of poly(fluorene-vinylene) derivatives, the photovoltaic properties of this copolymer were studied by Jin et al. (2006). The poly(9,9-dioctylfluorenyl-2,7-vinylene) [poly(FV)] and poly[2-(3'-dimethyldodecylsilylphenyl)-1,4-phenylenevinylene] [poly(m-SiPhPV)], were synthesized and used for the fabrication of efficient photovoltaic cells. The results show that novel copolymers composed of fluorenylvinylene and phenylenevinylene repeating units were found to have high molecular weights and exhibit good solubility in common organic solvents. Due to the high glass transition temperatures, these polymers are promising materials for photovoltaic applications. The photovoltaic cells prepared with poly(FV-co-m-SiPhPV) give the higher efficiency than those of with poly(FV) and poly(m-SiPhPV).

### **Theoretical investigation on conjugated polymers**

In theoretical point of view, structures, optical and electronic properties of conjugated polymers are under investigation. Due to the limitation of experimental systems, Fundamental study can improve the understanding of the phenomena of chemical compounds. In the fluorene system, the HF/6-31G(d) ground state geometry and potential curve of bifluorene (BF) were studied by Blondin *et al.* (2000). The results indicate that optimal conformation of BF is located at dihedral angle around 45° and 135°. In addition, the observed results show that the presence of alkyl chain at the 9-position of BF does not significantly change its potential curve. This strongly suggests that the presence of alkyl chains in corresponding polymer should not intrinsically change the conformation behavior of each repeating units. The structural properties of poly(2,7-fluorene) (PF) were also investigated by Briere *et al.* (2004). The ground state optimization was done by using DFT with plane wave basis set. The calculated dihedral angle of PF is 26° which is in agreement with experimental data.

The ground and excited states of fluorene-vinylene oligomers and its derivatives were calculated in Meeto et al. (2008). In this work, The ground state and the lowest singlet excited-state geometries of poly-(9,9-dialkylfluorene-2,7-vinylene) copolymer or PFV and its derivatives ( $F_mV_n-NH_2$ ), ( $F_mV_n-CN$ ), ( $F_mV_n-OCH_3$ ) and ( $F_mV_n-OH$ ) ( $m, n = 2-5$ ) were investigated based on density functional theory (DFT) and time-dependent DFT using B3LYP functional. The presence of substituents group at vinyl position leads to the twist conformations of all dimers. This can be explain by the steric hindrance effect of substituents to the  $\pi$ -orbital of vinylene unit. After electronic excitation, most of the derivative of FV dimers exhibits closed-planar structures at excitation state. The TDDFT calculated energy gaps of fluorene-vinylene based polymers are lower than those of experimental data. The fluorescent lifetime of these oligomers were predicted as well.

From our knowledge, until now, there is no theoretical investigation on the poly(fluorene-vinylene) copolymer available in the data based. A survey on fluorene-vinylene-like systems is only available route to collect the useful information. The ground and excited states of fluorene-phenylene (FP) based oligomers and polymers were studied by Gong *et al.* (2005). The closed-shell Hartree-Fock method and the DFT with various functionals were used to optimize ground stated structures. All derivatives are non-planar in their electronic ground states. Then the lowest singlet state was investigated by using CIS method. The results show that the primary electronic transition is originated from the HOMO to the LUMO orbital ( $S_1 \leftarrow S_0$ ).

Due to the limitation of CIS, TDDFT and RI-CC2 are interesting methods to perform the excited state calculation. Many calculations were done by TDDFT and RI-CC2 methods (Beenken and Lischka, 2005; Lukes *et al.*, 2005; Serrano-Andres *et al.*, 2005; Suramitr *et al.*, 2007). The results indicate that TDDFT and RI-CC2 methods are suitable for evaluating the excitation Properties of the low-lying excited states for small- and medium-sized molecules. For example, the vertical excitations and the fluorescent transition from the lowest excited state of methylene-bridged oligomers (Lukes *et al.*, 2005) were calculated using TDDFT, RI-CC2 and ZINDO/S methods. The RI-CC2 and ZINDO/S absorption and fluorescent spectra are agreed

quite well with the experiment. However, the TDDFT results are underestimated both absorption and fluorescent energies. The systematic decrease is found for larger systems ( $N > 4$ ).

The time-dependent density functional theory (TDDFT) (Gross *et al.*, 1990), a powerful tool for calculating excitation energies, is employed to extrapolate energy gaps of the polymers by the calculated excitation energies of their oligomers. It is pointed out that TDDFT systematically underestimated the excitation energies by 0.4-0.7 eV when compared to the experimental results (Ma *et al.*, 2002; Suramitr, 2005; Sriwichitkamol, 2006). The reason for this is due to the limitation of the current approximate exchange-correlation functional in correctly describing the exchange-correlation potential in the asymptotic region. However, reasonable results can still be expected here, because the Hartree-Fock (HF)/DFT hybrid functional such as B3LYP has been used which could partially overcome the asymptotic problem. For linear oligoenes, recent studies on the excited energies of the first dipole-allowed 1Bu states also showed that TDDFT calculations with the B3LYP functional can correctly reproduce the general trend of decreasing excitation energy with chain length, with a systematic underestimation of only approximately 0.3-0.5 eV. The survey on CASSCF TDDFT and RI-CC2 calculations have been performed on protonated and neutral Schiff bases (PSB and SB) (Aquino *et al.*, 2006). They found that CASSCF results are quite reliable even though overshooting of geometry changes is observed. TDDFT does not reproduce bond alternation well in the  $\pi\pi^*$  state. However, TDDFT with the B3LYP functional is expected to be a relatively reliable tool for evaluating the excitation energies of the low-lying excited states for small- and medium-sized molecules.

## METHODS OF CALCULATIONS

### Quantum Chemical Calculation

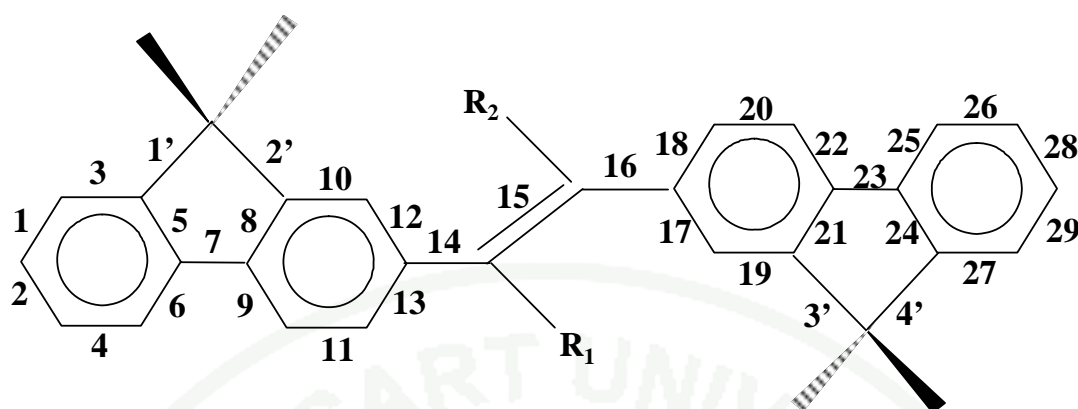
Theoretical chemistry (quantum computational chemistry) introduces very well defined mathematical approximations to end up chemistry problems. One of the challenging tasks for molecular orbital calculations is the important method in quantum chemistry to approximate structures and dynamics of molecular system. This approach provides a great promise in calculating electronic structures and predicting properties of variety of molecules. Until now, molecular orbital investigations have been introduced into research at molecular level to study mechanisms of action and to guide the design of more potent agents' novel nanostructures.

### Ground State Calculation

#### 1. Models of Calculation

Starting geometries of (FV)<sub>n</sub> oligomers and the derivatives were constructed by molecular modelling. Due to the computational cost reduction, the alkyl groups at 9-position on fluorene ring were replaced by hydrogen atoms. Moreover, there are some reports said that the alkyl substituents at the 9-position play an important role in the thermal stability and solubility and do not affect the electronic structure and optical property of fluorene-based polymer (Srivichitkamol *et al.*, 2006; Poolmee, *et al.*, 2005). There is also experimental evidence (Zeng et al., 2002) showed that the length of alkyl chain does not affect their optical properties such as the location of absorption maxima. Therefore, we might neglect the appearance of alkyl group at that position here. Consequently, the models and also the bond-numbering used in this study are shown in Figure 3.





Molecule	R <sub>1</sub>	R <sub>2</sub>
F <sub>2</sub> V	H	H
F <sub>2</sub> V-(CN) <sub>2</sub>	CN	CN
F <sub>2</sub> V-(NH <sub>2</sub> ) <sub>2</sub>	NH <sub>2</sub>	NH <sub>2</sub>
F <sub>2</sub> V-(OCH <sub>3</sub> ) <sub>2</sub>	OCH <sub>3</sub>	OCH <sub>3</sub>
F <sub>2</sub> V-(OH) <sub>2</sub>	OH	OH
F <sub>2</sub> V-CN	CN	H
F <sub>2</sub> V-NH <sub>2</sub>	NH <sub>2</sub>	H
F <sub>2</sub> V-OCH <sub>3</sub>	OCH <sub>3</sub>	H
F <sub>2</sub> V-OH	OH	H
F <sub>2</sub> V-CN-NH <sub>2</sub>	CN	NH <sub>2</sub>

**Figure 3** Schematic structure, bond and dihedral angle numbering of studied systems in *all-trans* conformations.

## 2. Conformational Analysis

In this study, poly(9,9-dialkylfluorenevinylene) was represented by 9H-fluorenevinylene as a model for calculations. To investigate the effect of substituent groups, side chains of oligomeric models were replaced by functional groups as shown in Figure 3. Potential energy surfaces of F<sub>2</sub>V and its derivatives were investigated by partial optimizations, based on B3LYP/6-31G(d) methods using Gaussian03 program package. The torsion potentials were calculated for the fixed

angles,  $\Theta$ , from the interval 0 to 180 degrees by changing 10 degrees step interval. In the case of asymmetric molecules, dihedral angles ( $\Theta_1$  and  $\Theta_2$ ) for both sides are investigated due to the different type of steric hindrance. The rotation angle is illustrated in Figure 4. Note that for model compound, hydrogen atom instead of alkyl group was used in order to simplify calculations. In this point of view, the electron donating effect and steric effect are dominated by an atom which is directly connected to backbone.

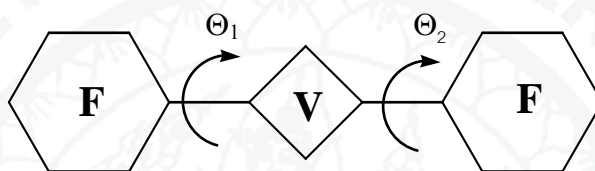


**Figure 4** Schematic diagram of dihedral angle used in this calculation.

Preliminary calculations of  $F_2V$  was performed by using AM1, HF/3-21G(d), HF/6-31G(d) and B3LYP/6-31G(d) methods. The ground ( $S_0$ ) electronic state of  $F_2V$  molecules is shown in Figure 5. From the B3LYP calculations, it is shown that the molecule has two potential minima at  $\Theta_1 = 0$  and 180 degrees corresponding to *cis* and *trans* conformations. Similarly, torsion energy curves obtained from AM1 and HF methods showed two minima but the locations of minima are around 30 and 150 degrees. The energy barriers from the equilibrium geometries to perpendicular conformations are different among these methods.

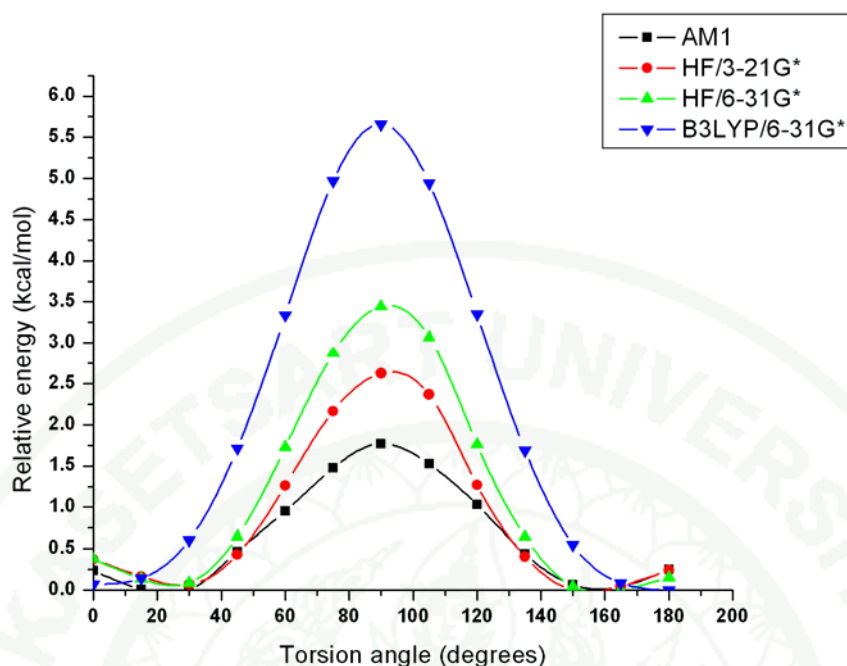


**Figure 5** Potential energy curves of torsional angle  $\Theta_1$  ( $\angle\text{C14-C15-C22-C23}$ ) obtained for  $\text{F}_2\text{V}$ . The curves were calculated by AM1, HF/3-21G(d), HF/6-31G(d) and B3LYP/6-31G(d) methods.

### 3. Ground State Geometry Optimization

Ground state geometries are optimized by the DFT method using the Becke three parameter hybrid (B3LYP) (Beck, 1993) and the second-order Møller–Plesset theory (MP2) (Møller and Plesset, 1934). The basis set 6-31G(d) was used (Gill *et al.*, 1992). The calculations are performed on Gaussian 03 program package (Frisch *et al.*, 2003). Furthermore, Geometry optimizations of fluorene-vinylene dimer ( $\text{F}_2\text{V}$ ) were carried out on Turbomole (5.7.1) program packages (Ahlich *et al.*, 1989). The DFT level using the resolution of the identity RI approximation (Weigend and Häser, 1997) with Perdew–Burke–Ernzerhof (Perdew *et al.*, 1996) (RI-PBE) functional was applied. The RI-CC2 (Christiansen *et al.*, 1995) method was applied for  $\text{F}_2\text{V}$  as well. The implementation of the resolution of the identity (RI) method allows the efficient treatment of larger molecules. The Dunning's basis sets SVP and TZVP were used (Dunning, T.H.Jr., 1971; Schäfer *et al.*, 1992; Schäfer *et al.*, 1994). Geometry parameters in term of bond lengths and bond torsion angles were collected. In general,

the bond lengths generated by these calculations were in good agreement with experimental values.

## **Excited State Calculation**

### **1. Excited State Structure**

The lowest singlet excited-state geometries of the fluorene-vinylene based oligomeric derivatives were optimized at TD-B3LYP/SVP levels of theory. All calculations were done using Turbomole version 5.7.1 program packages. For comparison, excited state properties were shown relatively with ground state parameters.

### **2. Electronic Property**

#### **2.1 HOMO-LUMO energy**

The HOMO-LUMO energy differences for fluorene-vinylene oligomers were calculated at B3LYP/6-31G(d) method and plotted against inverse chain length and extrapolated to zero which represented to the HOMO-LUMO energy gap of polymer at ground state electronic structure.

#### **2.2 Vertical Excitation Energy**

Since the energy gap is related to the lowest excitation energy of a polymer system, a recently developed tool, time-dependent density functional theory (TDDFT) was used to calculate the lowest excitation energy. The effects of substituent group on fluorine ring position were investigated. Vertical excitation energies (absorption energy) were computed with TD-B3LYP/SVP and TD-B3LYP/TZVP methods based on the ground state geometries and the results were compared with available experimental data. Polymer data are obtained from oligomer calculations by plotting the results against inverse chain length and extrapolating to

infinity (Andre' *et al.*, 1991). All calculations were done using the Gaussian 03 and Turbomole version 5.7.1 (Ahlrichs *et al.*, 1989) program packages.

### 2.3 Ionization Potential (IP) and Electron Affinity (EA)

Ionization Potential (IP) and Electron Affinity (EA) of all derivatives are computed by using B3LYP/6-31G(d) method. In this work, we have done IP and EA calculation of fluorene-vinylene derivatives by using the following equations

$$IP_{(eV)} = E_{\text{total (cation state with neutral opt.)}} - E_{\text{total (neutral opt.)}}$$

$$EA_{(eV)} = E_{\text{total (anion state with neutral opt.)}} - E_{\text{total (neutral opt.)}}$$

Where, neutral optimizations were done in B3LYP/6-31G(d) ground state optimizations. Then the single point calculations of cation and anion states based on those of optimal structures were followed by the same method. The IPs and EAs are obtained as functions of reciprocal chain length for the oligomers studies, with assumed linear extrapolation to infinite chain length.

### 2.4 Fluorescent Energy and Lifetime

In the fluorescence process, a molecule absorbs a photon and, after a certain delay, emits a photon of (generally) longer wavelength. Typically, both the absorbed and emitted photons are in the visible spectrum, but ultraviolet and infrared wavelengths are also possible. Molecules displaying this behavior (fluorophores) are usually rather complex organic chemicals. When the fluorescence process is repeated, the time delay between the absorption and the emission of a photon varies statistically for a fluorophore molecule. The average time delay is called the fluorescence lifetime, denoted by  $\tau$ . If a large number of fluorophore molecules are illuminated by a short pulse of light (Dirac pulse) at time  $t = 0$ , the intensity of the emitted fluorescence will vary according to



$$I(t) = I_0 \exp\left(-\frac{t}{\tau}\right), \quad t \geq 0$$

The fluorescence transition was obtained as the vertical de-excitation at the  $S_1$  optimized geometry (TD-B3LYP/SVP) of the excited state. As a result, the radiative lifetimes were also predicted. Radiative lifetimes were calculated on the basis of fluorescence energy and oscillator strengths according to the formula from Brandsen *et al.* (1983) (in au),

Fluorescence lifetime provides information useful in discrimination of particles. Extension of the conjugated backbone leads to a decrease of lifetimes.

## RESULTS AND DISCUSSION

### Ground State Calculation

#### 1. Conformational Analysis

Potential energy curves for rotation on bond 14 (see Figure 3) were obtained by calculating the variation of the total energy of F<sub>2</sub>V molecule with torsion angle  $\Theta_1$  (between the bonds 12, 14 and 15). The changes of rotation are in range of 0 to 180 degrees in interval of 10 degrees. From Karpfen *et al.* (1997) study, various conjugated and non-conjugated systems were investigated theoretically. They reported that the electron correlation contributions are largely different at various torsion angles due to the partial bond breaking of conjugated single bonds by internal rotation. The highest perpendicular barrier of bifluorenevinylene obtained by B3LYP calculations were attributed to the overestimation of the stability of the planar  $\pi$  systems by DFT methods. On the other hands, Bongini and Bottoni (1999) pointed out that the DFT approach provides a good description of the conformational properties of oligo and polythiophenes, which is in satisfactory agreement with the experimental evidence. Therefore, it will be useful to examine the potential energy and also structural parameters of fluorene-vinylene based molecules with B3LYP functional method.

The potential energy surface (PES) of bifluorene-vinylene obtained from B3LYP/6-31G(d) method is shown in Figure 6. Based on PES, minimum corresponds to an equilibrium structure, two minima around the planar conformations (0° and 180°) are observed. Consequently, the optimal inter-ring dihedral angles of fluorene-vinylene based oligomers are found to be planar (as shown in Table 5). We note that the similar shape of potential and barrier location with  $\Delta E = 0.22$  eV (5.0 kcal.mol<sup>-1</sup>) were obtained for the torsion of phenylene ring around the vinylene single bond at the B3LYP/cc-pVDZ theoretical level (Kwasniewski et al., 2003).

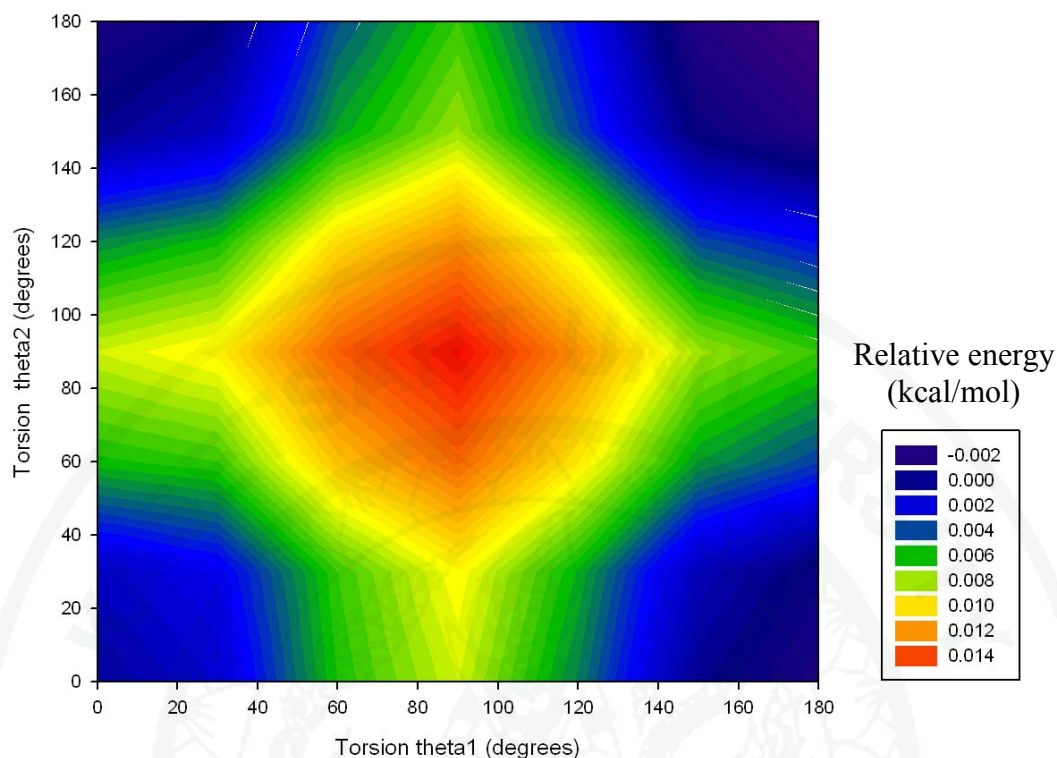


**Figure 6** Potential energy surface (PES) of torsional angle  $\theta_1$  ( $\angle\text{C14-C15-C22-C23}$ ) and  $\theta_2$  ( $\angle\text{C29-C28-C23-C22}$ ) obtained for  $\text{F}_2\text{V}$ . The curves were calculated by B3LYP/6-31G(d) methods.

Potential energy curves of all substituted compounds were shown in Figure 7 and 8. Torsion potential energy calculations were performed at B3LYP/6-31G(d) method. The presence of substituent groups decreased the energy barrier for the torsion of phenylene ring around the vinylene single bond. The presence of substituents groups on vinylene bridge give the structures which are stable in twisted form. The obtained potential curves exhibit two non-planar minima corresponding to the most stable *trans* or *cis* conformations. In the case of symmetric substitutions, the most stable conformation of  $\text{F}_2\text{V}$ ,  $\text{F}_2\text{V}-(\text{CN})_2$ ,  $\text{F}_2\text{V}-(\text{NH}_2)_2$ ,  $\text{F}_2\text{V}-(\text{OCH}_3)_2$ ,  $\text{F}_2\text{V}-(\text{OH})_2$  are at 180, 38, 150, 150, 35 degrees.

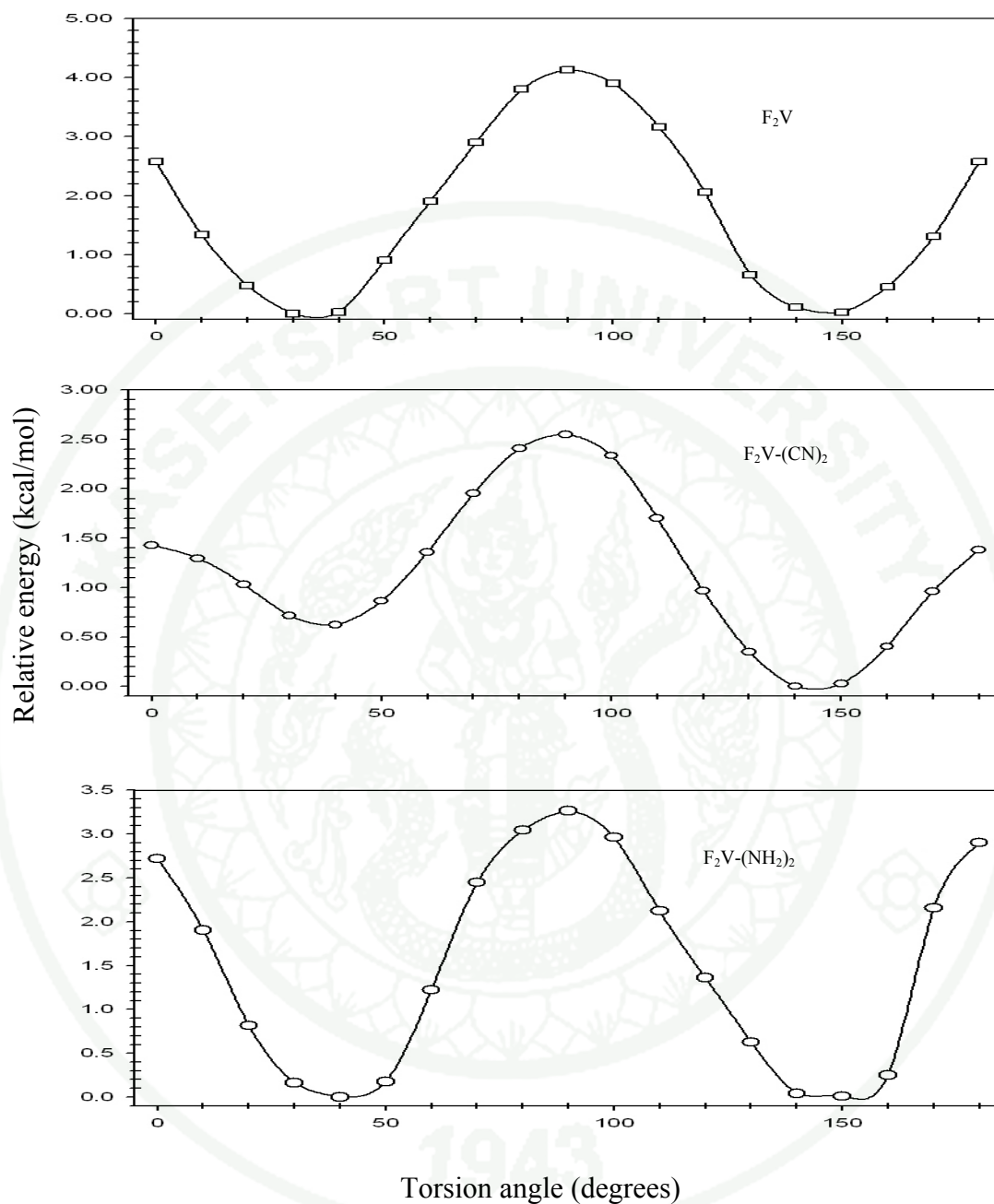


**Figure 7** One-dimensional dependence of the electronic ground state and vertically excited energies of studied symmetric systems on the torsion calculated at the B3LYP/6-31G(d) theoretical level.

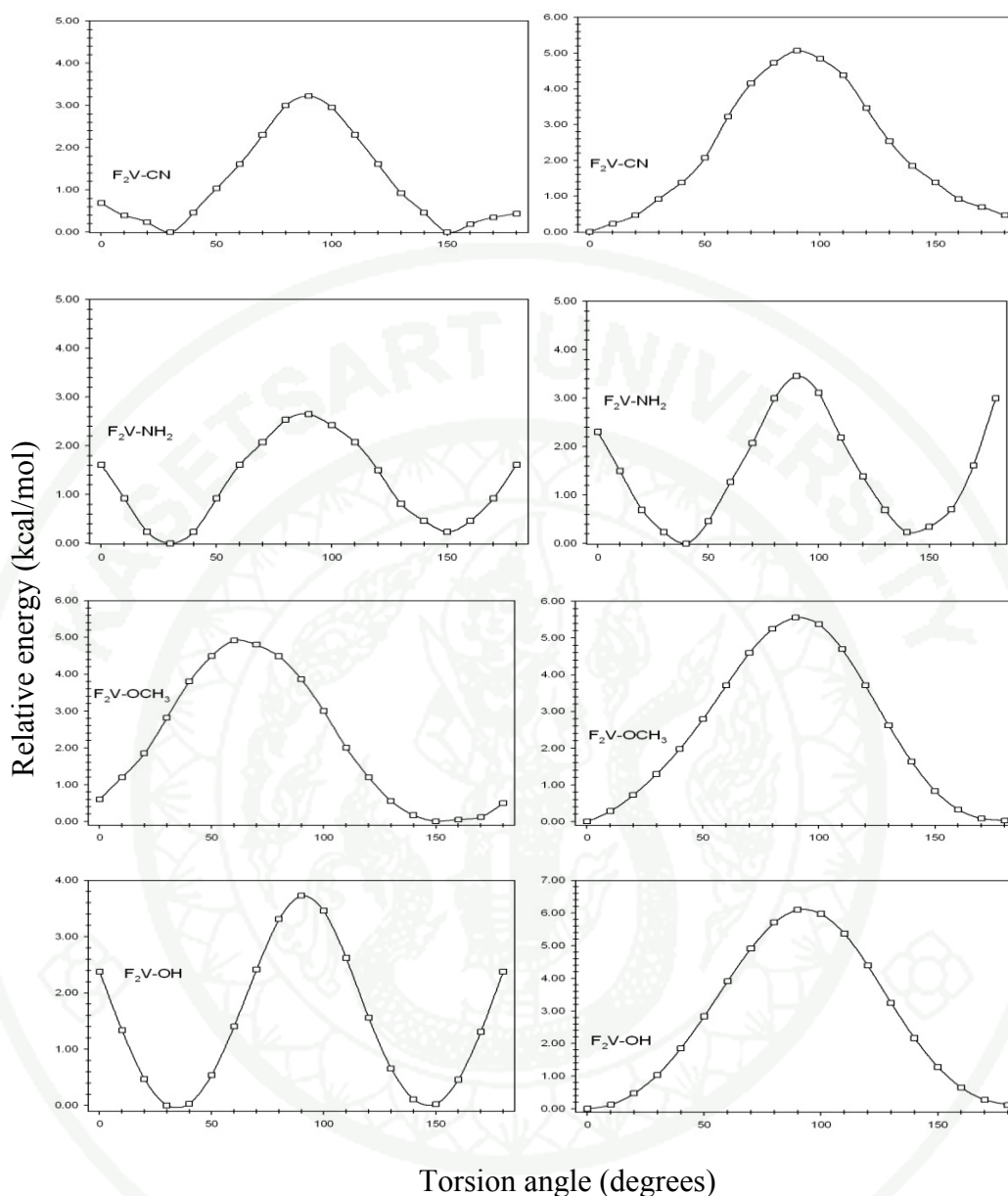


**Figure 8** One-dimensional dependence of the electronic ground state and vertically excited energies of studied asymmetric systems on the torsion calculated at the B3LYP/6-31G(d) theoretical level.

As can be seen in Figure 8, the torsional potential curves around the angles  $\Theta_1$  and  $\Theta_2$  exhibit ca two-times lower energy barriers for perpendicular arrangement than in the case of planar ones. The electronic ground state potential curves for mono-substituted molecules around the second dihedral angle  $\Theta_2$  have different shape. For the  $F_2V-CN$  molecule, the shape is similar to the potential curve of non-substituted



F<sub>2</sub>V molecule. The different situation is for the electron donor substituted molecules. The evaluated curve copies the shape of the dependence around the first dihedral angle except OH substitution. It seems that the strong electron-donor groups are able directly to affect through the double bond no. 15 the torsional motion on the opposite molecular side.

## 2. Ground stated geometry optimization.

In order to understand structural properties of the fluorene-vinylene copolymer and its derivatives, comparison between the ground state geometries in terms of bond lengths and torsionals angle was investigated. Molecular structure of fluorene-vinylene unit with the bond numbering is displayed in Figure 3. Optimized ground state geometries of F<sub>2</sub>V calculated by RI-PBE/SVP, B3LYP/6-31G(d), RI-CC2/SVP and MP2/6-31G(d) methods are displayed in Figure 9. The B3LYP/6-31G(d) and MP2/6-31G(d) method were calculated by G03 program and the other methods were calculated by Turbomole (5.7.1). According to these results, bond distances of F<sub>2</sub>V obtained from these methods are not significantly different. RI-CC2 method provides the shortest bond lengths in fluorene subunit and double bond (bond number 15) in vinyl unit while the single bond characters which are the inter-ring bond distances (bond number 14 and 16) and bond distances between two phenyl rings of fluorene subunit (bonds 7 and 23) are the longest. Bond lengths obtained from RI-PBE method shows the contrary behavior to those of RI-CC2. The bond distances gained from B3LYP method are in between those of others. Finally, MP2 bond distances are similar to the bonds obtained from the other methods.

Unfortunately, from our knowledge, there is no x-ray structure of fluorene-vinylene oligomer or polymer available in literature. Therefore, for the sake of comparison, we used x-ray structure of polyfluorene (Kawana *et al.*, 2002) as reference. Figure 9 indicated that bond distances obtained from these three methods are not significantly different to the x-ray distance. Due to limitation of computational time and resources, RI-CC2 method might not be an effective tool for the further

evaluations. Our calculated results indicated that B3LYP method with 6-31G(d) basis is the appropriated method for the further geometry optimizations.

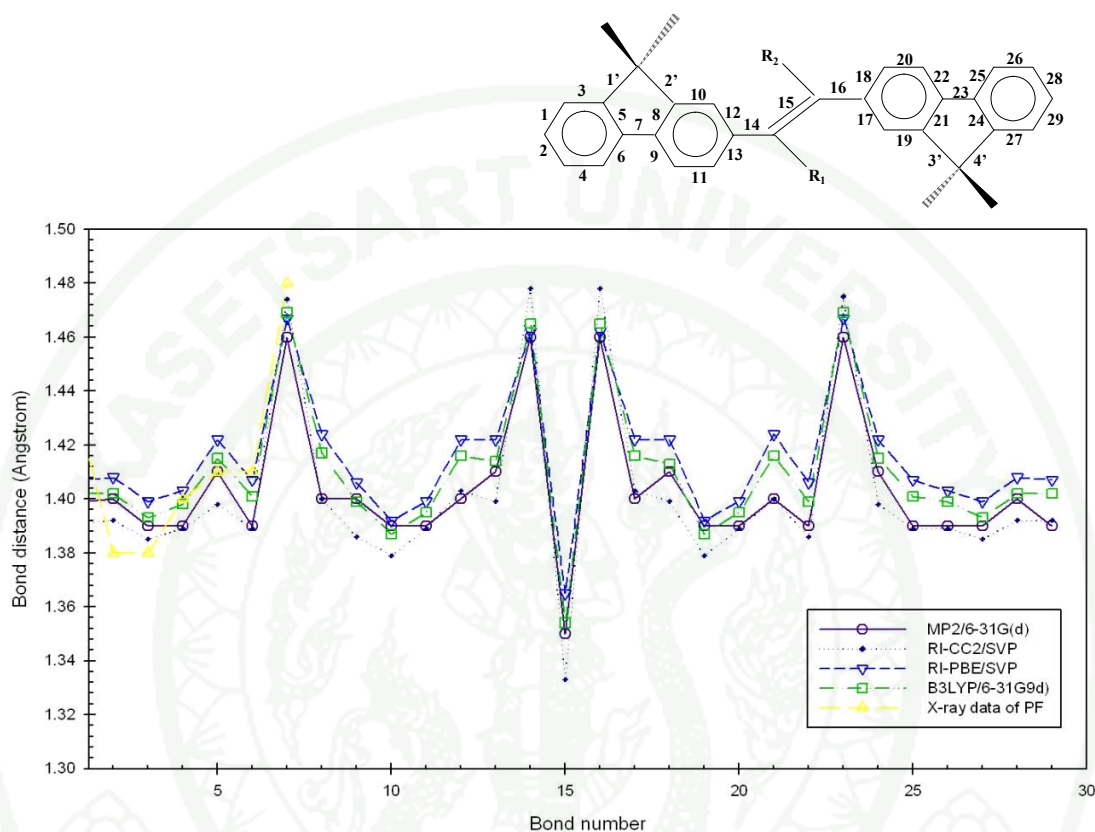
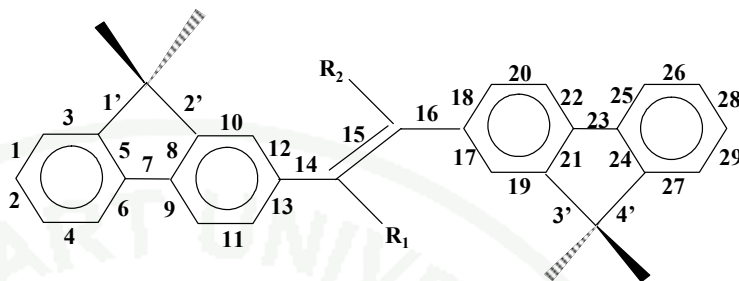


**Figure 9** Optimized bond lengths (in Å ) of F<sub>2</sub>V obtained from MP2/6-31G(d), RI-CC2/SVP, RI-PBE/SVP and B3LYP/6-31G(d) methods.

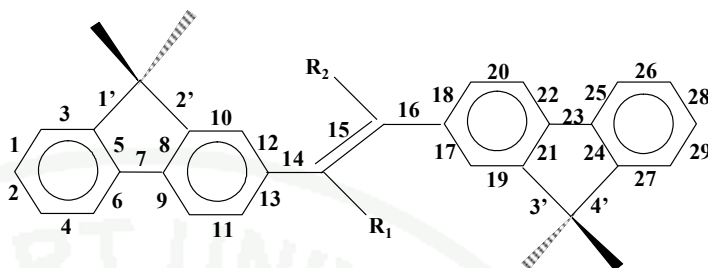
Then, geometries of the dimer of fluorene-vinylene (F<sub>2</sub>V) and its derivatives as fundamental models were analyzed and depicted in Table 1 and Table 2. The mutual comparison of optimal all-trans ground state <sup>1</sup>A geometries in terms of bond lengths and torsional angles can help us to understand the structural and energetic differences between the studied systems. The obtained minima were checked by the normal mode analysis. There are no imaginary frequencies for all optimal geometries at the present B3LYP/6-31G(d) level. This implied that the molecular structures might be the minimal structures.

**Table 1** Optimal bond lengths (in Å) for asymmetric substitution systems, obtained from B3LYP/6-31G(d) calculations.



Bond number	B3LYP/6-31G(d)					
	F <sub>2</sub> V	F <sub>2</sub> V-CN	F <sub>2</sub> V-NH <sub>2</sub>	F <sub>2</sub> V-OCH <sub>3</sub>	F <sub>2</sub> V-OH	F <sub>2</sub> V-CNN-H <sub>2</sub>
1	1.402	1.402	1.402	1.402	1.402	1.402
2	1.402	1.402	1.402	1.402	1.402	1.402
3	1.393	1.393	1.393	1.393	1.393	1.393
4	1.398	1.398	1.399	1.398	1.398	1.398
5	1.415	1.414	1.414	1.414	1.415	1.414
6	1.401	1.400	1.400	1.400	1.400	1.400
7	1.469	1.469	1.470	1.469	1.469	1.469
8	1.417	1.414	1.414	1.414	1.414	1.414
9	1.399	1.399	1.399	1.400	1.399	1.399
10	1.387	1.389	1.390	1.390	1.389	1.389
11	1.395	1.395	1.397	1.395	1.396	1.395
12	1.416	1.413	1.412	1.412	1.412	1.415
13	1.414	1.412	1.413	1.413	1.412	1.412
14	1.465	1.490	1.489	1.484	1.478	1.492
15	1.354	1.368	1.366	1.358	1.363	1.379
16	1.465	1.459	1.465	1.464	1.466	1.485
17	1.416	1.418	1.418	1.417	1.419	1.410
18	1.413	1.419	1.419	1.417	1.417	1.405
19	1.387	1.387	1.392	1.389	1.392	1.385
20	1.395	1.392	1.392	1.393	1.393	1.394
21	1.416	1.416	1.411	1.414	1.412	1.410
22	1.399	1.400	1.402	1.400	1.401	1.402
23	1.469	1.467	1.468	1.468	1.469	1.468
24	1.415	1.415	1.415	1.415	1.415	1.415
25	1.401	1.401	1.400	1.400	1.400	1.390
26	1.399	1.398	1.399	1.399	1.399	1.396
27	1.393	1.394	1.393	1.393	1.393	1.397
28	1.402	1.403	1.402	1.402	1.402	1.402
29	1.402	1.402	1.402	1.402	1.402	1.402

**Table 2** Optimal bond lengths (in Å) for symmetric substitution systems, obtained from B3LYP/6-31G(d) calculations.



Bond number	B3LYP/6-31G(d)				
	F <sub>2</sub> V	F <sub>2</sub> V-(CN) <sub>2</sub>	F <sub>2</sub> V-(NH <sub>2</sub> ) <sub>2</sub>	F <sub>2</sub> V-(OCH <sub>3</sub> ) <sub>2</sub>	F <sub>2</sub> V-(OH) <sub>2</sub>
1	1.402	1.401	1.402	1.402	1.402
2	1.402	1.403	1.402	1.402	1.402
3	1.393	1.394	1.394	1.393	1.393
4	1.398	1.398	1.399	1.399	1.399
5	1.415	1.414	1.415	1.415	1.415
6	1.401	1.400	1.400	1.400	1.400
7	1.469	1.468	1.469	1.468	1.468
8	1.417	1.414	1.412	1.413	1.414
9	1.399	1.400	1.400	1.399	1.398
10	1.387	1.389	1.392	1.390	1.389
11	1.395	1.394	1.395	1.395	1.395
12	1.416	1.412	1.414	1.414	1.415
13	1.414	1.414	1.415	1.415	1.417
14	1.465	1.488	1.486	1.484	1.478
15	1.354	1.379	1.372	1.365	1.367
16	1.465	1.488	1.486	1.484	1.478
17	1.416	1.412	1.414	1.414	1.415
18	1.413	1.414	1.415	1.415	1.417
19	1.387	1.389	1.392	1.390	1.389
20	1.395	1.393	1.395	1.395	1.395
21	1.416	1.414	1.412	1.413	1.414
22	1.399	1.400	1.401	1.399	1.399
23	1.469	1.468	1.469	1.468	1.468
24	1.415	1.414	1.415	1.415	1.415
25	1.401	1.400	1.400	1.400	1.400
26	1.399	1.398	1.399	1.399	1.399
27	1.393	1.394	1.394	1.393	1.393
28	1.402	1.403	1.402	1.402	1.402
29	1.402	1.401	1.402	1.402	1.402

According to the ground state optimized geometries of the derivatives, based on B3LYP/6-31G(d) calculation, the changes of atomic bond lengths of all derivatives (Figure 10 and 11) were compared to the fluorene-vinylene dimer. In all cases the smallest C–C bond distances are located in the central part of the fluorene rings (see bond numbers 3, 10, 19 and 27) and of the double bond on the vinylene bridge (see bond number 15). The largest bond lengths are found for the bond distances between two phenyl rings of fluorene subunit (bonds 7 and 23) which have a larger single bond character than the others. The single bonds 14 and 16 on vinylene bridge exhibit also the largest distances. The substitution of vinylene bridge affects only the bonds in the vicinity of added group, especially the bonds of vinylene bridge. The double bond number 15 and the neighbouring single bonds 14 and 16 are elongated while the bonds on rigid fluorene rings are very slightly shortened. Our calculations indicate that the differences in bond length changes for electron-withdrawing and electron-donating substitutions are significant only for vinylene bridge position. The most significant bond length differences were found to be at the inter-ring (in bond number 14 and 16) and the vinylene double bond (in bond number 15) of all *trans*-derivatives. The electron-withdrawing (CN) substitution elongates the bond length of about 0.03 Å while the electron-donating groups (NH<sub>2</sub>, OCH<sub>3</sub>, and OH) changed it only by 0.02 Å with respect to the F<sub>2</sub>V molecule. For the others, small extensions are in the range of 0.005 Å corresponding to both asymmetric and symmetric substitutions. Changing of bond distances are varied in the similar pattern even the molecules have different substituent groups. In comparison with mono-substituted molecules, the double bond on vinyl position of di-substituted molecules is more elongated. From these results we might say that substituents on vinyl position has a slightly affect to the bond distances.



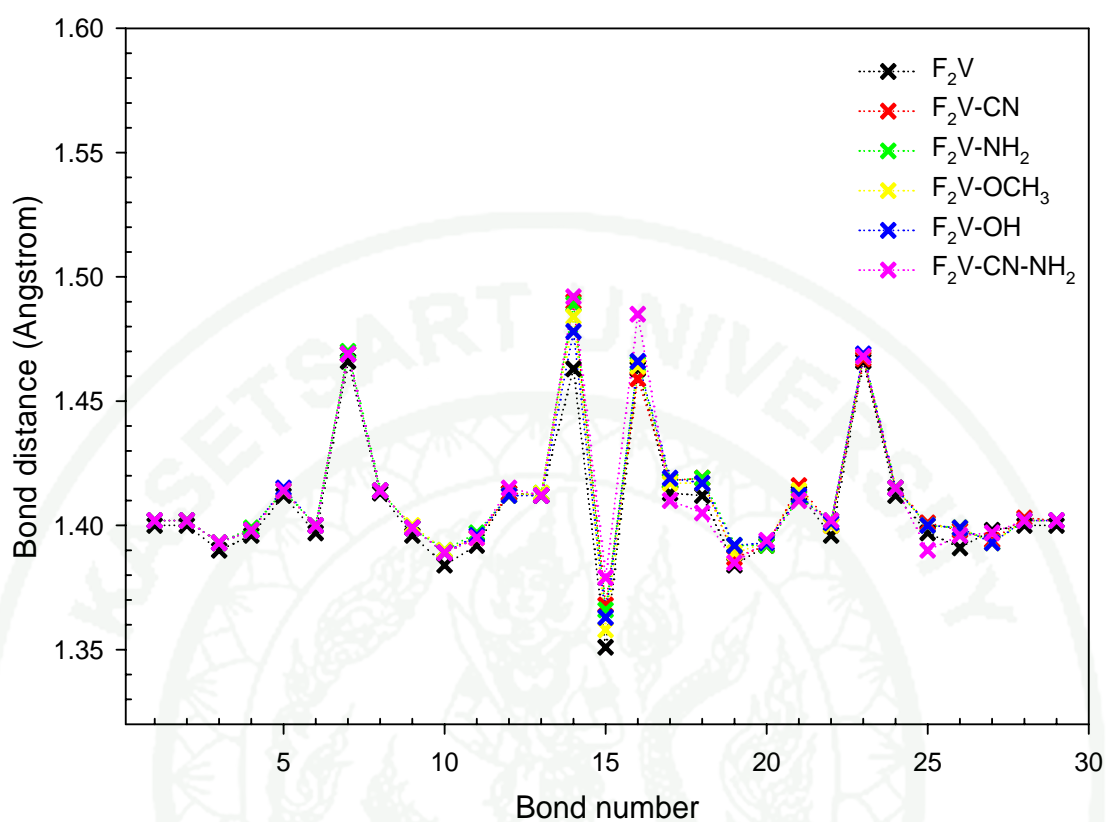


**Figure 10** Computed B3LYP/6-31G(d) bond lengths of the asymmetric substitution molecules under study. For notation see Figure 3.

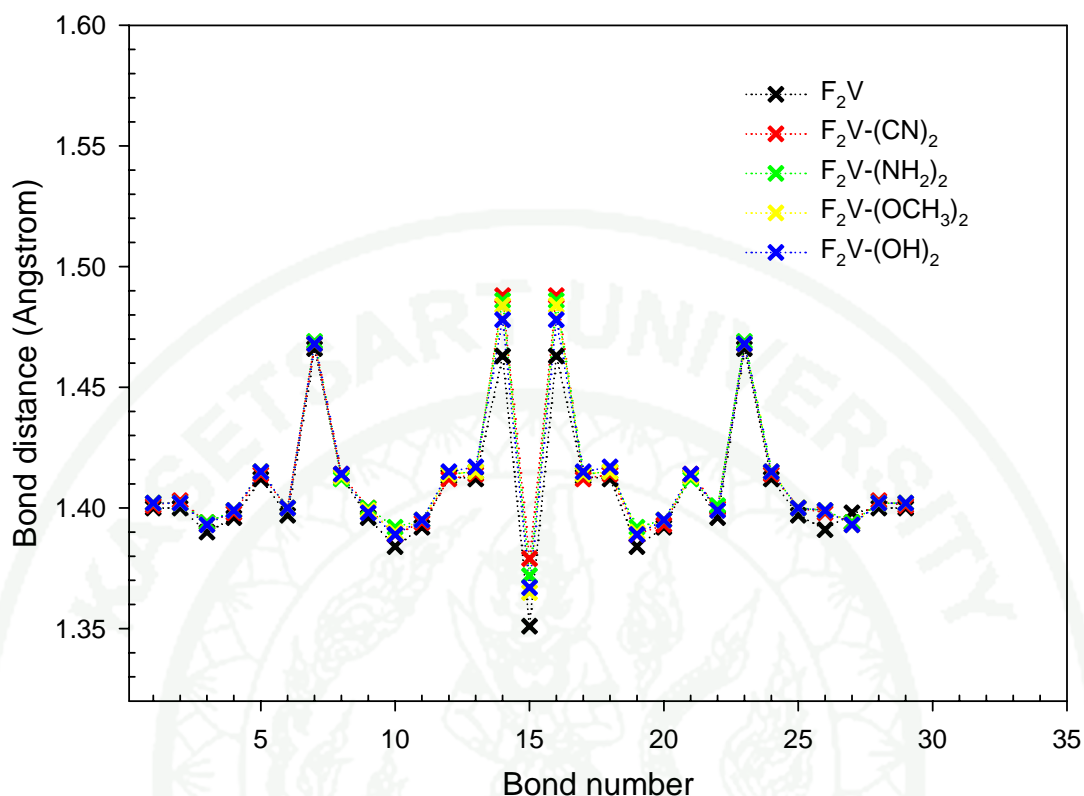


**Figure 11** Computed B3LYP/6-31G(d) bond lengths of the symmetric substitution molecules under study. For notation see Figure 3.

Next, considering similar structural properties of fluorene-vinylene oligomer, which extend from dimer to pentamer, the models were analyzed and compared based on optimized geometries of the ground state to study the chain length dependence on the oligomer bond length. Bond lengths of fluorene-vinylene oligomers obtained from B3LYP/6-31G(d) are shown in Figure 12 as an illustrated model. Yang, *et al.* (1996) calculated the structures of three series of copolymeric polyfluorene by B3LYP/6-31G(d) method and they found that the bond lengths and bond angles do not suffer appreciable variation with the oligomer size.

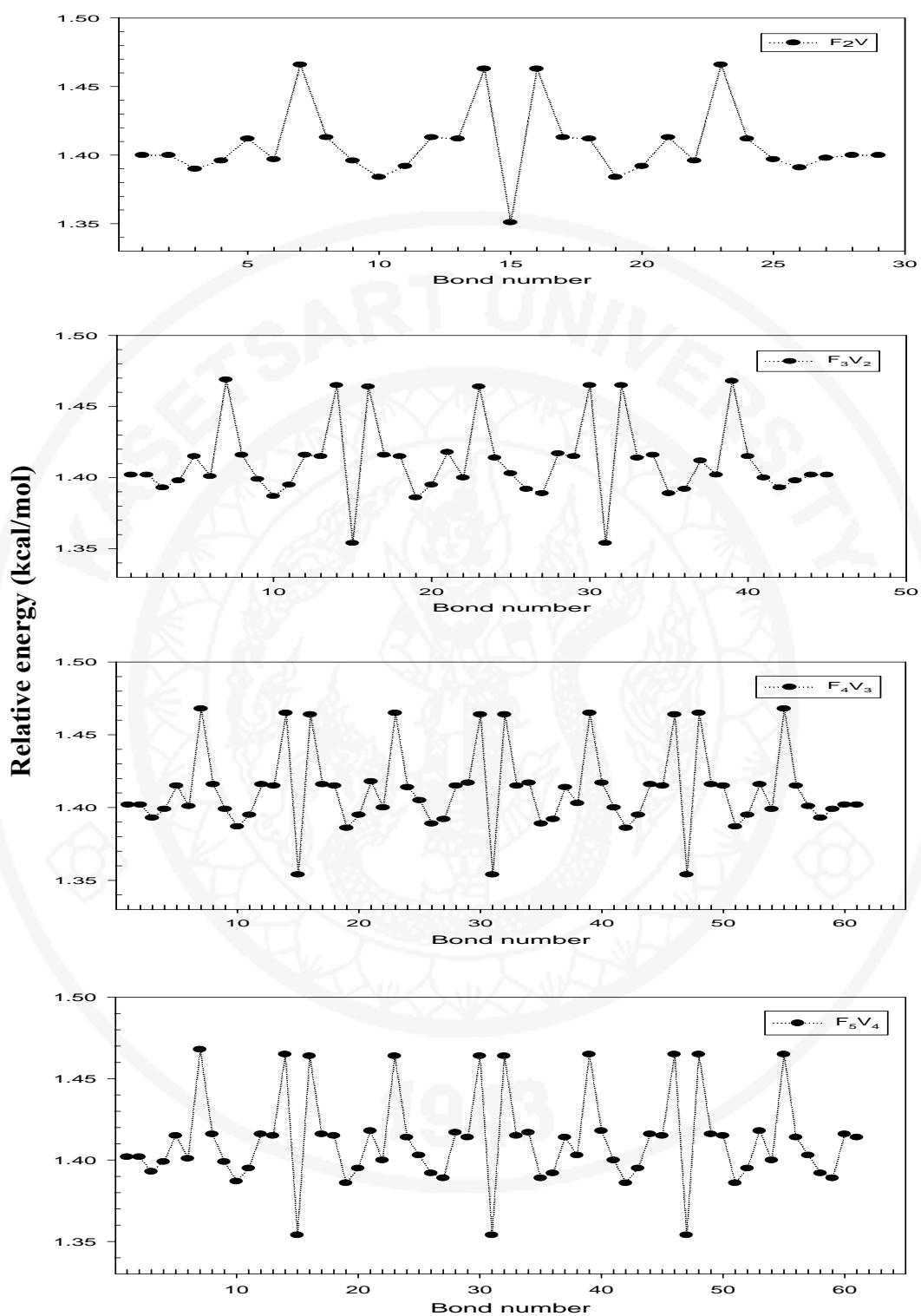


**Figure 12** Optimized bond distances of  $F_nV_m$  ( $n=2-5$  and  $m=1-4$ ) as obtained from B3LYP/6-31G(d) calculations, bond distances are given in Å unit (Y axis).

Corresponding to their results, it was found that the bond length does not display significantly variation with the oligomer size in the series of  $F_nV_m$ . Lukes *et al.* (2005, 2007) indicated that the elongation of the molecular chain leads only to small changes in the inter-ring distances of p-phenylene oligomers and the largest change occurs for a terminal ring becoming an inner one. From Chidthong *et al.* (2007) study, it was found that the inter-ring bond distances do not display appreciable variation with the oligomer size in the series of  $(FPy)_n$ . Moreover, the bond-changing pattern is varied systematically when molecular chain is elongated. These behaviors have been also found in the case of fluorene-vinylene oligomer and its derivatives. Therefore, one might said that the basic structures of the polymer can be described as their oligomers.

The data collected in Table 3 show that the dependence of the dihedral angles  $\Theta_1$  (between the bonds 12, 14 and 15) and  $\Theta_2$  (between the bonds 15, 16 and 17) between fluorene unit and the vinylene bridge on the substitution is significant. The B3LYP/6-31G(d) calculations indicate totally planar structure for the optimized  $F_2V$  molecule.

### 3. Bond Length Alternation (BLA)

Bond length changes in aromatic systems can also be described by bond length alternation (BLA) (Tretiak, *et al.*, 2002). The BLA values for selected molecular fragment can be defined as the differences in lengths between single and double bonds between non-hydrogen atoms. The positive (negative) sign of BLA indicates that the molecular unit has an aromatic (quinoid) isomer. With respect to this definition, the BLA value for central vinylene bridge may be evaluated as following

$$BLA = (d_{14} + d_{16}) - 2 d_{15},$$

where  $d$  symbols denote the bonds determined in Figure 3. As can be seen from data in Table 3, the mono-substitution with electron-withdrawing CN group leads to decrease of the BLA value by 0.006 Å with respect to the  $F_2V$  molecule. The next

presence of CN group has an additive influence on the BLA decrease. A small increase of BLA value is obtained for amino derivatives  $F_2V-NH_2$  and  $F_2V-(NH_2)_2$ . However, the increase of BLA for the  $F_2V-(NH_2)_2$  molecule is larger than two. For the push-pull system  $F_2V-CN-NH_2$ , the resulting influence of both groups has a compensate character. The BLA value is similar to the non-substituted  $F_2V$  molecule.

**Table 3** Optimal dihedral angles,  $\Theta_1$  (between the bonds 12, 14 and 15) and  $\Theta_2$  (between the bonds 15, 16 and 17), (in degrees) and BLA parameters (in Å) for *all-trans* conformations, obtained by B3-LYP/6-31G(d) calculations.

Molecule	$\Theta_1$	$\Theta_2$	BLA
$F_2V$	0	0	0.224
$F_2V-(CN)_2$	38	-38	0.218
$F_2V-(NH_2)_2$	45	-45	0.236
$F_2V-(OCH_3)_2$	32	-31	0.238
$F_2V-(OH)_2$	30	-30	0.222
$F_2V-CN$	28	-7	0.212
$F_2V-NH_2$	36	-31	0.227
$F_2V-OCH_3$	34	-7	0.232
$F_2V-OH$	25	31	0.218
$F_2V-CN-NH_2$	52	-44	0.223

According to the ground state and the lowest singlet excited state optimized geometries, based on B3LYP/6-31G(d) and TD-B3LYP/SVP calculations, respectively, the change of atomic bond length of all copolymer derivatives at ground state were compared to the fluorene-vinylene dimer as demonstrated in Figure 3.



## Excited State Calculation

### 1. Excited State Structure

The geometrical and energetic values are collected for the extremal points in Table 4. As can be seen in Figure 13, the non-substituted molecule  $F_2V$  has two planar minima and barrier for perpendicular arrangement ( $\Delta E = 0.245$  eV or  $5.65$  kcal.mol<sup>-1</sup>). We note that the similar shape of the potential and a barrier location with  $\Delta E = 0.22$  eV ( $5.0$  kcal.mol<sup>-1</sup>) were obtained for the torsion of phenylene ring around the vinylene single bond at the B3LYP/cc-pVDZ theoretical level (Kwasniewsky *et al.*, 2003). The presence of cyano or amino groups on vinylene bridge give structures which are stable in the twisted form. The obtained potential curves exhibit two non-planar minima corresponding to the most stable *trans* or *cis* conformations and two first-order saddle points. The most stable conformation of  $F_2V-(NH_2)_2$  molecule is at 45 degrees while the  $F_2V-(CN)_2$  molecule prefers *trans* conformation (144 degree). The mutual comparison of the energy barriers with respect to the  $F_2V$  molecule shows that the vinylene bridge substitution decreases the barrier at perpendicular arrangement. The cyano substitution decreases the barrier relative to  $F_2V$  by 0.092 eV (for  $F_2V-CN$ ) and by 0.128 eV (for  $F_2V-(CN)_2$ ). Although the amino substitution leads to the higher decrease of the perpendicular barrier relative to  $F_2V$  (0.108 eV for  $F_2V-NH_2$  and 0.169 eV for  $F_2V-(NH_2)_2$ ), the torsion at the planar arrangements is more restricted. The electronic ground state potential curves for mono-substituted molecules around the second dihedral angle  $\Theta_2$  have different shape. For the  $F_2V-CN$  molecule, the shape is similar to the potential curve of the non-substituted  $F_2V$  molecule. A different situation occurs for the  $F_2V-NH_2$  molecule. The second evaluated curve copies the shape of the dependence around the first dihedral angle. It seems that the strong electron-donor amino group is able directly to affect through the double bond no. 15 the torsional motion on the opposite molecular side. The mutual modification of the torsional potential with the amino or cyano groups is also observed for mixed  $F_2V-CN-NH_2$  molecule.

As can be seen in Figure 14, the torsional potential curves around the angles  $\Theta_1$  and  $\Theta_2$  exhibit two-times lower energy barriers for perpendicular arrangement than in the case of planar ones. In addition, the potential curve for the torsion around the angle  $\Theta_1$  (at the side of CN substitution) exhibits a more stable conformation at 132 degree. The energy difference with respect to the second minimum at 52 degree is 0.021 eV. This is a different situation that was presented for above mentioned potentials for  $F_2V-CN$  and  $F_2V-NH_2$  molecules. The discussed features may have therefore different but determining impact on the excitation-relaxation phenomena which may occur in various time-dependent optical experiments.

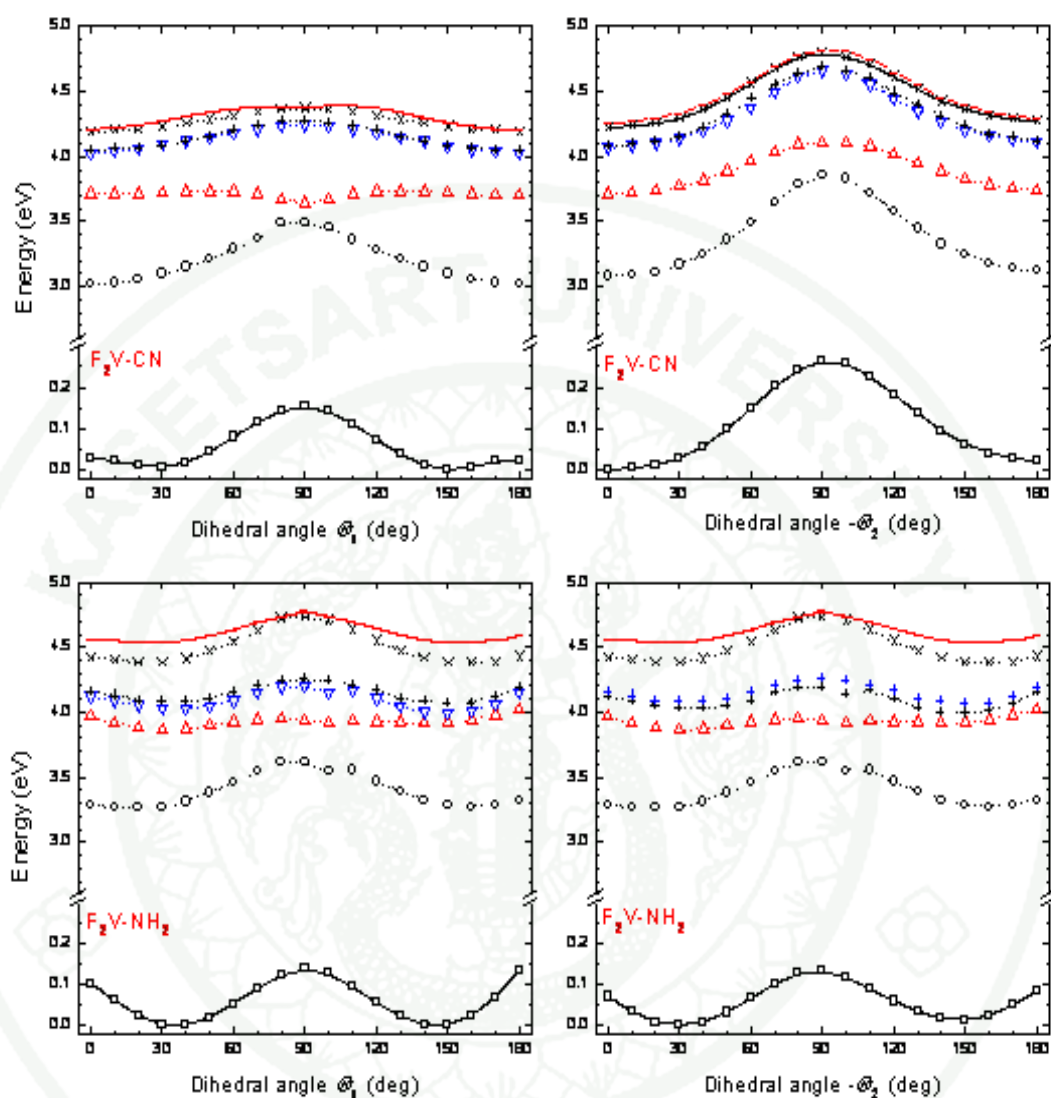


**Figure 13** One-dimensional dependence of the electronic ground state and vertically excited energies of the studied asymmetric systems on the torsion calculated at the B3LYP/6-31G(d) theoretical level. The ground-state energy minimum is taken as energy reference (see also Table 4). The open square denote electronic ground state and the next symbols indicate the first six excited states ( $S_1$ :  $\circ$ ;  $S_2$ :  $\Delta$ ;  $S_3$ :  $\nabla$ ;  $S_4$ :  $+$ ;  $S_5$ :  $\times$ ;  $S_6$ :  $-$ ).

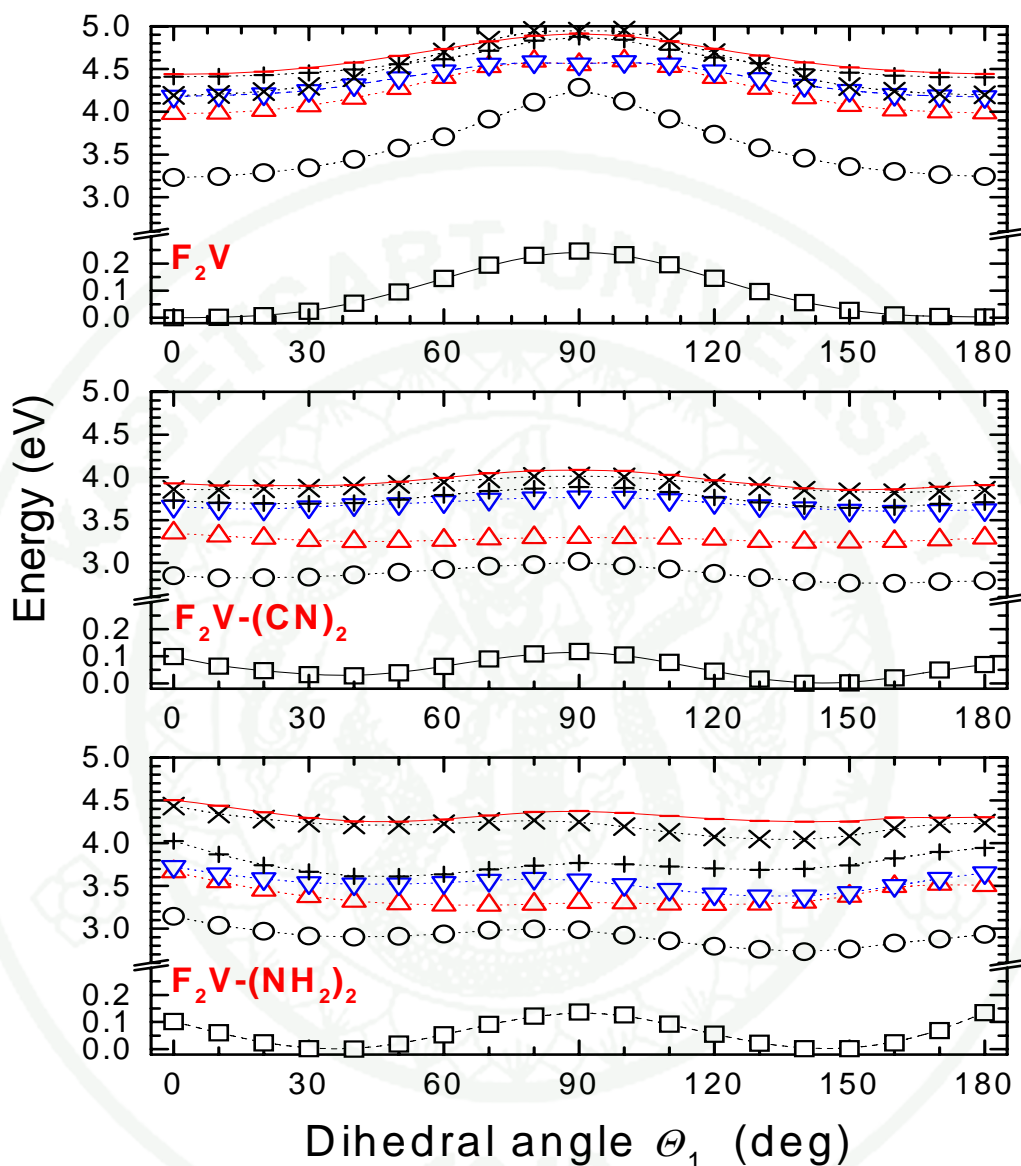


**Figure 14** One-dimensional dependence of the electronic ground state and vertically excited energies of studied symmetric systems on the torsion calculated at the B3LYP/6-31G(d) theoretical level. The ground-state energy minimum is taken as energy reference (see also Table 4). The open squares denote electronic ground state and the next symbols indicate the first six excited states (S1:  $\circ$ ; S2:  $\Delta$ ; S3:  $\nabla$ ; S4:  $+$ ; S5:  $\times$ ; S6:  $-$ ).

According to the ground state and the lowest singlet excited state optimized geometries, based on B3LYP/6-31G(d) and TD-B3LYP/SVP calculations, respectively, the change of atomic bond length of all copolymer derivatives at ground state were compared to the fluorene-vinylene dimer as demonstrated in Figure 15. The most significant bond length differences were found to be at the inter-ring (R14 and R16) and vinylene double bond (R15). For the others, small differences are in the range of  $\pm 0.005$  angstrom corresponding to all types of substituents. However, it was found that electron withdrawing substituents, such as CN group, make the inter-ring bonding much lengthening than a donating group ( $\text{NH}_2$ ,  $\text{OCH}_3$  and  $\text{OH}$ ) as compared with  $\text{F}_2\text{V}$ . In addition,  $\text{NH}_2$  substitution on vinylene unit can extend the inter-ring bonds (R14, R15 and R16). This might be due to the steric effect of  $\text{NH}_2$  group to a hydrogen atom on the fluorene unit and weak intramolecular hydrogen bonding occurred.

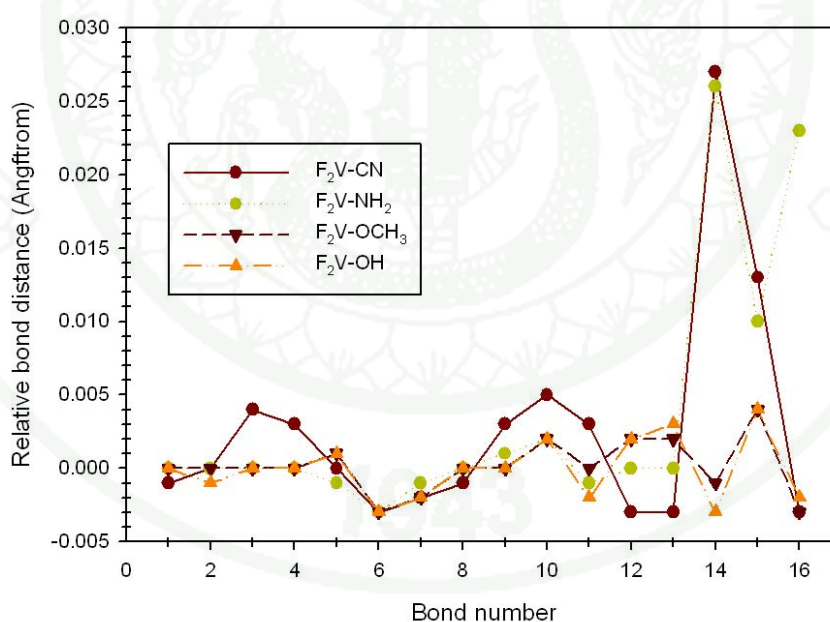


**Figure 15** Relative ground state and the first lowest excitation state bond lengths (in angstrom), calculated by B3LYP/6-31G(d) and TD-B3LYP/SVP methods, respectively, of the copolymer derivatives as compared to fluorene-vinylene dimer.



Comparison between all FV derivatives, all substituents can affect to the conjugation along polymer chain (Figure 16). The effect was due to steric hindrance and electronegativity of the substituent groups. Both electrons withdrawing (CN) and donating (NH<sub>2</sub>, OCH<sub>3</sub> and OH) groups can twist the inter-ring torsion angle by ca. 30 degrees. In addition, steric effect provides much more shift of torsion angle as found in the case of NH<sub>2</sub> and OCH<sub>3</sub> substituted groups. Especially in the case of F<sub>3</sub>V<sub>2</sub>-NH<sub>2</sub>, the ground state torsion angles are twisted both side of vinyl group (ground state:  $\phi_{F1-V1} = 150.3$  and  $\phi_{V1-F2} = 145.6$  degrees) and they are still unchanged after the excitation (excited state:  $\phi_{F1-V1} = 153.4$  and  $\phi_{V1-F2} = 144.2$  degrees). This steric effect on torsion of NH<sub>2</sub> substituent is also affected to inter-ring bonds that are stretched both side of vinyl group. From Chidthong, *et al.* (2007), it was found that excited state dihedral angles always shift to be planar or to the nearest planar structure. In our case, the results indicate that there are two types of changes which are corresponding to the type of substituent groups. Electron withdrawing groups (CN) make the inter-ring constrain even after excitation occurred as can be seen in the Figure 13 as there are slightly changes of torsion angles (less than 5 degrees). On the other hand, electron donating group (NH<sub>2</sub>, OCH<sub>3</sub> and OH) can handle only one side of torsion (torsion of F<sub>1</sub>-V<sub>1</sub> and F<sub>2</sub>-V<sub>2</sub> are tend to be close to planarity) while another side is about 150 degrees and can be shifted to near planar structure (165 degrees) after excitation process.

1943

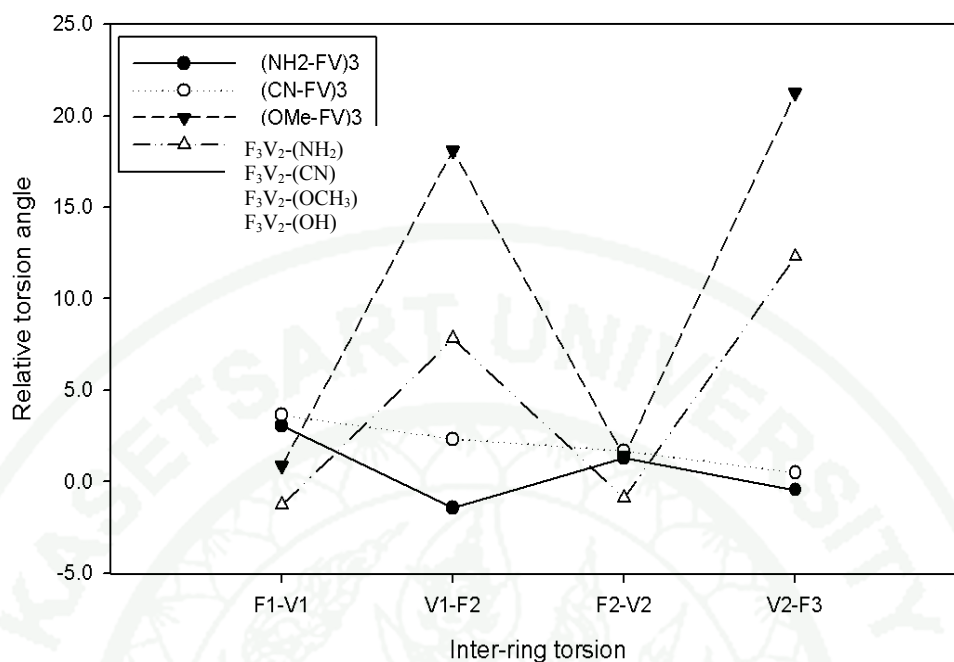


**Figure 16** Ground ( $S_0$ ) and excited ( $S_1$ ) states torsional angle changes (in degrees) of FV-derivatives. Optimized ground state geometries, calculated from B3LYP/6-31G(d) method and excited state geometries, by TD-B3LYP/SVP method.  $F_3V_2-NH_2$  is represented by solid circles,  $F_3V_2-CN$  by open circles,  $F_3V_2-OCH_3$  by solid triangles,  $F_3V_2-OH$  by open triangles.

**Table 4** Relative energies  $\Delta E$  and dihedral angles  $\Theta_1$  and  $\Theta_2$  of external points for torsional dependencies with respect to the most stable structure. The angles are in degrees and energies in eV or kcal/mol (values in parentheses).

Molecule	$\Theta_1$	$\Theta_2$	$\Delta E$
<b>F<sub>2</sub>V</b>	0	0	0.000 (0.00)
	90	0	0.245 (5.65)
	180	0	0.003 (0.07)
<b>F<sub>2</sub>V-(CN)<sub>2</sub></b>	0	-46	0.099 (2.28)
	38	-38	0.000 (0.00)
	90	-29	0.117 (2.70)
	144	-37	0.001 (0.02)
	180	-45	0.069 (1.59)
<b>F<sub>2</sub>V-(NH<sub>2</sub>)<sub>2</sub></b>	0	-57	0.224 (5.17)
	45	-45	0.000 (0.00)
	90	-39	0.076 (1.75)
	128	-37	0.038 (0.88)
	180	-45	0.298 (6.88)
<b>F<sub>2</sub>V-CN</b>	0	0	0.029 (0.67)
	28	-7	0.001 (0.02)
	90	0	0.153 (3.53)
	148	-7	0.000 (0.00)
	180	-1	0.024 (0.55)
	25	-90	0.293 (6.76)
	29	-180	0.049 (1.13)
<b>F<sub>2</sub>V-NH<sub>2</sub></b>	0	-31	0.102 (2.35)
	36	-31	0.000 (0.00)
	90	-28	0.137 (3.16)
	146	-24	0.002 (0.05)
	180	-38	0.134 (3.09)
	36	0	0.070 (1.61)
	35	-90	0.132 (3.04)
	35	-148	0.013 (0.30)
	39	-180	0.085 (1.96)

The chain length dependence on the oligomer torsion angles ( $\phi$ ), both at the ground and excited states was then investigated on fluorene-vinylene oligomers and its derivatives. Relative differences of the oligomer torsion angles were compared within the F<sub>n</sub>V<sub>m</sub> oligomers. The most interesting inter-ring torsional modes are the related torsions between vinylene and fluorene units (Table 5) along the oligomer

chain. Yang, *et al.* (2005) calculated the structures of three series of copolymeric polyfluorene by B3LYP/6-31G(d) method and they found that the bond lengths and bond angles do not suffer appreciable variation with the oligomer size. Corresponding to their results, it was found that the inter-ring dihedral does not display significantly variation with the oligomer size in the series of  $F_nV_m$ . The obtained results bring us to expect the polymer conformation by considering their oligomer geometries. Moreover, there is no remarkable change in the torsional angles between the two states. The vinylene unit apparently develops a good coplanarity with the fluorene unit in the alternating copolymer backbones. Ground state-torsion angles tend to slightly twist (around  $2^\circ$ - $3^\circ$ ) when increasing the chain length, whereas the excited state-torsion angles are thereby practically unaffected and keep a value of about  $180^\circ$ . This change is within the range of theoretical error.

**Table 5** Optimized inter-ring torsion angles,  $\phi$  (degrees) of  $F_nV_m$  ( $n=2-5$ ,  $m=1-4$ ) in the ground state ( $S_0$ ) and the lowest excited state ( $S_1$ ), obtained from B3LYP/6-31G(d) and TD-B3LYP/SVP calculations.

	Torsional angle, $\phi$ (degrees)							
	$F_2V$		$F_3V_2$		$F_4V_3$		$F_5V_4$	
	$S_0$	$S_1$	$S_0$	$S_1$	$S_0$	$S_1$	$S_0$	$S_1$
$F_1-V_1$	0	0.4	-0.4	0.8	-0.2	-0.3	-0.1	0
$V_1-F_2$	1.4	0.4	1.3	0.3	1	0.2	0.9	0.7
$F_2-V_2$			-179.2	-179.9	-179.4	-179.9	-179.5	-179.8
$V_2-F_3$			178.5	179.8	178.6	-180.0	178.7	179.4
$F_3-V_3$					0.5	0.2	0.4	0.3
$V_3-F_3$					-0.6	-0.2	-0.7	-0.4
$F_3-V_4$							178.8	179.8
$V_4-F_4$							-179.0	-179.7

## 2. HOMO-LUMO and Vertical Excitation Energy

In order to understand the physical origin of optical transitions for the selected excitation energies, it is useful to examine the relevant (highest) occupied and lowest unoccupied molecular orbitals that play a dominant role. As can be seen in Table 6, in all molecules for the lowest excitation energy, the electron is excited from the highest occupied molecular orbital (HOMO) to the lowest unoccupied molecular orbital (LUMO). This transition has  $\pi \rightarrow \pi^*$  character. However, the orbital presentation of the next transitions is different with respect to the substitution. As presented in Figure 17, the HOMO orbital of F<sub>2</sub>V molecule is located mostly on the double bond of vinylene bridge (bond no.15) and neighbouring bonds on fluorene units perpendicular oriented with respect to the chain (see bonds no. 12, 13 and 17, 18). The LUMO orbital is spread over the single bonds of vinylene bridge (bonds no. 14 and 16) and bonds on fluorene units which are oriented parallel with the molecular chain (see bonds no. 10, 11 and 19, 20). The presence of electron withdrawing cyano group in F<sub>2</sub>V-CN and F<sub>2</sub>V-(CN)<sub>2</sub> molecules increases the electron delocalization in HOMO over the fluorene units. On the other hand, the electron donating amino groups in F<sub>2</sub>V-NH<sub>2</sub> and F<sub>2</sub>V-(NH<sub>2</sub>)<sub>2</sub> molecules is responsible for the electron delocalization over the vinylene bond no. 15. The opposite situation is observed in the shape of LUMO orbitals for both types of derivatives. With respect to this fact, we can deduce that the optical transition for cyano derivatives is oriented from the fluorene units to the CN chromophore while for the amino derivatives it is spread from the central part to the fluorene units. This character is also reflected for the higher vertical excitations. The transitions from lower occupied orbitals to the LUMO orbital play important role for the CN derivatives. The transitions from HOMO orbital to the next unoccupied orbitals occur for the amino derivatives (see Table 6



**Table 6** The lowest excitation energies in eV and oscillator strengths (values in parentheses) for the optimal all-trans geometries. The values written in italics stand for the excitation contributions in percentage involved in each calculated transition (H denotes HOMO and L is LUMO).

Molecule	S <sub>1</sub>	S <sub>2</sub>	S <sub>3</sub>	S <sub>4</sub>	S <sub>5</sub>	S <sub>6</sub>	S <sub>7</sub>
<b>F<sub>2</sub>V</b>	3.23 (1.870) 99 %: H→L	3.98 (0.000) 60 %: H-1→L 38 %: H→L+1	4.18 (0.000) 50 %: H→L+3	4.19 (0.006) 68 %: H→L+2	4.41 (0.00) 43 %: H→L+2	4.44 (0.019) 33 %: H-2→L	4.44 (0.000) 60 %: H-3→L
<b>F<sub>2</sub>V-(CN)<sub>2</sub></b>	2.82 (0.907) 99 %: H→L	3.22 (0.000) 97 %: H-1→L	3.64 (0.009) 70 %: H-2→L	3.67 (0.000) 75 %: H-3→L	3.86 (0.004) 68 %: H-4→L	3.88 (0.000) 73 %: H-5→L	4.29 (0.336) 72 %: H-6→L
<b>F<sub>2</sub>V-(NH<sub>2</sub>)<sub>2</sub></b>	2.90 (0.586) 99 %: H→L	3.30 (0.000) 97 %: H→L+1	3.53 (0.009) 94 %: H→L+2	3.61 (0.000) 92 %: H→L+3	4.21 (0.016) 91 %: H→L+4	4.24 (0.000) 90 %: H→L+5	4.41 (0.713) 93 %: H-2→L+1
<b>F<sub>2</sub>V-CN</b>	3.08 (1.424) 99 %: H→L	3.72 (0.096) 91 %: H-1→L	4.08 (0.002) 98 %: H-2→L	4.08 (0.016) 62 %: H-3→L	4.22 (0.007) 42 %: H-5→L	4.26 (0.006) 44 %: H-4→L	4.39 (0.063) 75 %: H→L+1
<b>F<sub>2</sub>V-NH<sub>2</sub></b>	3.29 (1.099) 99 %: H→L	3.86 (0.251) 87 %: H→L+1	4.03 (0.013) 67 %: H→L+2	4.08 (0.021) 69 %: H→L+3	4.40 (0.079) 83 %: H-1→L	4.54 (0.023) 39 %: H→L+6	4.58 (0.027) 41 %: H→L+5

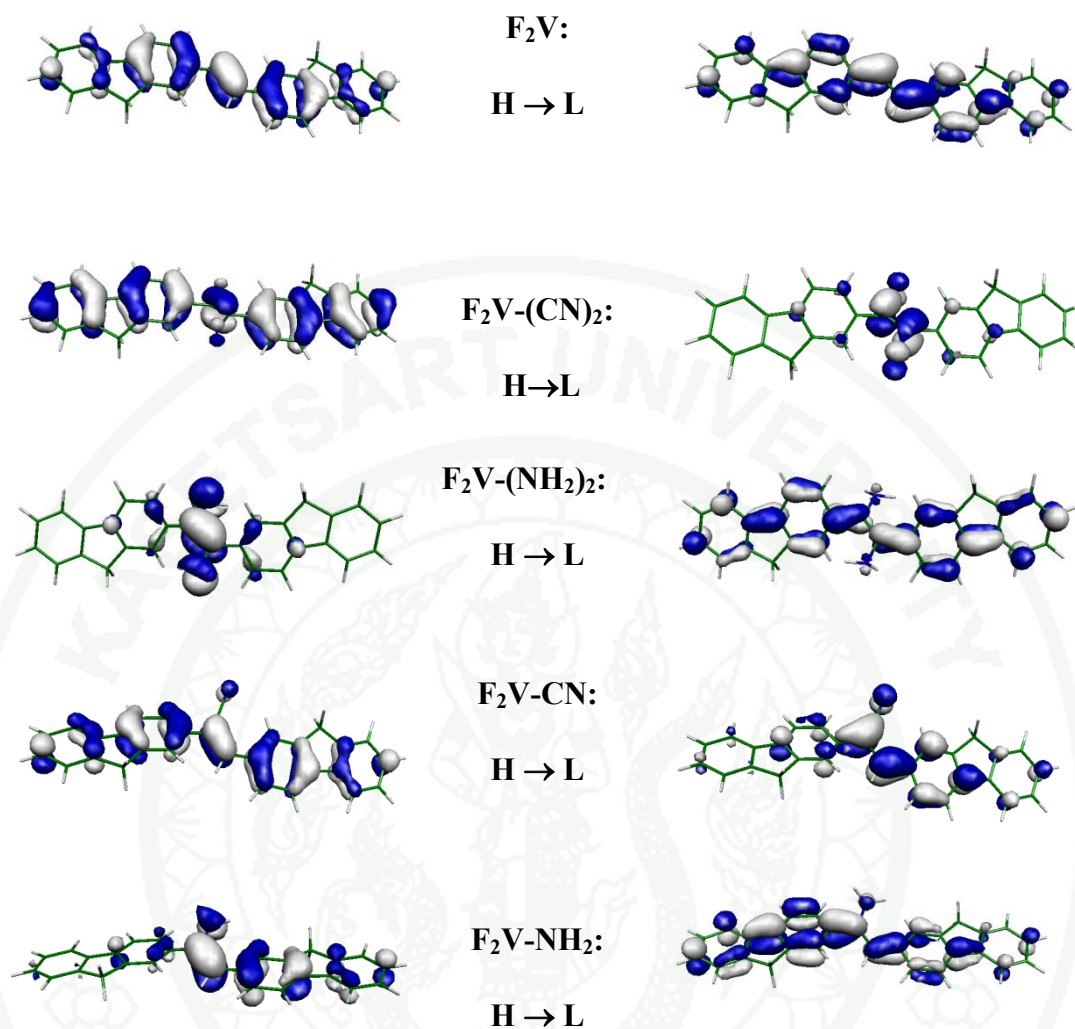


**Figure 17** Plots of the B3LYP/6-31G(d) molecular orbitals contributing significantly to the lowest energy transitions of studied molecules in *all-trans* conformation. H denotes HOMO and L is LUMO.

The B3LYP/6-31G(d) method was used on the basis of the ground state optimized structures to compute vertical electronic excitation energies, HOMO energies, and absorption spectra of all oligomers were investigated in this work (Table 7 and Figure 18). The vertical excitations energies with highest oscillator strength ( $\pi$ - $\pi^*$  transition) of each polymer calculated by TD-B3LYP/SVP and TD-B3LYP/TZVP methods were collected and extrapolated by linear regression technique. It was found that excitation energies of these materials are quite lower than the experimental data. There are 2.08 eV for  $F_nV_m$  and 2.40, 2.13, 2.41 and 2.24 eV for its derivatives,  $F_3V_2$ -CN,  $F_3V_2$ -NH<sub>2</sub>,  $F_3V_2$ -OCH<sub>3</sub> and  $F_3V_2$ -OH, respectively, which are calculated from TD-B3LYP/SVP method. The differences between experiment (Jin *et al.*, 2002; Jin *et al.*, 2003) and calculated energy gaps are slightly higher than standard criteria (0.3 eV) even the high basis set (TZVP) was used (2.19 eV for  $F_nV_m$  and 2.11, 2.37, 2.35 and 2.11 eV for its derivatives,  $F_3V_2$ -CN,  $F_3V_2$ -NH<sub>2</sub>,  $F_3V_2$ -OCH<sub>3</sub> and  $F_3V_2$ -OH, respectively). Corresponding to calculated excitation energies, absorption wavelengths calculated from TD-DFT method with both basis sets are much longer than those of experiments. Our results are in the same trend with studies of Geogieva *et al.* (2005). They varied the size of basis set in electronic calculation of coumarin system. The extension of basis set from SVP to TZVP leads to small decrease in excitation energy for  $\pi \rightarrow \pi^*$  transition and to an increase of the excitation energy for  $n \rightarrow \pi^*$  transition. Moreover, they compared the calculated energy gap in gas phase and in an aqueous solvent condition (with PCM model) as well. The presence of solvent can slightly decrease the energy gap of coumarin and gives a good agreement with experimental results.

Some reports suffered from this theoretical deviation, Hutchison *et al.* (2002, 2003) and Brocks *et al.* (1993) pointed out that density-functional theory (DFT) method within the local-density approximation (LDA) can compute equilibrium geometries in excellent agreement with experiments for both conjugated organic oligomers and polymers. However, DFT method calculated band gaps are typically on the order of 40% smaller than the experimental optical absorption band-gap data for conjugated

organic materials. polymers. Suramitr, *et al.* (2005) studied on oligophenylenevinylene derivatives and also found that extrapolated excitation energies calculated by TD-DFT are underestimated when compared to the experiment. However, there exist several successful investigations on the TD-DFT excitation energy prediction. Because the excitation energy of polymers depends on the planarity along chain length, polymers that suffered from the steric hindrance on the inter-ring position show higher energy (blue shift) than others. It can be clearly seen in the case of  $F_3V_2-NH_2$  and  $F_3V_2-OCH_3$ , the  $E_{exc}$  calculated from TD-B3LYP/SVP and TD-B3LYP/TZVP (values in parenthesis) methods are quite similar, 2.40(2.37), 2.41(2.35), respectively. Poolmee *et al.* (2004) performed the calculation on fluorene thiophene copolymer and they showed that TD-DFT excitation energies using DFT and AM1 optimized geometries provide a good energy gap due to the shortening inter-ring distance and planarity of oligomer structure.

**Table 7** Extrapolated excitation energy ( $E_{exc}$ ), oscillator strength ( $f$ ), HOMO energy, and absorption wavelength ( $\lambda_{abs}$ ) of the derivatives calculated from TD-B3LYP/SVP and TD-B3LYP/TZVP methods, the values in parenthesis are experimental results. Column 1 indicates the oligomers and polymers ( $n, m = \infty$ ) for different copolymers.

	TD-B3LYP/SVP				TD-B3LYP/TZVP			
	$E_{exc}$ (eV)	$f$	HOMO (eV)	$(\lambda_{abs})$ (nm.)	$E_{exc}$ (eV)	$f$	HOMO (eV)	$(\lambda_{abs})$ (nm.)
$F_n V_m$								
<i>dimer</i>	3.10 (3.08) <sup>c</sup>	2.11	-5.03 (-5.49) <sup>c</sup>	400.5 (368) <sup>c</sup>	3.01 (3.08) <sup>c</sup>	2.01	-5.25 (-5.49) <sup>c</sup>	411.2 (368) <sup>c</sup>
<i>trimer</i>	2.74 (2.83) <sup>c</sup>	3.20	-4.89 (-5.35) <sup>c</sup>	452.6 (398) <sup>c</sup>	2.67 (2.83) <sup>c</sup>	3.09	-5.09 (-5.35) <sup>c</sup>	463.6 (398) <sup>c</sup>
<i>tetramer</i>	2.57 (2.74) <sup>c</sup>	4.24	-4.83 (-5.34) <sup>c</sup>	481.1 (413) <sup>c</sup>	2.61 (2.74) <sup>c</sup>	4.10	-5.03 (-5.34) <sup>c</sup>	470.7 (413) <sup>c</sup>
<i>pentamer</i>	2.49 (2.69) <sup>c</sup>	5.29	-4.80 (-5.33) <sup>c</sup>	497.2 (419) <sup>c</sup>	2.52 (2.69) <sup>c</sup>	4.87	-5.09 (-5.33) <sup>c</sup>	492.7 (419) <sup>c</sup>
Eg ( $n, m = \infty$ )	2.08 (2.6) <sup>a</sup>				2.19 (2.6) <sup>a</sup>			
$F_n V_m$ -CN								
<i>dimer</i>	2.94	1.54	-5.59	421.3	2.88	1.48	-5.80	430.1
<i>trimer</i>	2.64	2.27	-5.52	468.8	2.60	2.19	-5.70	476.0
<i>tetramer</i>	2.52	3.06	-5.45	491.2	2.48	2.97	-5.65	499.3
<i>pentamer</i>	2.47	4.01	-5.44	502.7	2.43	3.89	-5.64	510.7
Eg ( $n, m = \infty$ )	2.13 (2.4) <sup>b</sup>				2.11 (2.4) <sup>b</sup>			
$F_n V_m$ -NH <sub>2</sub>								
<i>dimer</i>	3.31	1.18	-4.88	374.3	3.25	1.17	-5.11	381.6
<i>trimer</i>	3.00	1.99	-4.74	412.7	2.95	1.97	-4.97	419.9
<i>tetramer</i>	2.88	2.87	-4.68	430.1	2.83	2.84	-4.91	437.6
<i>pentamer</i>	2.75	3.50	-4.60	451.1	2.71	3.46	-4.82	458.2
Eg ( $n, m = \infty$ )	2.40				2.37			



**Table 7** (Continued)

	TD-B3LYP/SVP				TD-B3LYP/TZVP			
	$E_{exc}$ (eV)	$f$	HOMO (eV)	$(\lambda_{abs})$ (nm.)	$E_{exc}$ (eV)	$f$	HOMO (eV)	$(\lambda_{abs})$ (nm.)
$F_n V_m\text{-OCH}_3$								
<i>dimer</i>	3.18	1.95	-4.86	389.1	3.12	1.91	-5.08	396.7
<i>trimer</i>	2.90	2.76	-4.80	427.2	2.85	2.70	-5.02	435.2
<i>tetramer</i>	2.79	3.45	-4.83	443.8	2.74	3.38	-5.03	451.9
<i>pentamer</i>	2.73	4.33	-4.84	454.5	Na	Na	Na	Na
Eg ( $n,m = \infty$ )	2.41				2.35			
$F_n V_m\text{-OH}$								
<i>dimer</i>	3.21	1.32	-4.94	386.0	3.16	1.29	-5.17	292.1
<i>trimer</i>	2.84	2.04	-4.77	436.9	2.80	2.06	-5.00	442.6
<i>tetramer</i>	2.70	2.73	-4.70	458.3	2.67	2.76	-4.96	464.0
<i>pentamer</i>	2.65	3.61	-4.68	468.2	2.61	3.62	-4.91	474.3
Eg ( $n,m = \infty$ )	2.24				2.21			

<sup>a</sup> Jin *et al.*, 2002<sup>b</sup> Jin *et al.*, 2003<sup>c</sup> Lui *et al.*, 2007

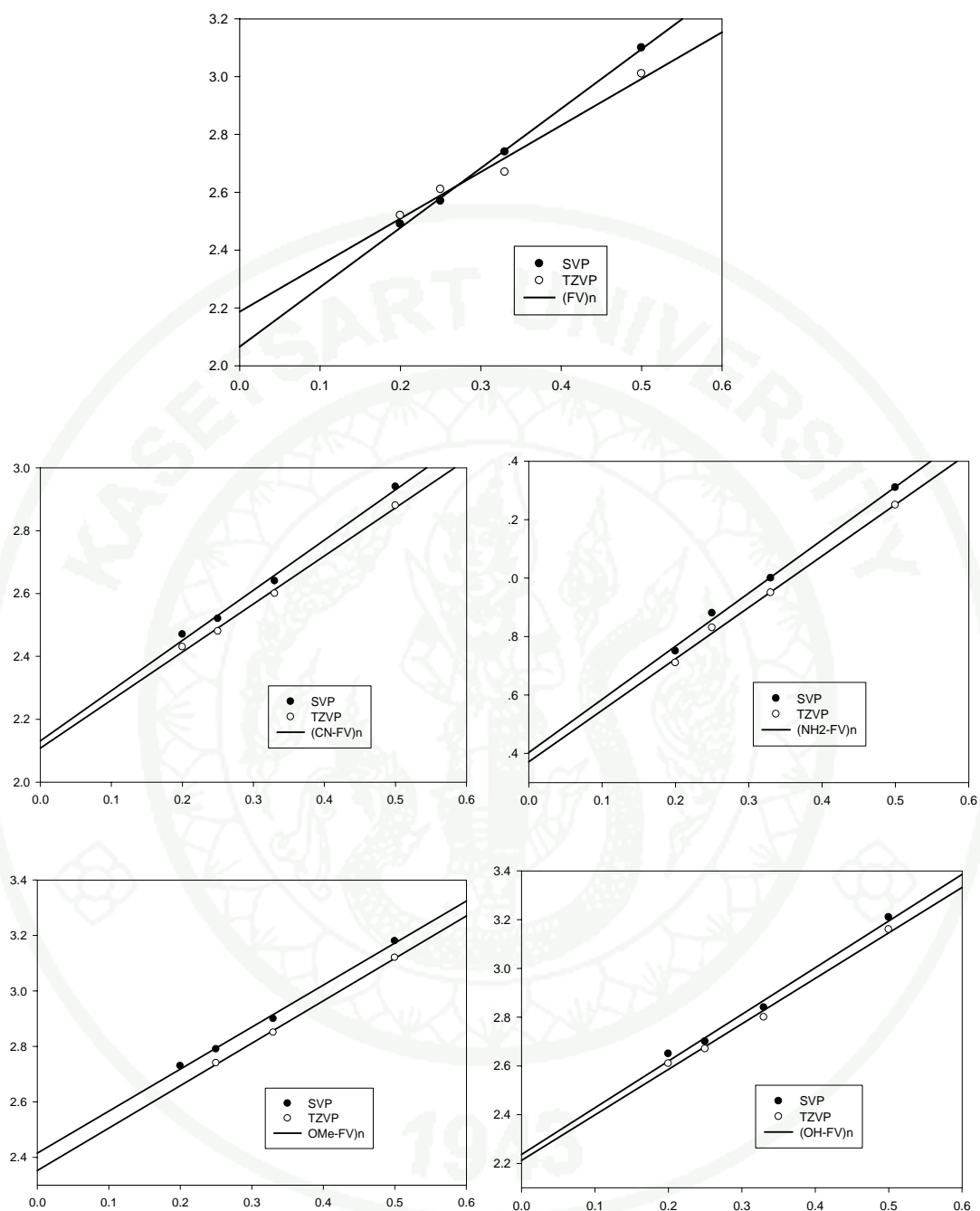
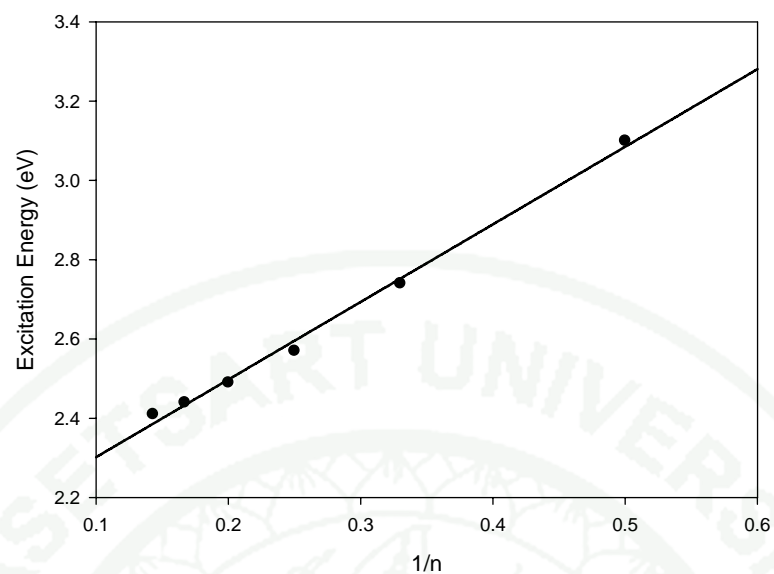


**Figure 18** Calculate excitation energies of PFV, PFV-CN, PFV-NH<sub>2</sub>, PFV-OCH<sub>3</sub> and PFV-OH by TDB3LYP method with SVP and TZVP basis sets based on ground state geometries optimized by B3LYP/6-31G(d) method.

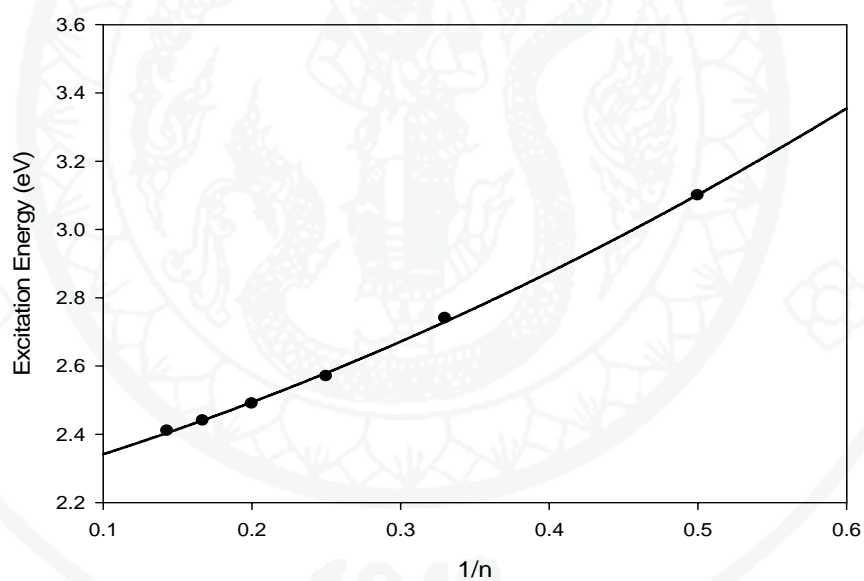
In the case of FV oligomers, there are experimental data of HOMO energy absorption wavelength and excitation energy of each oligomer (Table 7) studies by Liu *et al.*, (2007). It can be seen that our calculated HOMO energies and excitation energies of fluorene-vinylene oligomers are in good agreement with the experimental data. However, the linear extrapolation of the excitation energies with respect to inverse oligomer units is quite lower to the experimental value. Jansson, *et al.* (2007) studies the effect of conjugation lengths of singlet and triplet excited states of oligofluorene (dimer to heptamer) and uses an empirical relationship proposed by Meier *et al.* (1997). From their results, the linear relationships between excitation energies and  $1/n$  are observed only in range of  $n$  less than 5 with corresponding to the fitting parameter. For  $n > 5$ , excitation energy seems to be in constant value. Finally they suggest that in order to get more accurate excitation energy for the infinite fluorene oligomer, one need to use higher order polynomial fitting function.

Similarly, in fluorene-vinylene system, we extend the oligomer units up to heptamer ( $n = 7$ ) in order to investigate the dependence of the order of fitting function. Figure 19 (a and b) shows the first order and the second order fitting function of excitation energies of fluorene-vinylene oligomers when the numbers of units are from 2 to 7 units. The extrapolated excitation energies of polyfluorenevinylene obtained from linear and polynomial fittings are 2.11 and 2.21 eV, respectively. Interestingly, the results show that the polynomial extrapolated excitation energy is closer to the experimental value.

1943



(a)



(b)

**Figure 19** Correlation of the excitation energies of fluorene-vinylene oligomers with the inverse chain units (dimer to heptamer). The energies are calculated by B3LYP/6-31G(d) method.

### 3. Ionization Potential and Electron Affinity

One of the obstacles in performing conjugated polymer devices is their charge transfer properties. One major problem with organic polymers for such applications is that they are usually much better at accepting and transporting holes than electrons. Therefore, limitation of polymer applications in electronics field such as organic light-emitting displays (LEDs) is reached. Ionization potentials (IPs) and electron affinities (EAs) are used to estimate the energy barrier for the injection of both holes and electrons into the polymer. Methods for adjusting them should be considered. Many ways have been used to modulate IPs, EAs, and band gaps of polyfluorenes derivatives including conjugation length control, as well as the introduction of electron-donating or -accepting groups to the parent chromophore (Levesque *et al.*, 2001).

In this work, we have done IP and EA calculation of fluorene-vinylene derivatives by using the following equations

$$\begin{aligned} \text{IP}_{(\text{eV})} &= E_{\text{total (cation state with neutral opt.)}} - E_{\text{total (neutral opt.)}} \\ \text{EA}_{(\text{eV})} &= E_{\text{total (anion state with neutral opt.)}} - E_{\text{total (neutral opt.)}} \end{aligned}$$

Where, neutral optimizations were done in B3LYP/6-31G(d) ground state optimizations. Then the single point calculations of cation and anion states based on those of optimal structures were followed. The IPs and EAs are obtained as functions of reciprocal chain length for the oligomers studies, with assumed linear extrapolation to infinite chain length. Calculated IP and EA of FV oligomers, CN, OCH<sub>3</sub> and OH derivatives are shown in Table 8. For PFV, CN-PFV, OCH<sub>3</sub>-PFV and OH-PFV, the energies required to create a hole in the polymer are 5.1, 5.7, 5.2 and 4.9, respectively. The calculated IP of PFV is nearly equal to the experimental one (5.3 eV).



**Table 8** Ionization Potential (IP), Electron Affinity (EA), Highest Occupied Molecular Orbital (HOMO) and Lowest Unoccupied Molecular Orbital (LUMO) of FV based oligomers calculated by B3LYP/6-31G(d).

Oligomer	IP (eV)	EA (eV)	HOMO (eV)	LUMO (eV)
FV-H				
n=2	6.17	-0.56	-5.04	-1.69
n=3	5.81	-0.93	-4.89	-1.84
n=4	5.61	-1.14	-4.83	-1.92
n=5	-	-	-	-
n=∞	5.06 (5.3)*	-1.71 (1.6)*	-4.62	-2.15
FV-CN				
n=2	6.71	-1.24	-5.59	-2.37
n=3	6.4	-1.64	-5.5	-2.55
n=4	6.22	-1.84	-5.45	-2.62
n=5	6.02	-1.97	-5.37	-2.76
n=∞	5.64	-2.45	-5.26	-2.96
FV-OCH <sub>3</sub>				
n=2	5.95	-0.27	-4.79	-1.36
n=3	5.68	-0.65	-4.81	-1.55
n=4	5.61	-0.91	-4.83	-1.68
n=5	5.49	-1.06	-4.84	-1.76
n=∞	5.22	-1.56	-4.87	-2.01
FV-OH				
n=2	6.19	-0.23	-4.94	-1.42
n=3	5.77	-0.66	-4.77	-1.62
n=4	5.55	-0.88	-4.70	-1.70
n=5	5.42	-1.02	-4.68	-1.74
n=∞	4.90	-1.54	-4.49	-1.97

\*Lui *et al.*, 2007

#### 4. Fluorescence Energy and Lifetime

Fluorescence energies and lifetimes computed with the TD-B3LYP/SVP method using  $S_1$  optimized geometries are collected in Table 9. The extrapolated fluorescence energies obtained from the TD-B3LYP/SVP method since the linear relationship between the fluorescence energies on the reciprocal chain lengths are supposed. According to Table 9, it is shown that the fluorescence energies of every molecule are red shift from the excitation energies. There are 1.74, 2.00, 1.73 and 1.78 eV for CN, OCH<sub>3</sub>, OH and based structure, respectively. Radiative lifetimes have been computed for spontaneous emission by using the Einstein transition probabilities on the basis of fluorescence energy and oscillator strengths (Brandsen and Joachain, 1983) (in au).

Fluorescence lifetime provides information useful for the discrimination of particles. Extension of the conjugated backbone leads to a decrease of lifetimes. The lifetimes of these molecules are slightly different by ca. 0.2-0.4 ns. The lifetimes of FV based molecule and CN, OCH<sub>3</sub> and OH substituents are 1.0, 0.8, 1.0, and 0.6 ns, respectively. Among the three derivatives, the OCH<sub>3</sub> shows the lowest lifetime which is close to polyfluorene-vinylene. Recently, Gruber and coworkers (2006) determined the fluorescence lifetime of PFV by using mathematical fitting of the photoluminescence decay time-resolved spectrum. The resulting lifetime shows two time constants, 0.68 and 1.31 ns. The presence of two lifetimes probably due to an excited state deactivation process of the main chain, induced by the vinylene moiety. In addition, the second decay time might be occurred by the green-emission of the keto-defect in polymer chain. From the table 9, Calculated fluorescent lifetime of PFV is 0.6 ns. which is in good agreement with the available experimental data.

**Table 9** Calculated fluorescence energies ( $E_{flu}$ ) and radiative lifetimes of FV oligomers as obtained from TD-B3LYP/SVP calculations. Geometries were optimized at TD-B3LYP/SVP level.

	TD-B3LYP/SVP	
	$E_{flu}$ (eV)	Lifetime (ns)
PFV	1.78	0.6 (0.68)*
CN-PFV	1.74	1.0
NH <sub>2</sub> -PFV	1.77	0.6
OCH <sub>3</sub> -PFV	2.00	0.8
OH-PFV	1.73	1.0

\*Gruber *et al.*, 2006

## CONCLUSION

The (TD)-B3LYP method was used for the systematic theoretical investigation of the photo-physical properties of substituted model bifluorenevinylene compounds. The various substitutions of the vinylene unit by electron-acceptoring (CN) and/or electron-donating (NH<sub>2</sub>, OCH<sub>3</sub> and OH) groups were considered. DFT with B3LYP functional geometry was found to be a suitable method to estimate both structural parameters and electronic properties of poly-(9,9-dialkylfluorene-2,7-vinylene). Substitution at the vinylene unit by various functional groups was considered and resulting in FV derivatives. There were electron-withdrawing CN group and electron-donating groups, NH<sub>2</sub>, OCH<sub>3</sub> and OH groups. FV oligomers exhibits planar structures but all substituted oligomers display torsional shifts from the planarity ( $\theta = 7$ -50 degrees). Therefore, substitution leads to the twisting of the molecular fragment on the side of substitutions.

Theoretical excited state calculations of modeling polymeric systems are underestimated to those of the available experimental data. The obtained results indicate that substituents on vinylene unit can exhibit different electronic properties of the whole polymer. According to our results, we suggested that polyfluorene-vinylene with methoxy substitution on vinylene unit is an interesting material to be further synthesized as this copolymer demonstrates to give a high excitation energy within the fluorene-vinylene derivatives under this investigation.

In the case of the F<sub>2</sub>V-NH<sub>2</sub> molecule, the amino group is also responsible for the non-planarity on the non-substitute side. The next impact of the chemical modification of vinylene bridge is connected with the changes of electronic ground state torsional potentials of the fluorene unit around the single bond. The non-substituted molecule F<sub>2</sub>V has two planar minima and the barrier for perpendicular arrangement. For example, the presence of electron-withdrawing (cyano) or electron-donating (amino) groups on vinylene bridge is responsible for the restriction of the

torsional motion at the barriers located for planar and perpendicular arrangements. The energy barriers are also dependent on the substitution.

The TDDFT torsional potential energy curves in the vertically excited states were also investigated in this work. From our calculations, we do not find any indication of state crossings of the  $S_1$  state with higher ones for all investigated systems. The symmetric bi-substitution very effectively decreases the sensitivity of the evaluated potential curves on the torsion. The potential energy curves for the next higher excited states of  $F_2V$  molecule are quite closely spaced to each other and show multiple intersections (around 70 degree to 120 degree). On the other hand, the substitution can modulate the separation of crossing region of potential curves between the next lowest excited states. The absence of the intersections of excited states around the stable structures and relative well separation of the lowest excited state around the minima enable us to perform the molecular dynamics studies of investigation.



## LITERATURE CITED

- Ahlrichs, R., M. Bär, M. Häser, H. Horn and C. Kölmel. 1989. Electronic structure calculations on workstation computers: The program system turbomole. **Chem. Phys. Lett.** 162(3): 165-169.
- Ando, M., S. Murakami and H. Naito. 2003. Charge carrier transport properties of poly(9,9-dioctylfluorene) thin films. **Synth. Met.** 135: 285-286.
- Andre', J.A., J. Delhalle and J.-L. Bre'das. 1991. **Quantum chemistry aided design of organic polymers. An introduction to the quantum chemistry of polymers and its applications.** World Scientific London.
- Anuragudom, P., S.S. Newaz, S. Phanichphant and T.R. Lee. 2006. Facile Horner-Emmons synthesis of defect-free poly(9,9-dialkylfluorenyl-2,7-vinylene). **Macromolecules.** 39: 3494-3499.
- Aouchiche, H.A., S. Djennane and A. Bouccekine. 2004. DFT study of conjugated biheterocyclic oligomers exhibiting a very low HOMO-LUMO energy gap. **Synth. Met.** 140: 127-133.
- Appel, H., E.K.U. Gross and K. Burke. 2003. Excitations in Time-Dependent Density-Functional Theory. **Phys. Rev. Lett.** 90: 043005-1-4.
- Aquino, A.J.A., M. Barbatti and H. Lischka. 2006. Excited-state properties and environmental effects for protonated Schiff bases: A theoretical study; Chem. Phys. Chem. 7(10): 2089-2096.
- Babel, A. and S.A. Jenekhe. 2002. Electron transport in thin-film transistors from an n-type conjugated polymer. **Adv. Mater.** 14(5): 371-374.

- Becke, A.D. 1993. A new mixing of Hartree-Fock and local density-functional theories. **J. Chem. Phys.** 98: 1372–1377.
- Becker, B., H. Spreitzer, K. Ibrom and W. Kreuder. 1999. New insights into the microstructure of GILCH-polymerized PPVs. **Macromolecules.** 32: 4925-4932.
- Beenken, W.J.D. and H. Lischka. 2005. Structural broadening and diffusion by torsional motion in biphenyl. **J. Chem. Phys.** 123: 14431-14436.
- Bernius, M., M. Inbasekaran, E. Woo, W. Wu and L. Wujkowski. 2000. Light-emitting diodes based on fluorene polymers. **Thin Solid Films.** 363: 55-57.
- \_\_\_\_\_, M. Inbasekaran, J. O'Brien and W. Wu. 2000. Progress with light-emitting polymers. **Adv. Mat.** 12: 1737-1750.
- Bittihn, R., G. Ely and F. Woeffler. 1987. Polypyrrole as an electrode material for secondary lithium cells. **Makromol. Chem. Macromol. Symp.** 8: 51-59.
- Blondin, P., J. Bouchard, S. Beaupre, M. Belletete, G. Durocher and M. Leclerc. 2000. Molecular design and characterization of chromic polyfluorene derivatives. **Macromolecules.** 33: 8945-8952.
- Bongini, A., F. Brioni and M. Panunzio. 1997. Conformational analysis of 3,3', 3,4' - and 4,4' -dimethoxy-2,2' -bithiophenes as models for related polymers. **J. Chem. Soc., Perkin Trans.** 2: 927 – 930.
- Brandsen, B.H. and C.J. Joachain. 1983. **Physics of Atoms and Molecules.** Longman Group Limited.
- Braun, D. and A.J. Heeger. 1991. Visible light emission from semiconducting polymer diodes. **Appl. Phys. Lett.** 58:1982-1984.

- Bredas, J.L., R. Silbey, D. S. Boudreaux and R. R. Chance. 1983. Chain-length dependence of electronic and electrochemical properties of conjugated systems: polyacetylene, polyphenylene, polythiophene, and polypyrrole. **J. Am. Chem. Soc.** 105(22): 6555-6559.
- Briere, J.F. and M. Cote. 2004. Electronic, structural, and optical properties of conjugated polymers based on carbazole, fluorene, and borafluorene. **J. Phys. Chem. B.** 108: 3123-3129.
- Brocks, G., P.J. Kelly and R. Car. 1993. Structure and properties of polymers calculated by Ab initio molecular dynamics. **Synth. Met.** 57(2-3): 4243-4248.
- Burke, K., J. Werschnik and E.K.U. Gross. 2005. Time-dependent density functional theory: Past, present, and future. **J. Chem. Phys.** 123: 062206-1-9.
- Burroughes, J.H., D.D.C. Bradley, A.R. Brown, R.N. Marks, K. Mackay and R.H. Friend. 1990. Light-emitting diodes based on conjugated polymer. **Nature.** 347: 539-541.
- Chiang, C.K., C. R. Fincher, Jr., Y.W. Park, A.J. Heeger, H. Shirakawa, E.J. Louis, S. C. Gau and A.G. Macdairmid. 1977. Electrical conductivity in doped polyacetylene. **Phys. Rev. Lett.** 39: 1098-1101.
- Chidthong, R., S. Hannongbua, A.J.A. Aquino, P. Wolschann and H. Lischka. 2007. Excited state properties, fluorescence energies, and lifetime of a (fluorene-pyridene) copolymer, based on TD-DFT investigation. **J.Comput.Chem.** 28: 1735-1742.
- Cho, H.N., D.Y. Kim, J.K. Kim and C.Y. Kim. 1997. Control of band gaps of conjugated polymers by copolymerization. **Synth. Met.** 91: 293-296.

- Christiansen, O., H. Koch and P. Jørgensen. 1995. The second-order approximate coupled cluster singles and doubles model CC2. **Chem. Phys. Lett.** 243: 409-418.
- Chu, Q., Y. Pang, L. Ding and F.E. Karasz. 2002. Synthesis, chain rigidity, and luminescent properties of poly[(1,3-phenyleneethynylene)-alt-tris(2,5-dialkoxy-1,4-phenyleneethynylene)]s. **Macromolecules.** 35: 7569-7574.
- Claudio, G.C. and E.R. Bittner. 2002. Ground-state potential energy curves of phenylenevinylene oligomers. **Chem. Phys.** 276: 81-91.
- Cornil, J., D. Beljonne, R.H. Friend and J.L. Bredas. 1994. Optical absorption in poly(p-phenylene vinylene) and poly(2,5-dimethoxy-1,4-paraphenylene vinylene) oligomers. **Chem. Phys. Lett.** 223(1-2): 82-88.
- \_\_\_\_\_, I. Gueli, A. Dkhissi, J.C. Sancho-Garcia, E. Hennebicq, J.P. Calbert, V. Lemaure, D. Beljonne and J.L. Bredas. 2003. Electronic and optical properties of polyfluorene and fluorine-based copolymers: A quantum-chemical characterization. **J. Chem. Phys.** 118(14): 6615-6623.
- Delaere, D., M.T. Nguyen and L.G. Vanquickenborne. 2003. Structure-properties relationships in phosphole-containing pi-conjugated systems: A quantum chemical study. **J. Phys. Chem.** 107: 838-846.
- Dunning, T.H.J. 1971. Gaussian basis functions for use in molecular calculations. III. Contraction of (10s6p) atomic basis sets for the first-row atoms. **J. Chem. Phys.** 55(2): 716-723.
- Fincher, C.R., D.L. Peebles, A.J. Heeger, M.A. Druy, Y. Matsumura, A.G. Macdiarmid, H. Shirakawa and S. Ikeda. 1978. Anisotropic properties of pure and doped polyacetylene. **Solid State Commun.** 27: 489-494.

- Frisch, M.J., G.W. Trucks, H.B. Schlegel, G.E. Scuseria, M.A. Robb, J.R. Cheeseman, J.A. Montgomery Jr., T. Vreven, K.N. Kudin, J.C. Burant, J. M. Millam, S.S. Iyengar, J. Tomasi, V. Barone, B. Mennucci, M. Cossi, G. Scalmani, N. Rega, G.A. Petersson, H. Nakatsuji, M. Hada, M. Ehara, K. Toyota, R. Fukuda, J. Hasegawa, M. Ishida, T. Nakajima, Y. Honda, O. Kitao, H. Nakai, M. Klene, X. Li, J.E. Knox, H.P. Hratchian, J.B. Cross, C. Adamo, J. Jaramillo, R. Gomperts, R.E. Stratmann, O. Yazyev, A.J. Austin, R. Cammi, C. Pomelli, J.W. Ochterski, P.Y. Ayala, K. Morokuma, G.A. Voth, P. Salvador, J.J. Dannenberg, V.G. Zakrzewski, S. Dapprich, A.D. Daniels, M.C. Strain, O. Farkas, D.K. Malick, A.D. Radbuck, K. Raghavachari, J.B. Foresman, J.V. Ortiz, Q. Cui, A.G. Baboul, S. Clifford, J. Cioslowski, B.B. Stefanov, G. Liu, J. Liashenko, P. Piskorz, I. Komaromi, R.L. Martin, D.J. Fox, T. Keith, M.A. Al-Laham, C.Y. Peng, A. Nanayakkara, M. Challacombe, P.M.W. Gill, B. Johnson, W. Chen, M.W. Wong, C. Gonzalez, J.A. Pople. 2003. **GAUSSIAN 03**, Revision B.03, Gaussian Inc., Pittsburgh, PA.
- Furche, F., and K. Burke. 2005. Time-dependent density-functional theory in quantum chemistry. **Annual Reports in Computational Chemistry**. 1: 19–30
- \_\_\_\_\_ and R. Ahlrichs. 2002. Adiabatic time-dependent density functional methods for excited state properties. **J. Chem. Phys.** 117: 7433-7447.
- Gamerith, S., M. Gaal, L. Romaner, H.G. Nothofer, R. Guntner, P.S. de Freitas, U. Scherf and E.J.W. List. 2003. Comparison of thermal and electrical degradation effects in polyfluorenes. **Synth. Met.** 139: 855-858.
- Georgieva, I., N. Trendafilova, A. Aquino and H. Lischka. 2005. Excited state properties of 7-Hydroxy-4-methylcoumarin in the gas phase and in solution. A theoretical study. **J. Phys. Chem. A.** 109(51): 11860-11869.



- Gill, P.M.W., B.G. Johnson, J.A. Pople and M.J. Frisch. 1992. The performance of the Becke-Lee-Yang-Parr (B-LYP) density functional theory with various basis sets. **Chem. Phys. Lett.** 197: 499-505.
- Gong, Z. and J.B. Lagowski. 2005. Electronic structure properties of fluorene-phenylene monomer and its derivatives: TDDFT study. **J. Mol. Struct. (THEOCHEM)**. 729: 211-222.
- Grell, M., D.D.C. Bradley, X. Long, T. Chamberlain, M. Inbasekaran, E.P. Woo and M. Soliman. 1998. Chain geometry, solution aggregation and enhanced dichroism in the liquid-crystalline conjugated polymer poly(9,9-dioctylfluorene). **Acta Polym.** 49:439-444.
- Grisorio, R., P. Mastorilli, C.F. Nobile, G. Romanazzi, G.P. Suranna, G. Gigli, C. Piliego, G. Ciccarella, P. Cosma, D. Acierno and E. Amendola. 2007. Synthesis, spectral stability, and electroluminescent properties of random poly(2,7-fluorenylenevinylene-co-3,6-carbazolylenevinylene) obtained by a Suzuki-Heck Cascade reaction. **Macromolecules**. 40: 4865-4873.
- Gross, E.K.U. and W. Kohn. 1985. Local density-functional theory of frequencydependent linear response. **Phys. Rev. Lett.** 55: 2850-2852.
- Gross, M., D.C. Muller, H.G. Nothofer, U. Scherf, D. Neher, C. Brauchle and K. Meerholz. 2000. Improving the performance of doped pi-conjugated polymers for use in organic light-emitting diodes. **Nature**. 405: 661-665.
- Gruber, J., R.W.C. Li, L.H.J.M.C. Aguiar, T. L. Garcia, H.P.M. de Oliveira, T.D.Z. Atvars and A.F. Nogueira. 2006. Electrochemical synthesis, characterization and photophysics of a poly(fluorenylene vinylene) derivative. **Synth. Met.** 156:104-109.

Heeger, A.J. et al., MacDiarmid, A.G. et al., Shirakawa, H. et al. 1977. Electrical Conductivity in Doped Polyacetylene. **J. Phys. Rev. Lett.** 39: 1098-1101.

\_\_\_\_\_. 2001. Semiconducting and metallic polymers: The fourth generation of polymeric materials. **Phys. Chem. B.** 105(36): 8475-8491.

Hirata, S. and M. Head-Gordon. 1999. Time dependent density functional theory within the Tamm-Dancoff approximation. **Chem. Phys. Lett.** 314: 291-299.

Hsu, C.P., S. Hirata and M. Head-Gordon. 2001. Excitation energies from time-dependent density functional theory for linear polyene oligomers: butadiene to decapentaene. **J. Phys. Chem. A.** 105(2): 451-458.

Hutchison, G.R., M.A. Ratner and T.J. Marks. 2002. Accurate prediction of band gaps in neutral heterocyclic conjugated polymers. **J. Phys. Chem. A.** 106: 10596-10605.

\_\_\_\_\_, Y.J. Zhao, B. Delley, A.J. Freeman, M.A. Ratner and T.J. Marks. 2003. Electronic structure of conducting polymers: Limitations of oligomer extrapolation approximations and effects of heteroatoms. **Phys. Rev. B.** 68: 035204-035216.

Hwang, D.H., J.D. Lee, J.M. Kang, S. Lee, C.H. Lee and S.H. Jin. 2003. Syntheses and light-emitting properties of poly(9,9-di-noctylfluorenyl-2,7-vinylene) and PPV copolymers. **J. Mater. Chem.** 13:1540-1545.

\_\_\_\_\_, J.M. Kang, J.H. Eom, M.J. Park, H.J. Cho, J.I. Lee, H.Y. Chu, C. Lee, S.H. Jin and S.K. Shim. 2009. Stable green light-emission from poly[9,9-bis(40-n-octyloxyphenyl)fluorenyl-2,7-vinylene] synthesized via the Gilch polymerization route. **Curr. Appl. Phys.** 9: 441-447.

- Inbasekaran, M., E. Woo, W. Wu, M. Bernius, and L. Wujkowski. 2000. Fluorene homopolymers and copolymers. **Synth. Met.** 111-112: 397-401.
- Jansson, E., P.C. Jha and H. Ågren. 2007. Chain length dependence of singlet and triplet excited states of oligofluorenes: A density functional study. **Chem. Phys.** 336(2-3): 91-98.
- Jin, S.H., J.M. Shim, S.J. Jung, S.C. Kim, B.V.K. Naidu, W.S. Shin, Y.S. Gal, J.W. Lee, J.H. Kim and J.K. Lee. 2006. Photovoltaic properties of poly[(9,9-dioctylfluorenyl-2,7-vinylene)-co-{2-(3'-dimethyldodecylsilylphenyl)-1,4-phenylenevinylene}] for electro-active devices. **Macromol. Res.** 14: 524-529.
- \_\_\_\_\_, H.J. Park, J.Y. Kim, K. Lee, S.P. Lee, D.K. Moon, K.J. Lee and Y.S. Gal. 2002. Poly(fluorenevinylene) derivative by Gilch polymerization for light-emitting diode applications. **Macromolecules.** 35: 7532-7534.
- Jin, Y., J. Ju, J. Kim, S. Lee, J. Y. Kim, S.H. Park, S-M. Son, S.H. Jin, K. Lee, and H. Suh. 2003. Design, synthesis, and electroluminescent property of CN-poly(dihexylfluorenevinylene) for LEDs. **Macromolecules.** 36: 6970-6975.
- \_\_\_\_\_, K. Kim, S.H. Park, S. Song, J. Kim, J. Jung, K. Lee, and H. Suh. 2007. Increased efficiencies of the copolymers with fluoro groups in vinylene units. **Macromolecules.** 40: 6799-6806.
- Kallinger, C., M. Hilmer, A. Haugeneder, M. Perner, W. Spirk, U. Lemmer, J. Feldmann, U. Scherf, K. Müllen, A. Gombert and V. Wittwer. 1998. A flexible conjugated polymer laser. **Adv. Mat.** 10(12): 920-923.
- Karpfen, A., C.H. Choi and M. Kertesz. 1997. Single-bond torsional potentials in conjugated systems: a comparison of ab Initio and Density Functional results. **J. Phys. Chem. A.** 101(40): 7426-7433.

- Kawana, S., M. Durrell, J. Lu, J.E. Macdonald, M. Grell, D.D.C. Bradley, P.C. Jukes, R.A.L. Jones and S.L. Bennett. 2002. X-ray diffraction study of the structure of thin polyfluorene films. **Polymer**. 43(6): 1907-1913.
- Kim, D.Y., H.N. Cho and C.Y. Kim. 2000. Blue light emitting polymers. **Prog. Polym. Sci.** 25: 1089-1139.
- Kwasniewski, S.P., L. Claes, J.P. Francois and M.S. Deleuze. 2003. High level theoretical study of the structure and rotational barriers of trans-stilbene. **J. Chem. Phys.** 118: 7823-7836.
- Lee, J.I., G. Klaerner and R.D. Miller. 1999. Oxidative stability and its effect on the photoluminescence of poly(fluorene) derivatives: end group effects. **Chem. Mater.** 11: 1083-1088.
- Lemmer, U., S. Heun, R.F. Mahrt, U. Scherf, M. Hopmeier, U. Siegner, E.O. Göbel, K.Müllen and H. Bässler. 1995. Aggregate fluorescence in conjugated polymers. **Chem. Phys. Lett.** 240: 373-378.
- Löegdlund, M., P. Dannetun, C. Fredriksson, W.R. Salaneck and J.L. Brédas. 1994. Theoretical study of the interaction between sodium and oligomers of poly(p-phenylenevinylene) and poly(p-phenylene). **Synth. Met.** 67(1-3): 141-145.
- Lévesque, I, A. Donat-Bouilluda, Y. Tao, M. D'Iorio, S. Beaupré, P. Blondin, M. Ranger, J. Bouchard and M. Leclerc. 2001. Organic tunable electroluminescent diodes from polyfluorene derivatives. **Synth. Met.** 122(1): 79-81.
- Li, Z. and H. Meng. 2007. **Organic Light-Emitting Materials and Devices**. Taylor & Francis Group, New York.

- Lopez, L.C., P. Strohmriegl and T. Stübinger. 2002. Synthesis of poly (fluorenevinylene-co-phenylenevinylene) by suzuki coupling. **Macromol. Chem. Phys.** 203(13): 1926-1930.
- Lui, Q., W. Lui, B. Yao, H. Tian, Z. Xie, Y. Geng and F. Wang. 2007. Synthesis and chain-length dependent properties of monodisperse oligo(9,9-di-n-octylfluorene-2,7-vinylene)s. **Macromolecules.** 40(6): 1851-1857.
- Lukes, V., A. Aquino and H. Lischka. 2005. Theoretical study of vibrational and optical spectra of methylene-bridged oligofluorenes. **J. Phys. Chem. A.** 109: 10232-10238.
- \_\_\_\_\_ and H.F. Kauffmann. 2007. Dependence of optical properties of oligo-para-phenylenes on torsional modes and chain length. **J. Phys. Chem. B.** 111(28): 7954-7962.
- Ma, J., S. Li and Y. Jiang. 2002. A Time-Dependent DFT study on band gaps and effective conjugation lengths of polyacetylene, polyphenylene, polypentafulvene, polycyclopentadiene, polypyrrole, polyfuran, polysilole, polyphosphole, and polythiophene. **Macromolecules.** 35: 1109-1115.
- Meeto, W., S. Suramitr, S. Vannarat and S. Hannongbua. 2008. Structural and electronic properties of poly(fluorene–vinylene) copolymer and its derivatives: Time-dependent density functional theory investigation. **Chem. Phys.** 349: 1-8.
- Meier, H., U. Stalmach and H. Kolshorn. 1997. Effective conjugation length and UV/vis spectra of oligomers. **Acta. Polym.** 48(9): 379-384.
- Mermillod, M., J. Tanguy and F. Petiot. 1986. A study of chemically synthesized polypyrrole as electrode material for battery application. **Electrochem. Soc.** 133(6): 1073-1079.



- Mikroyannidis, J.A., L. Fenenko and C. Adachi. 2006. Synthesis and photophysical characteristics of 2,7-fluorenevinylene-based trimers and their electroluminescence. **J. Phys. Chem. B.** 110: 20317-20326.
- Møller, C. and M.S. Plesset. 1934. Note on an approximation treatment for many-electron systems. **Phys. Rev.** 46: 618-622.
- Nomura, K., H. Morimoto, Y. Imanishi, Z. Ramhani and Y. Geerts. 2001. Efficient synthesis of high molecular weight trans-poly(9,9-di-n-octylfluorene-2,7-vinylene) by acyclic diene metathesis (ADMET) polymerization by the molybdenum initiator. **J. Polym. Sci. Part A: Polym. Chem.** 39: 2463-2470.
- Onida, G., L. Reining, and A. Rubio. 2002. Electronic excitations: density functional versus many-body Green's-function approaches. **Rev. Mod. Phys.** 74: 601-659.
- Pan, J.F., S.J. Chua and W. Huang. 2000. Conformational analysis on biphenyls with theoretical calculations: modeling torsions in poly(para-phenylene)s with side chains. **Thin Solid Films.** 363: 1-5.
- \_\_\_\_\_. 2001. Conformational analysis (ab initio HF/3-21G\*) and optical properties of poly(thiophene-phenylene-thiophene) (PTPT). **Chem. Phys. Lett.** 363: 18-24.
- Pei, Q. and Y. Yang. 1996. Efficient photoluminescence and electroluminescence from a soluble polyfluorene. **J. Am. Chem. Soc.** 118: 7416-7417.
- Perdew, J.P., M. Ernzerhof and K. Burke. 1996. Rationale for mixing exact exchange with density functional approximations. **J. Chem. Phys.** 105: 9982-9985.

- Poolmee, P. and S. Hannongbua. 2004. Theoretical investigation on energy gap of fluorene-thiophene copolymer. **J. Theor. Comp. Chem.** 3(4): 481-489.
- \_\_\_\_\_, M. Ehara, S. Hannongbua and H. Nakatsuji. 2005. SAC–CI theoretical investigation on electronic structure of fluorene–thiophene oligomers. **Polymer.** 46: 6474-6481.
- Rault-Berthelot, J. and J. Simonet. 1985. The anodic oxidation of fluorene and some of its derivatives. **J. Electrochem. Soc.** 132: 187-192.
- Ranger, M., D. Rondeau, and M. Leclerc. 1997. New Well-defined poly(2,7-fluorene) derivatives: photoluminescence and base doping. **Macromolecules.** 30: 7686-7691.
- Runge, E. and E.K.U. Gross. 1984. Density-functional theory for time-dependent systems. **Phys. Rev. Lett.** 52: 997-1000.
- Saha, B., M. Ehara and H. Nakatsuji. 2007. Investigation of the electronic spectra and excited-state geometries of poly(para-phenylene vinylene) (PPV) and poly(para-phenylene) (PP) by the symmetry-adapted cluster configuration Interaction (SAC-CI) method. **J. Phys. Chem. A.** 111(25): 5473-5481.
- Sailor, M.J., E.J. Ginsburg, C.B. Gorman, A. Kumar, R.H. Grubbs and N.S. Lewis. 1990. Thin-films of n-Si/poly-(CH<sub>3</sub>)<sub>3</sub> Si-cyclooctatetraene-conducting polymer solar-cells and layered structures. **Science.** 249(4973): 1146-1149.
- Salzner, U., P.G. Pickup, R.A. Poirier and J.B. Lagowski. 1998. Accurate method for obtaining band gaps in conducting polymers using a DFT/hybrid approach. **J. Phys. Chem. A.** 102: 2572-2578.

- Schäfer, A., H. Horn and R. Ahlrichs. 1992. Fully optimized contracted gaussian basis sets for atoms Li to Kr. **J. Chem. Phys.** 97: 2571-2577.
- \_\_\_\_\_, C. Huber and R. Ahlrichs. 1994. Fully optimized contracted gaussian basis sets of triple zeta valence quality for atoms Li to Kr. **J. Chem. Phys.** 100: 5829-5835.
- Scherf, U. and E.J.W. List. 2002. Semiconducting polyfluorenes towards reliable structure–property relationships. **Adv. Mater.** 14: 477-487.
- Scott, J.C., J.J.D. Samuel, J.H. Hou, C.T. Rettner and R.D. Miller. 2006. Monolayer transistor using a highly ordered conjugated polymer as the channel. **Nano Lett.** 6(12): 2916-2919.
- Serrano-Andres, L. and M. Merchan. 2005. Quantum chemistry of the excited state: 2005 overview. **J. Mol. Struct. (THEOCHEM).** 729: 99-108.
- Souza, M.M.d., G. Rumbles, I. R. Gould, H. Amer, I. D. W. Samuel, S. C. Moratti, and A. B. Holmes. 2000. A theoretical and experimental study of cyano- and alkoxy-substituted phenylenevinylene model compounds. **Synth. Met.** 111-112: 539-543.
- Sriwichitkamol, K., S. Suramitr, P. Poolmee and S. Hannongbua. 2006. Structures, adsorption spectra and electronic properties of polyfluorene and Its derivatives; a theoretical study. **J. Theo. & Comput. Chem.** 5: 595-608.
- Suramitr, S., T. Kerdcharern, T. Sriksirin and S. Hannongbua. 2005. Electronic properties of alkoxy derivatives of poly(para-phenylenevinylene), investigated by time dependent density functional theory calculations, computational and theoretical polymer science. **Synth. Met.** 155(1): 27-34.

- \_\_\_\_\_, S. Hannongbua and P. Wolschann. 2007. Conformational analysis and electronic transition of carbazole-based oligomers as explained by density functional theory. **J. Mol. Struct. (THEOCHEM)**. 807: 109-119.
- Tasch, S., A. Niko, G. Leising and U. Scherf. 1996. Highly efficient electroluminescence of new wide band gap ladder-type poly(para-phenylenes). **Appl. Phys. Lett.** 68: 1090-1092.
- Tomozawa, H., D. Braun, S.D. Phillips, A.J. Heeger, and H. Kroemer. 1987. Metal-polymer Schottky barriers on cast films of soluble poly(3-alkylthiophenes). **Synth. Met.** 22: 63-69.
- Tretiak, S., A. Saxena, R.L. Martin, and A.R. Bishop. 2002. Conformational dynamics of photoexcited conjugated molecules. **Phys. Rev. Lett.** 89(9): 097402-1-097402-4.
- Van Gisbergen, S.J.A., A. Rosa, G. Ricciardi and E.J. Baerends. 1999. Time-dependent density functional calculations on the electronic absorption spectrum of free base porphyrin. **J. Chem. Phys.** 111(6): 2499-2506.
- Wu, L., T. Sato, H.Z. Tang and M. Fujiki. 2004. Conformation of a polyfluorene derivative in solution. **Macromolecules**. 37: 6183-6188.
- Yang, Y., Q. Pei and A.J. Heeger. 1996. Efficient blue polymer light-emitting diodes from a series of soluble poly(paraphenylene)s. **J. Appl. Phys.** 79: 934-939.
- Yang, L., A.M. Ren, J.K. Feng, J.F. Wang. 2005. Theoretical investigation of optical and electronic property modulations of  $\pi$ -conjugated polymers based on the electron-rich 3,6-dimethoxy-fluorene unit. **J. Org. Chem.** 70(8): 3009-3020.

Zeng, G., S.J. Chua and W. Huang. 2002. Influence of donor and acceptor substituents on the electronic characteristics of poly(fluorine-phenylene). **Thin Solid Films.** 417: 194-197.







## APPENDICES

## APPENDIX A

### Theoretical Background

#### 1. Density Functional Theory

Methods that are rooted in the so-called density functional theory are currently regarded as very promising since are able to include a large amount of correlation effects in a formalism that essentially requires very similar computational resources as the Hartree-Fock procedure. In fact the algorithms of the approach, in which the electron density is described in terms of one-electron basis functions, are very similar to the single-determinant HF algorithm. This property has helped to establish density functional methods as a standard tool for chemistry and physics.

While the concept of expressing part or all of the molecular energy as a functional of the electron density goes back to the early days of quantum theory, Density Functional Theory (DFT) was put on a rigorous theoretical foundation by the Hohenberg-Kohn theorem. It states that there exists unique density  $\rho$  that yield the exact ground energy of system. The subsequent work of Kohn and Sham laid the basis for practical computational applications of the DFT to real systems. The basis of their formalism are the so-called Kohn-Sham equations.

$$H\Psi_i = E_i\Psi_i \quad (1)$$

in which the Hamiltonian  $H$  is defined as

$$H = \left( -\frac{1}{2}\nabla^2 + V_{\text{KS}} \right) \quad (2)$$

where  $V_{\text{KS}}$  is a local potential defined such that the total density of the non-interacting system

$$\rho = \sum_i |\Psi_i|^2 \quad (3)$$

is the same as the density of the “real” system.  $V_{KS}$  has the three components  $V_{ext}$ ,  $V_C$  and  $V_{XC}$  containing the nuclear and external, Coulomb potential of the electrons and the exchange-correlation interactions.

$$E_{KS} = V_{ext} + \sum_{\mu\nu} P_{\mu\nu} H_{\mu\nu} + \frac{1}{2} \sum_{\mu\nu\lambda\sigma} P_{\mu\nu} P_{\lambda\sigma} \mathfrak{J} + E_x(P) + E_C(P) \quad (4)$$

In most cases the expressions for  $E_C$  and  $E_X$  cannot be computed analytically and must be obtained by numerical methods. The key difference between the Hartree-Fock and Kohn-Sham approaches to the SCF methods is the term  $E_{XC}$ , which was mostly omitted in above discussion. In HF theory, this  $E_{XC}$  is written as

$$E_{XC}^{HF} = \frac{1}{2} \sum_{\mu\nu\lambda\sigma} (P_{\mu\nu}^\alpha P_{\lambda\sigma}^\alpha P_{\mu\nu}^\beta P_{\lambda\sigma}^\beta) (\mu\nu / \lambda\sigma) \quad (5)$$

while the KS theory introduces a functional

$$E_{XC}^{HF} = \int f(\rho^\alpha, \rho^\beta, \gamma_{\alpha\alpha}, \gamma_{\alpha\beta}, \gamma_{\beta\beta}) d\mathbf{r} \quad (6)$$

for the description. The density gradient invariants  $\gamma$  ( $\gamma_{xy} = \nabla \rho_x \nabla \rho_y$ )

### Density Functionals

It is often customary to make a partition of the density functional into an exchange and correlation part for the separation of

$$E_{XC}(\rho) = E_X(\rho) + E_C(\rho) \quad (7)$$

Although distinction between exchange and correlation contributions is somewhat artificial in the context of DFT, the above separation considerably simplifies the discussion. It should, however, be explicitly noted that the definition of  $E_C$  does not correspond to the *ab initio* EC since correlation has, by definition, meaning only in a mean field approximation and DFT is not using such an approximation. The exchange part, on the other hand, follows closely the HF definition of exchange, does however not necessarily reproduce the exact exchange.

### Exchange

The exchange energy of a uniform spin-polarized gas of spin density  $\rho_\sigma$  is

$$E_X^S = -\sum \int \rho^\sigma(r) f_X^S(\rho_\sigma(r)) dr \quad (8)$$

with  $f_X^S(\rho_\sigma(r)) = \alpha_X [\rho_\sigma(r)]^{\frac{1}{3}}$  and  $\alpha_X = \frac{3}{2} \left( \frac{3}{4\pi} \right)^{\frac{1}{3}}$ . The exchange expression is sometimes labeled *Slater exchange*, thus the superscript *S*. This exchange expression serves as a base for other functional, which can be conveniently expressed in terms of their enhancement factor  $F_X$  over the exchange of the uniform electron gas

$$E_X = -\sum_\sigma \int \rho_\sigma(r) f_X^S(\rho_\sigma(r)) F_X(\rho_\sigma, \gamma_{\sigma\sigma}(r)) dr \quad (9)$$

For instance, the exchange functional proposed by Perdew and Wang uses the following factor:

$$F_X^{PW}(s) = \left[ 1 + 0.0864 \frac{s^2}{m} + bs^4 + cs^6 \right]^m \quad (10)$$

with  $m = 1/15$ ,  $b = 14$ ,  $c = 0.2$  and  $s = (24\pi^2)^{-1/3} \sqrt{\gamma_{\sigma\sigma} / \rho^{4/3}}$   $\gamma_{\sigma\sigma}$  here is again the squared density gradient  $\nabla_{\sigma}^2$ . One of the most used exchange functionals is that of Becke 1988, which is often labeled B88 or simply  $B$ .

$$F_x^B = 1 - \frac{\beta}{\alpha_x} \frac{x^2}{1 + 6\beta \sinh^{-1}(x)} \quad (11)$$

which uses the values  $x = \sqrt{\gamma_{\sigma\sigma} / \rho^{4/3}}$  and  $\beta = 0.0042$  in order to maintain correct boundary conditions. In a different approach, Perdew and Wang proposed an exchange formula that is designed from purely first principles.

$$F_x^{PW91} = \frac{1 + (a_1 s)(a_2 s) \sinh^{-1} + (a_3 + a_4 \exp(-100s^2))s^2}{1 + (a_1 s)(a_2 s) \sinh^{-1} + a_5 s^4} \quad (12)$$

where  $a_1 = 0.19645$ ,  $a_2 = 7.7956$ ,  $a_3 = 0.2743$ ,  $a_4 = -0.1508$ ,  $a_5 = 0.004$  and  $s$  the same as in eq. 32.

In practice, the three above exchange functionals are very similar, and are in fact based on minor corrections to the previous ones. Therefore they can be expected to produce very similar results. The enhancement over the simple electron gas, however, are significant enough and usually constitute a major improvement.

### Correlation

While it is possible to obtain  $E_C$  by some numerical methods from  $E_{XC}$  and the already known EX (cf. eq. 31) for the uniform electron gas, it is much more common to use separate correlation functionals. Distinction is made between local and gradient corrected functionals, referring to absence or presence of first order terms of the density  $\rho_{\sigma}$ . The local functional proposed by Vosko, Wilk and Nusair (VWN) was



obtained using Pad'e approximated interpolations of Ceperley and Alder results of their accurate quantum Monte Carlo calculations for the homogeneous electron gas. The functional is,

$$E_c^{VWN} = \frac{A}{2} \left[ \ln \frac{x^2}{X(x)} + \frac{2b}{Q} \tan^{-1} \frac{Q}{2x+b} - \frac{bx_0}{X(x_0)} \left( \ln \frac{(x-x_0)^2}{X(x)} + \frac{2(b+2x_0)}{Q} \tan^{-1} \frac{Q}{(2x+b)} \right) \right] \quad (13)$$

where the functions  $x = r_b^{1/2}$ ,  $X(x) = x^2 + bx + c$  and  $Q = (4c - b^2)^{1/2}$  and the constants are  $A = 0.0621814$ ,  $x_0 = -0.409286$ ,  $b = 13.0720$  and  $c = 42.7189$ .  $r_b$  represents the Wigner-radius and is defined by  $1/\rho = \frac{4\pi}{3}(r_b)^3$ . Together with the exchange expression from eq. 40 this constitutes what is often called the local density approximation (LDA) or local spin density approximation (LSDA) when spin is considered (Gies and Gerhardt, 1987).

Due to the experiences with the LDA and as a consequence of some of its shortcomings, recent developments have resulted in a number of gradient corrections to local functionals like the aforementioned VWN or a completely new class of gradient corrected functionals.

Another frequently used functional has been published by Lee, Yang and Parr. It replaces both the local and the gradient part of the LDA correlation functional.

$$E_c^{LYP} = -a \frac{1}{1+d\rho^{-1/3}} \left\{ \rho + b\rho^{-2/3} \left[ C_F \rho^{-5/3} - 2t_w + \frac{1}{9} \left( t_w + \frac{1}{2} \nabla^2 \rho \right) \right] e^{-2c\rho^{-1/3}} \right\} \quad (14)$$

where  $t_w = \frac{1}{8} \left( \frac{|\nabla \rho|^2}{\rho} - \nabla^2 \rho \right)$  and  $C_F = \frac{3}{10} (3\pi^2)^{2/3}$ ,  $a = 0.04918$ ,  $b = 0.132$ ,  $c = 0.2533$

and  $d = 0.349$

## Hybrid Functionals

More recently, following an approach proposed by Becke, the combination of DFT functionals with *ab initio* formulations led to a class of expressions which are essentially a mixture of both DFT and HF contributions with fitted coefficients for each contribution. The aim of this approach is to provide expressions that include the full exchange contribution and avoid side-effects arising from a complete replacement of the DFT exchange expression by the HF one. As an example, the B3LYP functional looks like this:

$$E_{XC}^{B3LYP} = a_{x0}E_X^S + (1 - a_{x0})E_X^{HF} + a_{x1}\Delta E_X^B + E_C^{VWN} + a_C\Delta E_C^{LYP} \quad (15)$$

with  $a_{x0} = 0.80$ ,  $a_{x1} = 0.72$  and  $a_C = 0.81$ , which are values fitted for a selected set of molecules to reproduce the heat of formation. The term  $E_X^{HF}$  is calculated using the Kohn-Sham orbitals in the manner of the HF procedure by computing the exchange integrals  $(\mu\nu / \nu\mu)$ . The B3LYP functional often uses  $\Delta E_C^{3LYP} = E_C^{LYP} - E_C^{VWN}$ .

## 2. Time Dependent Density Functional Theory

Ground-state DFT is based on the papers by Hohenberg and Kohn, and by Kohn and Sham. The main results are that the density of system is identical to the density of an associated non-interacting particle system moving in a local potential  $v_s(r)$  defined by the Kohn-Sham equations (atomic units are used throughout):

$$\left[ -\frac{1}{2}\nabla^2 + v_s[\rho(r)] \right] \varphi_i(r) = \varepsilon_i \varphi_i(r) \quad (16)$$

Here the local potential  $v_s[\rho](r)$  is the so-call Kohn-Sham potential, consisting of the external potential  $v_{ext}$  (the Coulomb field of the nuclei and external fields if present), the Hartree potential  $v_H$ , which is trivially calculated from the density, and the *xc* potential  $v_{xc}$  which is the only unknown part:

$$v_s(r) = v_{ext}(r) + v_H(r) + v_{xc}(r) \quad (17)$$

The Kohn-Sham orbitals  $\varphi_i$  move in the effective field  $v_s$  which depends upon the electron density  $\rho(r)$ . This density is exactly obtained by summing the squares of the Kohn-Sham orbitals and multiplying by their occupation numbers  $n_i$ .

$$\rho(r) = \sum_i^{occ} n_i |\varphi_i(r)|^2 \quad (18)$$

As the KS potential  $v_s(r)$  and the density  $\rho(r)$  are inter-dependent, the equation have to be solved in a Self-Consistent Field (SCF) procedure, which means that one iteratively adapts the effective potential  $v_s$  and the density  $\rho$  until the difference in the energy between two subsequent cycles is sufficiently small. In the most straightforward fashion, this can be performed by mixing the density of the previous cycle with a small part of the density in the present cycle. This “simple damping” approach usually converges very slowly, and in practice the Direct Inversion in the Iterative Subspace (DIIS) procedure by Pulay and co-workers, is much to be preferred. In the DIIS approach, not only the result of previous cycle, but the results of all, or many, previous cycles is taken into account, in order to obtain the optimal guess for the next cycle. If one is close to self-consistency, this procedure converge the SCF equation above.

In order to solve the KS equations an approximation for the exchange-correlation (xc) potential  $v_{xc}(r)$  is required and the simplest one is the LDA which is based upon the local density of the system. The GGAs go beyond this and take the local gradient of the density into account as well, allowing for a much improved accuracy in the results for energies and geometries. Many other approximations, for examples those based directly on the KS orbitals, are also available.

The usual ground state DFT scheme enables one to determine the density, and consequently the dipole moment, of a molecule with or without external electric fields

(Van Gisbergen *et. al.*, 1999). This affords the determination of the static polarizability and hyperpolarizability tensors  $\alpha$ ,  $\beta$  and  $\gamma$  by performing calculations in small electric fields of varying magnitudes and directions. In this so-call finite field (FF) approach, the tensor are then determined from finite difference techniques. The main advantage of this approach is that no programming work is needed. Any standard DFT code will allow the determination of static properties in this manner. However, for the determination of higher order tensors, such as  $\gamma$ , one need very well converged solution to the KS equations in order to make reliable predictions, which may be technically hard to achieve and which will certainly lead to considerable increase in CPU time consuming.

The most fundamental disadvantage of the FF approach, however, is that one has access to static properties only. The frequency-dependent polarizability and hyperpolarizability tensors are not accessible. Excitation energies and oscillator strengths can also not be obtained from the FF calculations. This is an important drawback of the FF approach, as it makes a direct comparison with experimental results are impossible. Especially for hyperpolarizabilities, it is known that there are substantial differences between the frequency-dependent and zero frequency results.

If one is interested in the time dependent properties mentioned above, a time dependent theory is required. There is a statement that, under curtain quite general conditions, there is an one-to-one correspondence between time-dependent one-body densities  $\rho(r,t)$  and time dependent one-body potentials  $v_{\text{ex}}(r,t)$ , for a given initial state. That is, a given evolution of the density can be generated by at most one time-dependent potential as derived by Runge and Gross (Rung and Gross, 1984);

$$i \frac{\partial}{\partial t} \varphi_i(r,t) = \left[ -\frac{\nabla^2}{2} + v_s(r,t) \right] \varphi_i(r,t) \equiv F_s \varphi_i(r,t) \quad (19)$$

Then, one can define a fictitious system of noninteracting electrons moving in a time-dependent effective potential, whose density is precisely that of the real

system. The time dependent potential is known as Kohn-Sham (KS) potential  $v_s(r,t)$  which is subdivided in the same manner as its static counterpart:

$$v_s(r,t) = v_{ext}(r,t) + v_H(r,t) + v_{xc}(r,t) \quad (20)$$

the Hatree potential being explicitly given by:

$$v_H(r,t) = \int dr' \frac{\rho(r',t)}{|r-r'|} \quad (21)$$

In practice, we always need to approximate unknown functional. An obvious and simple choice for TDDFT is adiabatic local density approximation (ALDA), sometime called time-dependent LDA. The time dependent  $xc$  potential  $v_{xc}[\rho](r,t)$  being an unknown functional of the time dependent density  $\rho(r,t)$  now given by:

$$\rho(r,t) = \sum_i^{occ} n_i |\varphi_i(r,t)|^2 \quad (22)$$

If a certain approximation for the time dependent  $xc$  potential  $v_{xc}(r,t)$  has been chosen, the TDKS equations can be solved iteratively to yield the time dependent density of system, which may be exposed to an external time dependent electric field. If one is interested in the effects due to extremely large laser fields, the perturbative expansion of the dipole moment become meaningless, and the TDKS equations have to be solved non-perturbatively. This has until now been performed for atoms, by Ullrich and Gross (Hirata *et.al.*, 1999), and more recently also by others, and gives access to such effects as higher harmonic generation (HHG). These applications fall into three general categories: nonperturbative regimes, linear (and higher-order) response, and ground-state applications. When the perturbing field is weak, as in typical spectroscopic experiments, perturbation theory applies. Then, instead of needing knowledge of the functional  $v_{xc}[\rho](r,t)$  at densities that are changing significantly with time, which might differ substantially from a ground-state density,



This potential is needed in the vicinity of the initial state, which is taken to be a nondegenerate ground-state. These changes are characterized by a new functional, the exchange-correlation kernel (Gross *et al.*, 1985). The exchange-correlation kernel is much more manageable than the full time-dependent exchange-correlation potential, because it is a functional of the ground-state density alone. Analysis of the linear response then shows (Appel *et al.*, 2003) that the latter is (usually) dominated by the response of the ground-state Kohn-Sham system, but corrected by TDDFT via matrix elements of the exchange-correlation kernel. In the absence of Hartree-exchange-correlation effects, the allowed transitions are exactly those of the ground-state Kohn-Sham potential. But the presence of the kernel shifts the transition frequencies away from the Kohn-Sham values to the true values. Several approaches to extracting excitations from TDDFT for atoms, molecules, and clusters are currently being used. The standard approach in quantum chemistry is to very efficiently convert the search for poles of response functions into a large eigenvalue problem (Furche *et al.*, 2005), in a space of the single-particle excitations of the system. The eigenvalues yield transition frequencies, while the eigenvectors yield oscillator strengths. This allows use of many existing fast algorithms to extract the lowest few excitations. The TDDFT has been programmed into most standard quantum chemical packages and after a molecule's structure has been found, it is usually not too costly to extract its low-lying spectrum. Moreover, the number of these TDDFT response calculations for transition frequencies is growing exponentially at the present (Burke *et al.*, 2005). Challenges remain for the application of TDDFT to solids (Onida *et al.*, 2002), because the present generation of approximate functionals (local and semi-local) loses important effects in the thermodynamic limit, but much work (some reported in this book) is currently in progress.

However, the drawback of this is that the calculations are very time consuming, forbidding the treatment of medium-sized molecules. If one restricts oneself to properties which are accessible through perturbative methods, as we will do here, a much more efficient approach is possible, allowing the treatment of large molecules (>100 atoms). This approach will be the subject of the next section. For

more information on time dependent DFT in general, the reader is referred to the excellent reviews by Gross and co-workers.

### 3. Second-Order Approximate Coupled-Cluster

The CC2 model is an approximated coupled-cluster singles-and-doubles (CCSD) method which has been proposed in 1995 by Christiansen, Jørgensen and Koch for response calculations on molecules which are out of reach for CCSD and higher correlated methods. It is one of the simplest correlated ab initio methods for excited states and yields energies for singly-excited states which are correct through second-order in the electron-electron interaction (dynamic electron correlation), as the well-known second-order Møller-Plesset perturbation theory (MP2) does for ground states. It is thus well-suited for the study of excited states of large closed-shell (or at least "single-reference") molecules. In difference to the perturbative doubles corrections CIS(D) to the widely used configuration interaction singles (CIS) method and similar perturbative approaches to excited states which use non-degenerate perturbation theory, CC2 is not limited to energetically isolated states. A feature, which is important in the search of excited state equilibrium structures. In several applications CC2 has been shown to be a viable tool for such studies.

As MP2 and other related methods based on a second-order treatment of electron correlation, CC2 can be implemented very efficiently with a so-called resolution of the identity approximation for the integrals which describe the electron-electron interaction and thereby made applicable to relatively large molecules, which have been intractable with conventional implementations. As demonstrated in the mid 1990's by Weigend and Häser for MP2, the computational costs and demands (CPU time, memory and disk space) are for most applications reduced by orders of magnitudes.

During the last years we have in our group developed the RI-CC2 code of the Turbomole packages, an implementation of CC2 with the resolution-of-the-identity approximation which includes

- ground and excitation energies
- transition matrix elements (e.g. oscillator or rotatory strength)
- first-order properties (expectation values)
- analytic gradients for ground and excited states

### **The Turbomole Program**

Turbomole is the ab initio electronic calculation that implements various quantum chemistry algorithms. This program was developed by group of prof. Reinhart Ahlrichs at the University of Karlsruhe. In 2007, the TURBOMOLE GmbH (Ltd) was founded by the main developers of the program: R. Ahlrichs, F. Furche, C. Hättig, W. Klopper, M. Sierka and F. Weigend. The company took over the responsibility for the coordination of the scientific development of the program, to which it holds all copy and intellectual property rights. For the further program development, all researchers interested in TURBOMOLE development can submit project proposals to the company. The proposals are reviewed by the founding members of TURBOMOLE GmbH.

With almost 20 years of continuous development TURBOMOLE has become a valuable tool used by academic and industrial researchers. It is used in research areas ranging from homogeneous and heterogeneous catalysis, inorganic and organic chemistry to various types of spectroscopy, and biochemistry.

Presently TURBOMOLE is one of the fastest and most stable codes available for standard quantum chemical applications. Unlike many other programs, the main focus in the development of TURBOMOLE has not been to implement all new methods and functionals, but to provide a fast and stable code which is able to treat molecules of industrial relevance at reasonable time and memory requirements.

## Outstanding features of TURBOMOLE

- Direct and semi-direct algorithms with adjustable main memory and disk space requirements
- Full use of all finite point groups
- Efficient integral evaluation
- Stable and accurate grids for numerical integration
- Low memory and disk space requirements

## Feature list

- Key methods
  - Restricted, unrestricted, and restricted open-shell wave functions
  - Density Functional Theory (DFT) including most of the popular exchange-correlation functionals, i.e. LDA, GGA, hybrid functional
  - Hartree-Fock (HF) and DFT response calculations: stability, dynamic response properties, and excited states
  - Two-component relativistic calculations including spin-orbit interactions for all exchange- correlation functional
  - Second-order Møller-Plesset (MP2) perturbation theory for large molecules
  - Second-order approximate coupled-cluster (CC2) method for ground and excited states
  - Treatment of Solvation Effects with the Conductor-like Screening Model (COSMO)
  - Universal force field (UFF)

- Key properties
  - Structure optimization to minima and saddle points (transition structures)
  - Analytical vibrational frequencies and vibrational spectra for HF and DFT, numerical for all other methods
  - NMR shielding constants for DFT, HF, and MP2 method
  - Ab initio molecular dynamics (MD)
- DFT and HF ground and excited states
  - Efficient implementation of the Resolution of Identity (RI) and Multipole Accelerated Resolution of Identity (MARI) approximations allow DFT calculations for molecular systems of unprecedented sizes containing hundreds of atoms
  - Ground state analytical force constants, vibrational frequencies and vibrational spectra
  - Empirical dispersion correction for DFT calculations
  - Eigenvalues of the electronic Hessian (stability analysis)
  - Frequency-dependent polarizabilities and optical rotations
  - Vertical electronic excitation energies
  - Transition moments, oscillator and rotatory strengths of electronic excitations, UV-VIS and CD spectra
  - Gradients of the ground and excited state energy with respect to nuclear positions; excited and ground state equilibrium structures; adiabatic excitation energies, emission spectra
  - Excited state electron densities, charge moments, population analysis
  - Excited state force constants by numerical differentiation of gradients, vibrational frequencies and vibrational spectra



- MP2 and CC2 methods
  - Efficient implementation of the Resolution of Identity (RI) approximation for enhanced performance
  - Closed-shell HF and unrestricted UHF reference states
  - Sequential and parallel (with MPI) implementation (with the exception of MP2-R12)
  - Ground state energies and gradients for MP2, spin-component scaled MP2 (SCS-MP2) and CC2
  - Ground state energies for MP2-R12
  - Excitation energies for CC2, ADC(2) and CIS(D)
  - Transition moments for CC2
  - Excited state gradients for CC2 and ADC(2)

## The Theory of Photophysical Processes

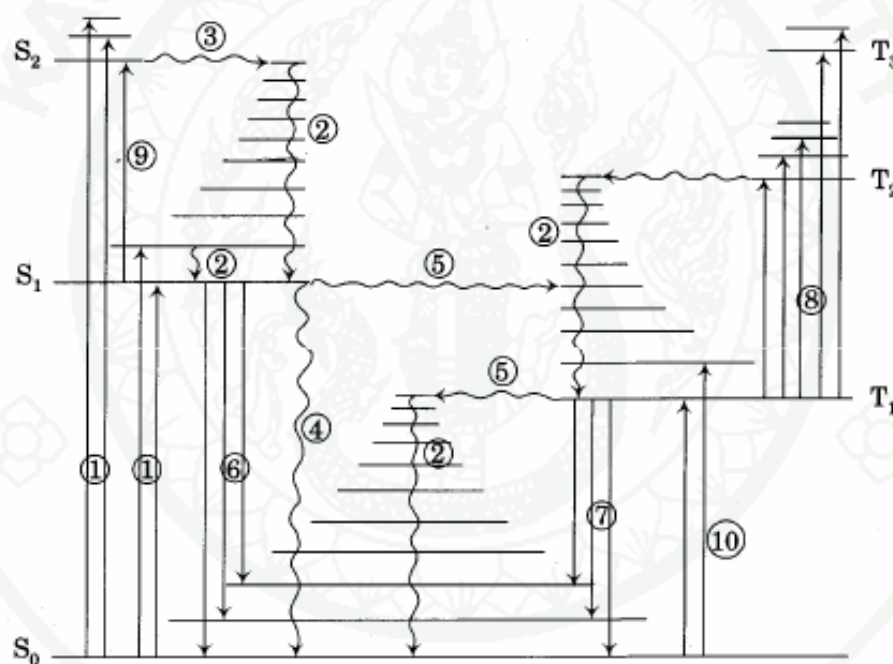
### 1. Photophysical Process

If a substance is irradiated with electromagnetic radiation, the energy of the incident photons may be transferred to the atoms or molecules raising them from the ground state to an excited state. This process, known as absorption, is accompanied by attenuation of the incident radiation at a particular frequency and can occur only when the energy difference between the two levels is exactly matched by the energy of the photons. The frequency of the radiation is given by

$$E_2 - E_1 = \Delta E = h\nu \quad (1)$$

where  $E_1$  and  $E_2$  are the energies of the two levels and  $\Delta E$  is the difference between them. The absorbed energy is rapidly lost to the surrounding by collisions allowing the system to revert or relax to the ground state. Sometimes the energy is not dissipated in this way but is re-emitted a few million seconds later-a process known as fluorescence.

A useful way of representing the energies of the electronic states of molecule is a Jablonski diagram, such as in Fig. A3. The vertical scale represents potential energy. The horizontal scale has no particular significance; it allows us to separate to singlet and triplet state manifolds (sets of energy levels) so that the excited states are more clearly distinguished. Superimposed on each electronic state is a set of vibrational energy levels. For the sake of clarity, a set of rotational energy levels superimposed on each vibrational level is not shown.



**Appendix Figure A1** Generalized Jablonski Diagram.

There are two kinds of photophysical processes indicated in Figure A1. Those interconversions denoted by straight lines are radiative processes, which occur through the absorption or emission of light. Those indicated by wavy lines are nonradiative processes, which occur without light being absorbed or emitted. The numbers on the lines are keys to the following definitions:

**1. Absorption of Light.** A ground state molecule ( $S_0$ ) may absorb a photon of light, thus becoming converted to an excited state. The most likely transitions are  $S_0 \rightarrow S_1$  or  $S_0 \rightarrow S_2$ , although  $S_0$  to higher excited singlet state transitions are also possible.

**2. Vibrational Relaxation.** The absorption from  $S_0$  to  $S_n$  involves an energy change from the 0<sup>th</sup> vibrational level of  $S_0$  to any vibrational level of the excited state. However, the  $v = 0$  is also the vibrational level is the level most populated at room temperature for the ground electronic state of molecule, and  $v = 0$  is also the vibrational level of the excited electronic state that is most likely to be populated at equilibrium. Unless the molecule dissociates before equilibrium can be obtained, there is a very rapid process (with a rate constant of about  $10^{12} \text{ sec}^{-1}$ ) that relaxed the higher vibrational level of the excited state to its 0th vibrational level in condensed phases (i.e., solids or liquids).

**3. Internal Conversion** is a non radiative process that converts a higher electronic state into a lower state of the same multiplicity (a higher singlet state into a lower singlet state or a higher triplet state into a lower triplet state). The name arises because the process occurs internally; the line for internal conversion is a horizontal one. This means that the the 0th vibrational level of  $S_2$  is converted into a vibrationally excited  $S_1$  can then relax to its 0th vibrational level. The rate constants for internal conversion are fast ( $> 10^{10} \text{ sec}^{-1}$ ), especially when the two states are close in energy.

**4. Radiationless Decay** is a process by which electronically excited states are returned to ground states (typically from  $S_1$  to  $S_0$ ) without the emission of light. Radiationless decay often has a slower rate constant (ca.  $< 10^6 \text{ sec}^{-1}$ ) than other forms of internal conversion because the energy gap between  $S_1$  and  $S_0$  is usually greater than that between  $S_2$  and  $S_1$  or other pairs of excited states.

**5. Intersystem Crossing**, the conversion of a singlet state into a triplet state (or vice versa), requires a spin flip of an electron. The probability of intersystem

crossing depends, among other things, on the energy gap between the singlet and triplet states, so values of  $k_{isc}$  vary from  $10^6$  to  $10^{10} \text{ sec}^{-1}$ . The  $T_n$  states is lower in energy than the corresponding  $S_n$  state because of the lower electron repulsion for unpaired electrons.

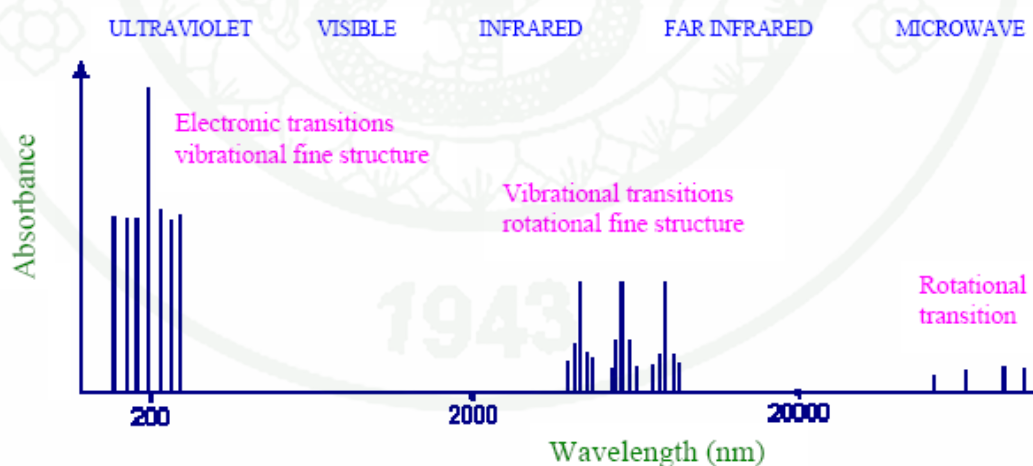
**Processes 2-5** are nonradiative processes. The following are radiative processes.

**6. Fluorescence** is the emission of light from an excited state to a ground state with the same multiplicity. Usually the emission is  $S_1 \rightarrow S_0$ , and generalization to that effect is known as Kasha's rule. However, anomalous fluorescence ( $S_2 \rightarrow S_0$ ) occurs in some compound, among them azulene, thiocarbonyl compounds, and some gaseous polyenes.

**7. Phosphorescence** is the emission of light from an excited state to a ground state with different multiplicity (usually from a triplet excited state to singlet ground state). This process involves both an electronic state change and a spin flip so, like  $S_0 \rightarrow T_n$  absorption, phosphorescence is a spin-forbidden process. **8. Triplet-Triplet Absorption.** A molecule in a triplet excited state may absorb a photon to give a higher triplet state, so a UV-Vis spectrum may be obtained, and the time-dependence of the excited state decay may be monitored. Flash spectroscopy is triplet-triplet absorption spectroscopy that can be an important technique for detecting triplet excited states.

**9. Singlet-Singlet Absorption.** Because triplet states may persist longer than singlet states, the only excitation of excited states possible during much of the development of photochemistry was triplet-triplet absorption. With the advent of picosecond and femtosecond spectroscopy, it has become possible also to measure transitions from one excited singlet state to another, higher energy excited singlet state.

**10. Singlet-Triplet Absorption**, like phosphorescence, is a spin-forbidden process, so ordinarily  $S_0 \rightarrow T_n$  transitions are not observed in UV-Vis spectroscopy. However, these transitions can be seen under certain conditions. For ultraviolet and visible wavelengths, one should expect that the absorption spectrum of a molecule (i.e., a plot of its degree of absorption against the wavelength of the incident radiation) should show a few very sharp lines. Each line should occur at a wavelength where the energy of an incident photon exactly matches the energy required to excite an electronic transition as shown in Figure A2. In practice it is found that the ultraviolet and visible spectrum of most molecules consists of a few humps rather than sharp lines. These humps show that the molecule is absorbing radiation over a band of wavelengths. One reason for this band, rather than line absorption is that an electronic level transition is usually accompanied by a simultaneous change between the more numerous vibrational levels. Thus, a photon with a little too much or too little energy to be accepted by the molecule for a ‘pure’ electronic transition can be utilized for a transition between one of the vibrational levels associated with the lower electronic state to one of the vibrational levels of a higher electronic state.



**Appendix Figure A2** Idealized Absorption Spectrum.



If the difference in electronic energy is 'E' and the difference in vibrational energy is 'e', then photons with energies of E, E+e, E+2e, E-e, E-2e, etc. will be absorbed. Furthermore, each of the many vibrational levels associated with the electronic states also has a large number of rotational levels associated with it. Thus a transition can consist of a large electronic component, a smaller vibrational element and an even smaller rotational change. The rotational contribution to the transition has the effect of filling in the gaps in the vibrational fine structure. In addition, when molecules are closely packed together as they normally are in solution, they exert influences on each other which slightly disturb the already numerous, and almost infinite energy levels and blur the sharp spectral lines into bands.

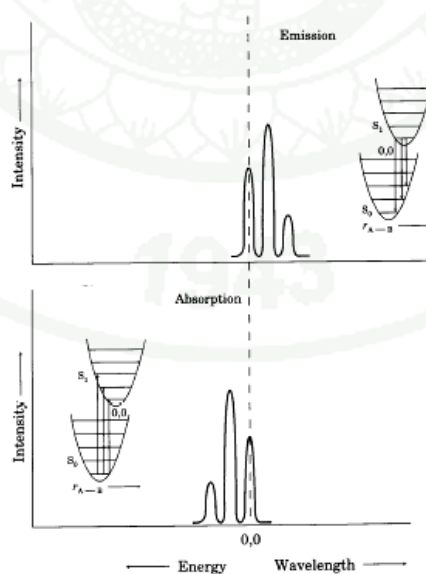
## 2. Fluorescence and Phosphorescence

For most organic molecules, fluorescence is the spontaneous emission of light from the  $v = 0$  vibrational level of the first excited singlet state to some vibrational level ( $v = 0, 1, 2, \dots$ ) of the (singlet) ground electronic state. As indicated in the top portion of Figure A3, the energy of the photon emitted in the  $v = 0$  to  $v = 0$  fluorescence is the same as the energy of the photon absorbed in the  $v = 0$  to  $v = 0$  transition if the geometry of the photoexcited molecule is nearly the same as that of the ground state molecule. However, all other fluorescence lines are at longer wavelengths (lower energy). Thus, the fluorescence and emission spectra should overlap at the 0,0 transition, providing confirmation of the 0,0 energy of the electronically excited state. In molecules such as anthracene, the  $\sigma$  bonding provides a molecular framework for the planar  $\pi$  system, and the  $\pi$  bonding results from population of many bonding MOs. Therefore promotion of one electron to an antibonding MO may not seriously distort the molecular geometry. In such cases there can be a nearly mirror image relationship between the absorption and fluorescence spectra of organic molecules, particularly when the spectra are plotted as intensity versus energy ( $\text{cm}^{-1}$ ) instead of wavelength. The similarity arises because the factors that make some  $v = 0$  to  $v = x$  transitions more probable than others also make some  $v = 0$  to  $v = x$  emissions more probable.

For some molecules, however, the geometry of the ground and excited states may be very different. As a result, there may be a large difference between  $\lambda_{\text{max}}$  for absorption and  $\lambda_{\text{max}}$  for emission, and the 0,0 transition may be weak or not present.

A similar relationship between geometry and a mirror image appearance of singlet-triplet absorption and phosphorescence is expected, but this is often difficult to determine experimentally, in fluid solution phosphorescence is usually reduced by diffusion-limited bimolecular interaction of the excited triplet compound and one or more ground state species. However, phosphorescence can often be observed by irradiating the compound in environments in which diffusion is quite slow, such as in an organic glass at liquid nitrogen temperature.

Singlet-triplet absorption is ordinarily difficult to detect because the transition is spin-forbidden. Heavy atom solvents or oxygen perturbation have been used to induce singlet-triplet absorption, but absorptions observed in this manner are weak, and it is important to establish that the observed absorption is not due to artifacts resulting from the solvent or additive.



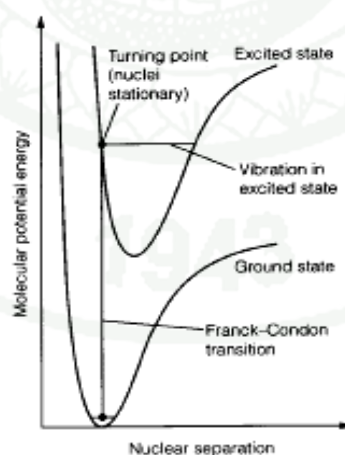
**Appendix Figure A3** Schematic representations of the origins of UV-Vis absorption (bottom) and fluorescence (top) spectra.

### 3. Franck-Condon principle

The different electronic states of a molecule are often associated with different shapes of molecule because the different electron distribution around the molecule changes the electrostatic Coulombic forces that maintain the nuclei in specific relative positions. Since nuclei are considerably more massive than electrons, the Franck-Condon principle states that:

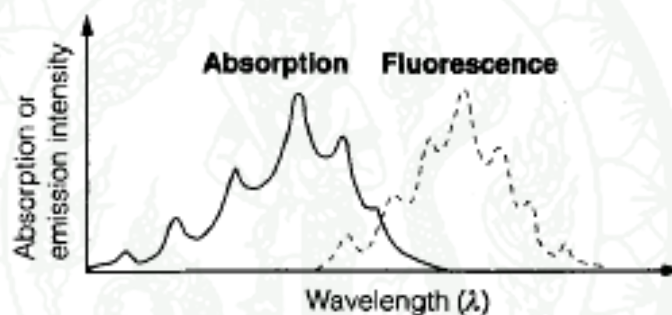
*An electronic transition takes place sufficiently rapidly that the nuclei do not change their internuclear positions during the transition.*

Consequently, when energy is absorbed in an electronic transition, the nuclei suddenly find themselves in a new force field and at positions which are not in equilibrium for the new electronic state. This is shown schematically in Figure A4, in which an electronic absorption from the ground state appears as a vertical line because of the Franck-Condon principle. The internuclear separation of the ground state becomes a turning point, the extent of maximum displacement, in a vibration of the excited state.



**Appendix Figure A4** Illustration of the Franck-Condon principle for vertical electronic transitions.

The vertical transition has the greatest transition probability but transitions to nearby vibrational levels also occur with lower intensity. Therefore, instead of an electronic absorption occurring at a single, sharp line, electronic absorption consists of many lines each corresponding to the stimulation of different vibrations in the upper state. This vibrational structure (or progression) of an electronic transition can be solved for small molecules in the gas-phase, but in a liquid or solid collision broadening of the transitions cause the lines to merge together and the electronic absorption spectrum is often a broad band with limited structure (Figure A5). The Franck-Condon principle also applies to downward transitions and accounts for the vibrational structure of a fluorescence spectrum.



**Appendix Figure A5** Relationship between the broad electronic absorption and fluorescence bands of liquids and solids.

## APPENDIX B

### Oral Presentation and Poster Contributions to Conferences

#### Oral Presentation I

Meeto, W., S. Suramitr, S. Vannarat and S. Hannongbua. **Ground and Excited States Geometries of Fluorenevinylene Based Oligomers: Time Dependent Density Functional Theory Study:** The 11th Annual National Symposium on Computational Science and Engineering (ANSCSE11), Prince of Songkla University (PSU), Phuket Campus, Thailand, 28-30 March 2007.



### Poster Presentation I

Meeto, W., S. Suramitr, P. Poolmee, K. Sriwichitkamol, and S. Hannongbua. **Effect of Conjugation Length on Structural and Electronic Properties of Conjugated Polymeric Compounds:** The abstract of 31<sup>st</sup> Congress on Science and Technology of Thailand (STT 2005), Suranaree University of Technology, Nakhon Ratchasima, Thailand, 18-20 October 2005.

### Poster Presentation II

Meeto, W., S. Suramitr, and S. Hannongbua. **Quantum Chemical Calculations on Structural and Electronic Properties of Poly(fluorenevinylene):** International Conference on Modeling in Chemical and Biological Engineering Sciences, Rama garden hotel, Bangkok, Thailand, 25-27 October 2006.

### Poster Presentation III

Suramitr, S., W. Meeto and S. Hannongbua. **Theoretical Investigation of Ground and Excited States Geometry of Conjugated Based on Carbazole Copolymers:** International Conference on Modeling in Chemical and Biological Engineering Sciences, Rama garden hotel, Bangkok, Thailand, 25-27 October 2006.

### Poster Presentation IV

Meeto, W., S. Suramitr, and S. Hannongbua. **Electronic Properties of the Poly(fluorenevinylene) Derivatives: Time Dependent Density Functional Theory Calculations:** German-Thai Symposium on Nanoscience and Nanotechnology, The Tide Resort, Bangsean Beach, Chonburi, Thailand, 27-28 September 2007.

## APPENDIX C

### Publications

#### Publication I

Meeto, W., S. Suramitr, S. Vannarat and S. Hannongbua. 2008. Structural and electronic properties of poly(fluorene–vinylene) copolymer and its derivatives: Time-dependent density functional theory investigation. **Chem. Phys.** 349: 1-8.

Available online at [www.sciencedirect.com](http://www.sciencedirect.com)

ScienceDirect

Chemical Physics 349 (2008) 1–8

Chemical  
Physics[www.elsevier.com/locate/chemphys](http://www.elsevier.com/locate/chemphys)

## Structural and electronic properties of poly(fluorene–vinylene) copolymer and its derivatives: Time-dependent density functional theory investigation

W. Meeto<sup>a,b</sup>, S. Suramitr<sup>a,b</sup>, S. Vannarat<sup>c</sup>, S. Hannongbua<sup>a,b,\*</sup><sup>a</sup> Department of Chemistry, Faculty of Science, Kasetsart University, Bangkok 10900, Thailand<sup>b</sup> Center of Nanotechnology, Kasetsart University, Bangkok 10900, Thailand<sup>c</sup> National Electronics and Computer Technology Center, Pathumthani 12120, Thailand

Received 14 December 2007; accepted 13 February 2008

Available online 20 February 2008

This work is dedicated to Professor Dr. Hans Lischka on an occasion of his 65th anniversary.

### Abstract

The ground state and the lowest singlet excited-state geometries of poly-(9,9-dialkylfluorene-2,7-vinylene) copolymer or PFV and its derivatives (NH<sub>2</sub>-FV)<sub>n</sub>, (CN-FV)<sub>n</sub>, (OMe-FV)<sub>n</sub> and (OH-FV)<sub>n</sub> (*n* = 2–5) were investigated based on density functional theory (DFT) and time-dependent DFT using B3LYP functional. The ground state and the lowest singlet excited-state geometries of the oligomers were optimized at the B3LYP/6-31G\* and TD-B3LYP/SVP levels, respectively. The calculated ground state geometries favor the aromatic type structure, while the electronic excitations lead to quinoid type distortion, which exhibited a shortening of the inter-ring bonds (about 0.03 Å). Absorption and fluorescence energies were extrapolated to infinite chain length making use of their good linearity with respect to 1/*n*. Extrapolated values of 2.19 eV for (FV)<sub>n</sub> was obtained by TD-B3LYP/TZVP method and 2.37, 2.11, 2.35 and 2.11 eV for its derivatives, (NH<sub>2</sub>-FV)<sub>n</sub>, (CN-FV)<sub>n</sub>, (OMe-FV)<sub>n</sub> and (OH-FV)<sub>n</sub>, respectively. The predicted energy gaps of the copolymer derivatives were calculated and compared to available experimental data. Fluorescence energies are 1.78, 1.74, 2.00 and 1.73 eV and the predicted radiative lifetime are 0.6, 1.0, 0.8 and 1.0 ns. for (FV)<sub>n</sub>, (CN-FV)<sub>n</sub>, (OMe-FV)<sub>n</sub> and (OH-FV)<sub>n</sub>, respectively. These fundamental structural and electronic informations can be useful in designing of novel conducting polymer materials.

© 2008 Elsevier B.V. All rights reserved.

**Keywords:** Fluorene–vinylene molecule; Energy gap; Vertical excitation energy; Density functional theory; Life time

### 1. Introduction

The application of the conjugated polymers was found to be useful as organic light-emitting diodes (OLEDs) since poly(*p*-phenylene vinylene) (PPV) was found to emit electroluminescence (EL) in 1990 [1]. This kind of light-emitting polymer can be fabricated on a flexible substrate and easily processed for specific purposes [2,3]. Compared with

single molecules, polymers have longer  $\pi$ -conjugation lengths, higher glass-transition temperatures, better film-forming properties, and stable film morphologies; there are further advantages on device fabrication such as higher quantum efficiencies, longer lifetime, and simplified processing by spin-coating.

Nowadays, poly(*p*-phenylenevinylene) (PPV) [1,4], and polyfluorenes (PFs) [5,6] and their derivatives are getting much academic and industrial interest. Recently, poly-(9,9-dialkylfluorene-2,7-vinylene) [7–10] or PFV (Fig. 1) was prepared by various synthetic methods such as acyclic diene metathesis (ADMET) polymerization [7], the Heck reaction [8], Horner–Emmons reaction [9] and Gilch

\* Corresponding author. Address: Department of Chemistry, Faculty of Science, Kasetsart University, Bangkok 10900, Thailand. Tel./fax: +66 25625555x2140.

E-mail address: [fscisph@ku.ac.th](mailto:fscisph@ku.ac.th) (S. Hannongbua).

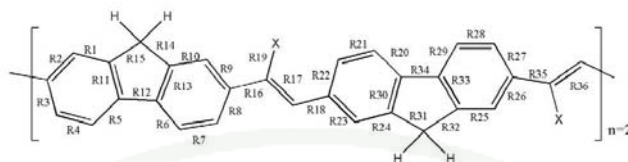


Fig. 1. Structure of poly(fluorene-vinylene) copolymer with replacing 9,9-alkyl group by hydrogen atoms and bond numbering used in this study.

polymerization [10]. This polymer shows good characteristics, such as high molecular weight, low dispersion, and facile purification. In addition, PFV is also a useful material for LED applications. There are some studies of fluorene-vinylene like system available in literatures. Barberis et al. [11] synthesized the three systems of twin molecules including fluorene-hexamethylene bridged (F) and found that it can emitted blue light (428–449 nm). It can also provide the highest photoluminescence (PL) quantum yield in THF solution (0.60). Anastopoulos et al. [12] used a femtosecond time resolved upconversion spectroscopy to measure the excitation energy transfer of poly(fluorenevinylene-co-phenylenevinylene). Pattern of emission wavelengths of this copolymer are depend on its mechanism when excitation process occurs. From our knowledge, there is no theoretical research studied on fluorene-vinylene copolymer and its derivatives, therefore, fundamental understanding on structural and energetic properties of this kind of copolymer could be beneficial knowledge for the design of novel copolymer.

Quantum chemical calculations have been proven to be an important tool for investigation of the relationships between electronic structures and optical properties of the  $\pi$ -conjugated materials. For the theoretical investigation on both the ground and excited states, several theoretical methods have been applied to conjugated polymers [13–17]. In particular, the time-dependence density functional theory (TDDFT) method was developed and used as a powerful tool for the excited-state investigation. Many research groups employed TDDFT to calculate energy gaps and used the extrapolating technique to predict the energy gaps of infinite chain length of various conducting polymers [18–21]. Many publications focus on TDDFT electronic properties related to ground state geometry of conducting polymers, while the properties based on the excited state are not widely investigated. Therefore, calculation of electronic of excited states is still a very challenging task, especially in the calculation of geometry relaxation effects in excited states. Wang et al. [22] used TDDFT method with extrapolation technique to investigate the ionization potentials (IPs), electron affinities (EAs), and HOMO–LUMO gaps ( $\Delta_{H-L}$ ) of fluorene-based conjugated polymer and found that the calculated results are in good agreement even it is slightly underestimated when compared with experimental values of polyfluorene. The same situation was found in the work of Lukes et al.

[23] which methylene-bridge oligofluorene was investigated by TDDFT, RI-CC2, and ZINDO/S methods, indicated that TDDFT results showed underestimated excitation and fluorescence energies. In case of excited-state calculations, Saha et al. [24] used SAC-CI method to investigate both ground and excited state properties of poly(*p*-phenylenevinylene) and poly(*p*-phenylene). The calculations were done with successful results when compared to the experimental data and reference TDDFT calculations with the mean average deviation from available experimental results lies within 0.2 eV. In addition, they point out that conventional TDDFT with the B3LYP functional should be used carefully, because it can provide inaccurate estimates of the chain length dependence of  $\pi$ – $\pi^*$  excitation energies for these molecules with long  $\pi$ -conjugated chains. From the work of Lukes et al. [25], excited-state properties of *p*-phenylene oligomers were investigated by using time-dependence DFT. The computed vertical excitation energy and fluorescence energy are underestimated when compared with experimental results. They also suggested that the limitation of the current approximate exchanges functionals in correctly describing the exchange–correlation potential in the asymptotic region. However, TDDFT can be helpful in understanding fundamentals of the electronic and optical characteristics of conjugated polymers and guiding the experimental efforts toward novel compounds with enhanced characteristics.

Thus, the main objective of this work are to investigate structural, electronic and optical properties of poly(fluorene-vinylene) copolymer and its derivatives by using density functional theory method. Fluorescence energies and radiative lifetimes were analyzed and predicted. The effect of substituents on oligomeric structures and electronic energies was also studied, since a novel conducting polymer will be further synthesized by substituting the electron donating and withdrawing groups on the vinyl position.

## 2. Method of calculations

In this study, fluorene (F) and vinylene (V) copolymers, consisted of (FV)<sub>n</sub> and its derivatives (NH<sub>2</sub>–FV)<sub>n</sub>, (CN–FV)<sub>n</sub>, (OMe–FV)<sub>n</sub> and (OH–FV)<sub>n</sub>, were studied. Structures of the dimer are illustrated in Fig. 2. The ground state and the lowest singlet excited-state geometries of the fluorene-vinylene based oligomers were optimized at the B3LYP/6-31G\* and TD-B3LYP/SVP levels of theory. In order to



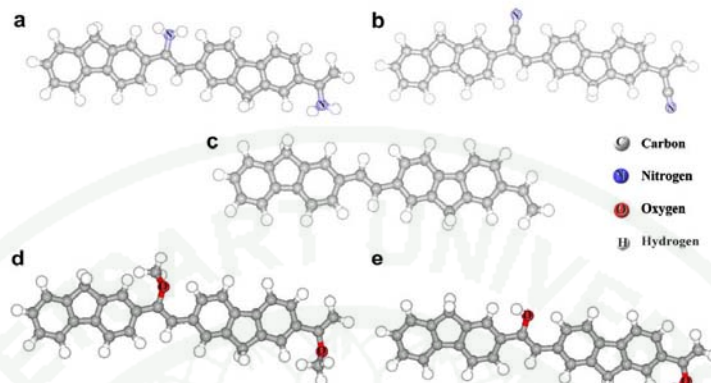


Fig. 2. Dimeric models of fluorene vinylene-based copolymers, (a)  $(\text{NH}_2 \text{ FV})_2$ , (b)  $(\text{CN FV})_2$ , (c)  $(\text{FV})_2$ , (d)  $(\text{OMe FV})_2$ , and (e)  $(\text{OH FV})_2$ .

save computational resources and time, the models for calculations were constructed by replacing alkyl groups ( $\text{C}_8\text{H}_{17}$ ) to the H-atom on the five-membered ring of the fluorene unit. Sriwichitkamol et al. [26] studied the effect of the alkyl group on fluorene oligomers and they proved that the length of alkyl group does not affect the structural and electronic properties of fluorene oligomers. In fact, the alkyl side chain is helpful in increasing the solubility of the polymer. The chain length of fluorene–vinylene derivative oligomers was expanded from dimer to pentamer. On the basis of the optimized geometries, the electronic absorption and fluorescence characteristics were calculated by TD-B3LYP/SVP method. Vertical excitation energies (absorption energy) were computed with TD-B3LYP/SVP and TD-B3LYP/TZVP methods based on the ground state geometries and the results were compared with available experimental data. In addition, an extrapolating technique was employed in the electronic calculations to estimate the energy gap of the polymers. The fluorescence transition was obtained as the vertical de-excitation at the optimized geometry of the excited state. As a result, the radiative lifetimes were also predicted. All calculations were done using the Gaussian 03 [41] and Turbomole version 5.7 [42] program packages, running on Linux 3.4 GHz PC.

### 3. Results and discussion

#### 3.1. Geometries of poly(fluorene–vinylene) copolymer and its derivatives

To understand structural and energetic properties of fluorene–vinylene copolymer and its derivatives, comparison between the ground and excited-state geometries in terms of bond length and torsional angle of these copolymers was investigated. Molecular structure of fluorene–vinylene unit with the bond numbering is displayed in Fig. 1. Then,

geometries of the dimer of fluorene–vinylene ( $\text{FV})_2$  and its derivatives as fundamental models were analyzed and their structures are present in Fig. 2. According to the ground state and the lowest singlet excited-state optimized geometries, based on B3LYP/6-31G\* and TD-B3LYP/SVP calculations, respectively, the change of atomic bond length of all copolymer derivatives at ground state were compared to the fluorene–vinylene dimer as demonstrated in Fig. 3. The most significant bond length differences were found to be at the inter-ring (R16 and R18) and vinylene double bond (R17). For the others, small differences are in the range of  $\pm 0.005 \text{ \AA}$  corresponding to all types of substituents. However, it was found that electron withdrawing

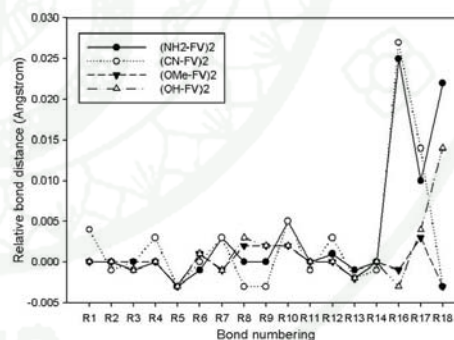


Fig. 3. Relative ground state and the first lowest excitation state bond lengths (in Å), calculated by B3LYP/6-31G\* and TD-B3LYP/SVP methods, respectively, of the copolymer derivatives as compared to fluorene vinylene dimer.  $(\text{NH}_2 \text{ FV})_2$  is represented by solid circle,  $(\text{CN FV})_2$  by open circle,  $(\text{OMe FV})_2$  by solid triangle, and  $(\text{OH FV})_2$  by open triangle.



substituents, such as CN group, make the inter-ring bonding much lengthening than a donating group (OMe, NH<sub>2</sub> and OH) as compared with (FV)<sub>2</sub>. In addition, NH<sub>2</sub> substitution on vinylene unit can extend the inter-ring bonds (R16, R17 and R18). This might be due to the steric effect of NH<sub>2</sub> group to a hydrogen atom on the fluorene unit and weak intramolecular hydrogen bonding occurred.

Next, considering similar structural properties of fluorene–vinylene oligomer, which extend from dimer to pentamer, the models were analyzed and compared based on optimized geometries of the ground state and the first lowest excited state. The relative bond distances of all FV oligomers are illustrated in Fig. 4. It was found that atomic bond lengths in parallel direction (bond numbering R1, R4, R7, R10, R12, R16, R18 and so on) become shorter and other bonds become longer forming a quinoid structure. For all FV-oligomers, the center of the quinoid structures is located at the linking bonds between fluorene units such as R16 and R18, as seen clearly in Fig. 4. Lukes et al. [25] indicated that the elongation of the molecular chain leads only to small changes in the inter-ring distances of *p*-phenylene oligomers and the largest change occurs for a terminal ring becoming an inner one. From Chidthong et al. [27] studied, they found that the inter-ring bond distances do not display appreciable variation with the oligomer size in the series of (FV)<sub>n</sub>. Moreover, the bond-changing pattern is varied systematically when molecular chain is elongated. These behaviors have been also found

in the case of fluorene–vinylene oligomer and its derivatives.

The chain length dependence on the oligomer torsion angles ( $\phi$ ), both at the ground and excited states was then investigated on fluorene–vinylene oligomers and its derivatives. Relative differences of the oligomer torsion angles were compared within the (FV)<sub>n</sub> oligomers. Ground state potential energy surface of FV dimer was calculated by B3LYP method and according to our calculations, it was found that there are two minima located on torsion around 0–15° and 165–180°. The most interesting inter-ring torsional modes are the related torsions between vinylene and fluorene units (Table 1) along the oligomer chain. Yang et al. [28] calculated the structures of three series of copolymeric polyfluorene by B3LYP/6-31G\* method and they found that the bond lengths and bond angles do not suffer appreciable variation with the oligomer size. Corresponding to their results, it was found that the inter-ring dihedral do not display significantly variation with the oligomer size in the series of (FV)<sub>n</sub>. The obtained results bring us to expect the polymer conformation by considering their oligomer geometries. Moreover, there is no remarkable change in the torsional angles between the two states. The vinylene unit apparently develops a good coplanarity with the fluorene unit in the alternating copolymer backbones. Ground state-torsion angles tend to slightly twist (around 2–3°) when increasing the chain length, whereas the excited state-torsion angles are thereby practically

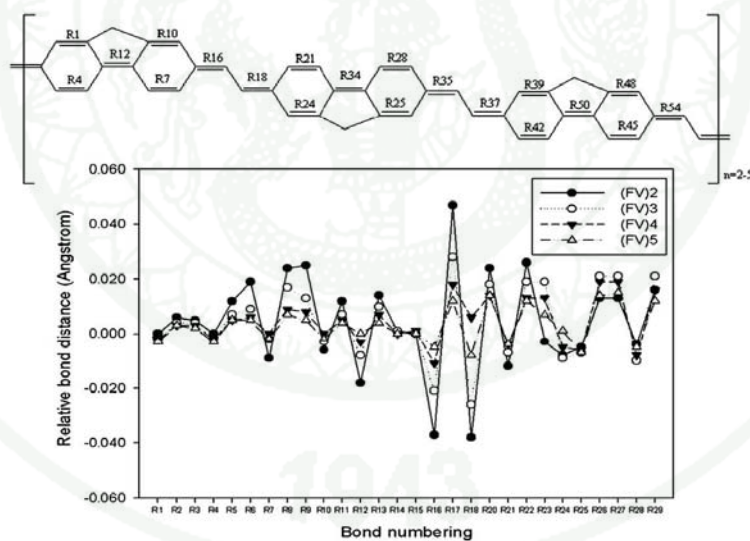


Fig. 4. Changes in bond length (in Å) of FV-derivatives between excitation from S<sub>0</sub> (B3LYP/6-31G\*) to S<sub>1</sub> (TD-B3LYP/SVP). (FV)<sub>2</sub> is represented by solid circle, (FV)<sub>3</sub> by open circle, (FV)<sub>4</sub> by solid triangle, (FV)<sub>5</sub> by open triangle.

Table 1  
Optimized inter-ring torsion angle,  $\phi$  ( $^\circ$ ) of  $(FV)_n$  ( $n = 2-5$ ) in the ground state ( $S_0$ ) and the lowest excited state ( $S_1$ ), obtained from B3LYP/6-31G\* and TD-B3LYP/SVP calculations

		Torsional angle, $\phi$ ( $^\circ$ )							
		$(FV)_2$		$(FV)_3$		$(FV)_4$		$(FV)_5$	
		$S_0$	$S_1$	$S_0$	$S_1$	$S_0$	$S_1$	$S_0$	$S_1$
F <sub>1</sub>	V <sub>1</sub>	179.1	179.6	178.0	179.2	179.5	179.7	179.9	180.0
V <sub>1</sub>	F <sub>2</sub>	179.2	179.6	178.4	179.7	179.4	179.8	178.8	179.3
F <sub>2</sub>	V <sub>2</sub>			179.8	179.9	179.7	179.9	179.9	179.8
V <sub>2</sub>	F <sub>3</sub>			178.9	179.8	179.8	180.0	178.9	179.4
F <sub>3</sub>	V <sub>3</sub>					177.9	179.8	175.7	178.7
V <sub>3</sub>	F <sub>4</sub>					177.6	179.8	175.7	178.6
F <sub>4</sub>	V <sub>4</sub>							179.8	179.8
V <sub>4</sub>	F <sub>5</sub>							179.0	179.7

unaffected and keeps a value of about  $180^\circ$ . This change is within the range of theoretical error.

Comparison between all FV derivatives, the results are shown in Table 2. Ground state potential energy surfaces of the dimeric derivatives were calculated, then, full optimization of the extended FV-based oligomers were performed. From this table, in the case of ground state torsion angle, it can be seen that all substituents can affect to the conjugation along polymer chain. The effect was due to steric hindrance and electronegativity of the substituent groups. Both electron withdrawing (CN) and donating (OMe, NH<sub>2</sub> and OH) groups can twist the inter-ring torsion angle by ca.  $30^\circ$ . In addition, steric effect provides much more shift of torsion angle as found in the case of NH<sub>2</sub> and OMe substituted groups. Especially in the case of  $(NH_2-FV)_3$ , the ground state torsion angles are twisted both side of vinyl group (ground state:  $\phi_{F1-V1} = 150.3^\circ$  and  $\phi_{V1-F2} = 145.6^\circ$ ) and they still unchanged after the excitation (excited state:  $\phi_{F1-V1} = 153.4^\circ$  and  $\phi_{V1-F2} = 144.2^\circ$ ). This steric effect on torsion of NH<sub>2</sub> substituent is also affected to inter-ring bonds that are stretched both side of vinyl group (Fig. 3). From Chidthong et al. [27], they found that excited state dihedral angles always shift to be planar or nearest planar structure. In our case, the results indicate that there are two types of change which is corresponding to type of substituent groups (Fig. 5). Electron withdrawing groups (CN) make the inter-ring constrain even after excitation occurred as can be seen in the Fig. 5 as there are slightly change of torsion angles (less than

Table 2  
Optimized torsion angle,  $\phi$  ( $^\circ$ ) of  $(NH_2-FV)_3$ ,  $(CN-FV)_3$ ,  $(OMe-FV)_3$ , and  $(OH-FV)_3$  in the ground state ( $S_0$ ) and the lowest excited state ( $S_1$ ), obtained from B3LYP/6-31G\* and TD-B3LYP/SVP calculations

		Torsional angle, $\phi$ ( $^\circ$ )							
		$(NH_2-FV)_3$		$(CN-FV)_3$		$(OMe-FV)_3$		$(OH-FV)_3$	
		$S_0$	$S_1$	$S_0$	$S_1$	$S_0$	$S_1$	$S_0$	$S_1$
F <sub>1</sub>	V <sub>1</sub>	150.3	153.4	151.9	155.5	174.1	175.0	179.3	178.0
V <sub>1</sub>	F <sub>2</sub>	145.6	144.2	173.1	175.5	144.7	162.8	146.7	154.5
F <sub>2</sub>	V <sub>2</sub>	152.0	153.2	152.2	153.9	174.7	176.1	179.6	178.7
V <sub>2</sub>	F <sub>3</sub>	145.1	144.7	173.1	173.6	144.4	165.6	146.2	158.5

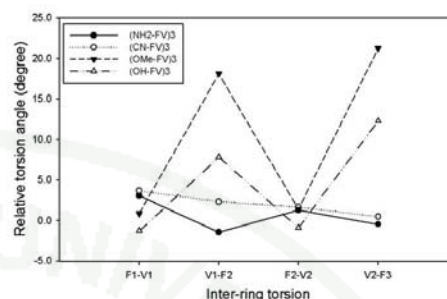


Fig. 5. Ground ( $S_0$ ) and excited ( $S_1$ ) states torsional angle changes (in  $^\circ$ ) of FV-derivatives. Optimized ground state geometries, calculated from B3LYP/6-31G\* method and excited-state geometries, calculated from TD-B3LYP/SVP method.  $(NH_2-FV)_3$  is represented by solid circle,  $(CN-FV)_3$  by open circle,  $(OMe-FV)_3$  by solid triangle,  $(OH-FV)_3$  by open triangle.

$5^\circ$ ). On the other hand, electron donating group (OMe, NH<sub>2</sub> and OH) can handle only one side of torsion (torsion of F<sub>1</sub>-V<sub>1</sub> and F<sub>2</sub>-V<sub>2</sub> are tend to be close to planarity) while another side is about  $150^\circ$  and can be shifted to near planar structure ( $165^\circ$ ) after excitation process.

### 3.2. Singlet vertical excitation energy

The B3LYP/6-31G\* method was used on the basis of the ground state optimized structures to compute vertical electronic excitation energies, HOMO energy, and absorption spectra of all oligomers were investigated in this work (Table 3). The vertical excitations energies with highest oscillator strength ( $\pi-\pi^*$  transition) of each polymer calculated by TD-B3LYP/SVP and TD-B3LYP/TZVP methods were collected and extrapolated by linear regression technique. It was found that excitation energies of these materials are quite lower than the experimental data. There are 2.08 eV for  $(FV)_n$  and 2.40, 2.13, 2.41 and 2.24 eV for its derivatives,  $(NH_2-FV)_n$ ,  $(CN-FV)_n$ ,  $(OMe-FV)_n$  and  $(OH-FV)_n$ , respectively, which are calculated from TD-B3LYP/SVP method. The difference between experiment [10,27] and calculated energy gaps are slightly higher than standard criteria (0.3 eV) even the high basis set (TZVP) was used (2.19 eV for  $(FV)_n$  and 2.37, 2.11, 2.39 and 2.11 eV for its derivatives,  $(NH_2-FV)_n$ ,  $(CN-FV)_n$ ,  $(OMe-FV)_n$  and  $(OH-FV)_n$ , respectively). Corresponding to calculated excitation energies, absorption wavelengths calculated from TD-DFT method with both basis sets are much longer than those of experiments. Our results are in the same trend with Wang et al. [22], Lukes et al. [23] and Geogieva et al. [30] studied. Extrapolated excitation energy of oligofluorene which is calculated from group of Wang showed slightly underestimated about 0.06 eV when compared to the experiment. While in our investigation, oligofluorenevinylene gives much higher deviation from



Table 3

Extrapolated excitation energy ( $E_{exc}$ ), oscillator strength ( $f$ ), HOMO energy, and absorption wavelength ( $\lambda_{abs}$ ) of the derivatives calculated from TD-B3LYP/SVP and TD-B3LYP/TZVP methods, the values in parenthesis are experimental results

	TD-B3LYP/SVP				TD-B3LYP/TZVP			
	$E_{exc}$ (eV)	$f$	HOMO (eV)	$\lambda_{abs}$ (nm)	$E_{exc}$ (eV)	$f$	HOMO (eV)	$\lambda_{abs}$ (nm)
<b>(NH<sub>2</sub> FV)<sub>n</sub></b>								
$n = 2$	3.31	1.18	−4.88	374	3.25	1.17	−5.11	382
$n = 3$	3.00	1.99	−4.74	413	2.95	1.97	−4.97	420
$n = 4$	2.88	2.87	−4.68	430	2.83	2.84	−4.91	438
$n = 5$	2.75	3.50	−4.60	451	2.71	3.46	−4.82	458
$E_g (n = \infty)$	2.40				2.37			
<b>(CN FV)<sub>n</sub></b>								
$n = 2$	2.94	1.54	−5.59	421	2.88	1.48	−5.80	430
$n = 3$	2.64	2.27	−5.52	469	2.60	2.19	−5.70	476
$n = 4$	2.52	3.06	−5.45	491	2.48	2.97	−5.65	499
$n = 5$	2.47	4.01	−5.44	503	2.43	3.89	−5.64	511
$E_g (n = \infty)$	2.13 (2.4) <sup>b</sup>				2.11 (2.4) <sup>b</sup>			
<b>(FV)<sub>n</sub></b>								
$n = 2$	3.10 (3.08) <sup>c</sup>	2.11	−5.03 (−5.49) <sup>c</sup>	401 (368) <sup>c</sup>	3.01 (3.08) <sup>c</sup>	2.01	−5.25 (−5.49) <sup>c</sup>	411 (368) <sup>c</sup>
$n = 3$	2.74 (2.83) <sup>c</sup>	3.20	−4.89 (−5.35) <sup>c</sup>	453 (398) <sup>c</sup>	2.67 (2.83) <sup>c</sup>	3.09	−5.09 (−5.35) <sup>c</sup>	464 (398) <sup>c</sup>
$n = 4$	2.57 (2.74) <sup>c</sup>	4.24	−4.83 (−5.34) <sup>c</sup>	481 (413) <sup>c</sup>	2.61 (2.74) <sup>c</sup>	4.10	−5.03 (−5.34) <sup>c</sup>	471 (413) <sup>c</sup>
$n = 5$	2.49 (2.69) <sup>c</sup>	5.29	−4.80 (−5.33) <sup>c</sup>	497 (419) <sup>c</sup>	2.52 (2.69) <sup>c</sup>	4.87	−5.09 (−5.33) <sup>c</sup>	493 (419) <sup>c</sup>
$E_g (n = \infty)$	2.08 (2.6) <sup>a</sup>				2.19 (2.6) <sup>a</sup>			
<b>(OMe FV)<sub>n</sub></b>								
$n = 2$	3.18	1.95	−4.86	389	3.12	1.91	−5.08	397
$n = 3$	2.90	2.76	−4.80	427	2.85	2.70	−5.02	435
$n = 4$	2.79	3.45	−4.83	444	2.74	3.38	−5.03	452
$n = 5$	2.73	4.33	−4.84	454	2.70	3.46	−4.82	458
$E_g (n = \infty)$	2.41				2.39			
<b>(OH FV)<sub>n</sub></b>								
$n = 2$	3.21	1.32	−4.94	386	3.16	1.29	−5.17	292
$n = 3$	2.84	2.04	−4.77	437	2.80	2.06	−5.00	443
$n = 4$	2.70	2.73	−4.70	458	2.67	2.76	−4.96	464
$n = 5$	2.65	3.61	−4.68	468	2.61	3.62	−4.91	474
$E_g (n = \infty)$	2.24				2.21			

Column 1 indicates the oligomers ( $n = 2-5$ ) and the polymers ( $n = \infty$ ) for different copolymers.

<sup>a</sup> Ref. [10]

<sup>b</sup> Ref. [29]

<sup>c</sup> Ref. [38]

the experimental results (calculated excitations are underestimated about 0.4 eV). For fluorenevinylene dimer, excitation energy and HOMO energy calculated from TDDFT/SVP method are overestimated in comparison to experimental data. These energies decreased when conjugation length are elongated. For oligofluorenevinylene (FV)<sub>n</sub> which  $n = 3-5$ , the excitation energies and HOMO energies are underestimated when compared to experimental results. Based on our TDDFT data, it was found that a significant underestimation of the excitation energies for the larger oligomers is in agreement with theoretical results of methylene-bridge oligofluorene [23]. In the work of Georgieva group, they varied the size of basis set in electronic calculation of coumarin system. The extension of basis set from SVP to TZVP led to small decrease in excitation energy for  $\pi-\pi^*$  transition and increase of excitation energy for  $n-\pi^*$  transition. Moreover, they compared the calculated energy gap in gas phase and in an aqueous solvent condition (with PCM model) as well. The presence

of solvent can slightly decrease the energy gap of coumarin and give a good agreement with experimental results. Some reports suffered from this theoretical deviation, Hutchison et al. [31] and Brooks et al. [32] pointed out that density functional theory (DFT) method within the local-density approximation (LDA) can compute equilibrium geometries in excellent agreement with experiment for both conjugated organic oligomers and polymers. However, DFT method calculated band gaps are typically on the order of 40% smaller than the experimental optical absorption band-gap data for conjugated organic materials, polymers. Suramitr et al. [33] studied on oligophenylenevinylene derivatives and also found that extrapolated excitation energies calculated by TD-DFT are underestimated when compared to the experiment. However, there are several successful investigations on the TD-DFT excitation energy prediction [34–37]. Because the excitation energy of polymer depends on planarity along chain length, polymers that suffered from the steric hindrance on the inter-ring

position show the higher energy (blue shift) than others. It can be clearly seen in the case of  $(\text{NH}_2\text{-FV})_n$  and  $(\text{OMe-FV})_n$ , and the  $E_{\text{exc}}$  calculated from TD-B3LYP/SVP and TD-B3LYP/TZVP (values in parenthesis) methods are 2.40(2.37), 2.41(2.39) eV, respectively. Poolmee et al. [34] performed the calculation on fluorene thiophene copolymer and they showed that TD-DFT excitation energies using DFT and AM1 optimized geometries provide a good energy gap due to the shortening inter-ring distance and planarity of oligomer structure.

In the case of FV oligomers, there are experimental data of HOMO energy absorption wavelength and excitation energy of each oligomer [38]. It can be seen that our calculated values are in good agreement with the experimental data. Jansson et al. [39] studied the chain length dependence of singlet and triplet excited states of oligofluorene ( $n = 2-7$ ) and used an empirical relationship proposed by Meier et al. [40]. From their results, the linear relationships between excitation energy and  $1/n$  are observed only in range of  $n$  less than 5 with corresponding to the fitting parameter. For  $n > 5$ , excitation energy seems to be in constant value. Finally they suggested that to get more accurate excitation energy for the infinite oligomer, one needs to use higher order polynomials.

### 3.3. Fluorescence energy and lifetime

Fluorescence energies and lifetime computed with the TD-B3LYP/SVP method using  $S_1$  optimized geometries are collected in Table 4. The extrapolated fluorescence energies obtained from the TD-B3LYP/SVP method since the linear relationship between the fluorescence energies on the reciprocal chain lengths are supposed. According to Table 4, it is shown that the fluorescence energies of every molecule are red shift from the excitation energies. There are 1.74, 1.78, 2.00, and 1.73 eV for  $(\text{CN-FV})_n$ ,  $(\text{FV})_n$ ,  $(\text{OMe-FV})_n$ , and  $(\text{OH-FV})_n$  respectively. Radiative lifetimes were calculated on the basis of fluorescence energy and oscillator strengths according to the following formula [43] (in a.u.),

$$\tau = \frac{c^3}{2(E_{\text{flu}})^2 f}$$

Table 4  
Extrapolated fluorescence energies ( $E_{\text{flu}}$ ) and radiative lifetimes versus inverse chain length of FV oligomers as obtained from TD-B3LYP/SVP calculations

	TD-B3LYP/SVP	
	$E_{\text{flu}}$ (eV)	Lifetime (ns)
$(\text{NH}_2\text{-FV})_n$		
$(\text{CN-FV})_n$	1.74	1.0
$(\text{FV})_n$	1.78	0.6 (0.46) <sup>a</sup>
$(\text{OMe-FV})_n$	2.00	0.8
$(\text{OH-FV})_n$	1.73	1.0

Geometries were optimized at TD-B3LYP/SVP level.

<sup>a</sup> Ref. [44].

where  $c$  is the velocity of light,  $E_{\text{flu}}$  is the fluorescence transition energy, and  $f$  is oscillator strength. Fluorescence lifetime provides information useful in discrimination of particles. Extension of the conjugated backbone leads to a decrease of lifetimes. The lifetime of these molecules are slightly difference by ca. 0.2–0.4 ns. Lifetime of  $(\text{FV})_n$ ,  $(\text{CN-FV})_n$ ,  $(\text{OMe-FV})_n$  and  $(\text{OH-FV})_n$  are 0.6, 0.8, 1.0 and 1.0 ns, respectively. Among the three derivatives, the  $(\text{OMe-FV})_n$  shows the lowest lifetime which is close to polyfluorene-vinylene. For the sake of comparison, a chemically similar system, poly(9,9-dihexylfluorene), was used as an experimental result. Fluorescence lifetime of poly(9,9-dihexylfluorene) in THF solution is 0.46 ns [44] which is in agreement with the lifetime of the predicted  $(\text{FV})_n$  (0.6 ns).

### 4. Conclusions

TD-DFT with B3LYP functional geometry was found to be a suitable method to estimate both structural parameters and electronic properties of poly-(9,9-dialkylfluorene-2,7-vinylene). Substitution on vinylene unit by various functional groups was considered and resulting FV derivatives;  $(\text{NH}_2\text{-FV})_n$ ,  $(\text{CN-FV})_n$ ,  $(\text{OMe-FV})_n$  and  $(\text{OH-FV})_n$  ( $n = 2-5$ ). Most of the derivative of FV copolymer exhibit planar structures at excitation state, whereas,  $\text{NH}_2$  and  $\text{OMe}$  substituted oligomers display small shift from the planarity. Theoretical excited-state calculations of modeling polymeric systems are quite underestimated to those of the available experimental data. The predicted fluorescence lifetime of  $(\text{FV})_n$  is in good agreement when compared with the chemically similar system, poly(9,9-dihexylfluorene). The obtained results indicate that substituents on vinylene unit can exhibit different electronic properties of the whole polymer. According to our results, we suggested that polyfluorene-vinylene with methoxy substitution on vinylene unit is an interesting material to be further synthesized as this copolymer demonstrates to give high excitation energy within the fluorene-vinylene derivatives under this investigation.

### Acknowledgements

We thank the Thailand Research Fund (TRF research scholar RSA5080005), the Thailand Graduated Institute of Science and Technology (TGIST), the Postgraduate Education and Research on Petroleum, Petrochemical Technology and Advanced Materials, Ministry of Education, and the Center of Nanotechnology Kasetsart University, Kasetsart University Research and Development Institute (KURDI) for financial support. Partial supporting by National Nanotechnology Center (NANOTEC), Ministry of Science and Technology, Thailand, through its program of Center of Excellence Network is grateful. Finally, Large scale research laboratory (LSR): ITANIUM of the National Electronics and Computer Technology Center (NECTEC), Ministry of Science and Technology,



LCAC and computing center of KU for computing resources and research facilities.

#### Appendix A. Supplementary material

Supplementary data associated with this article can be found, in the online version, at doi:10.1016/j.chemphys.2008.02.025.

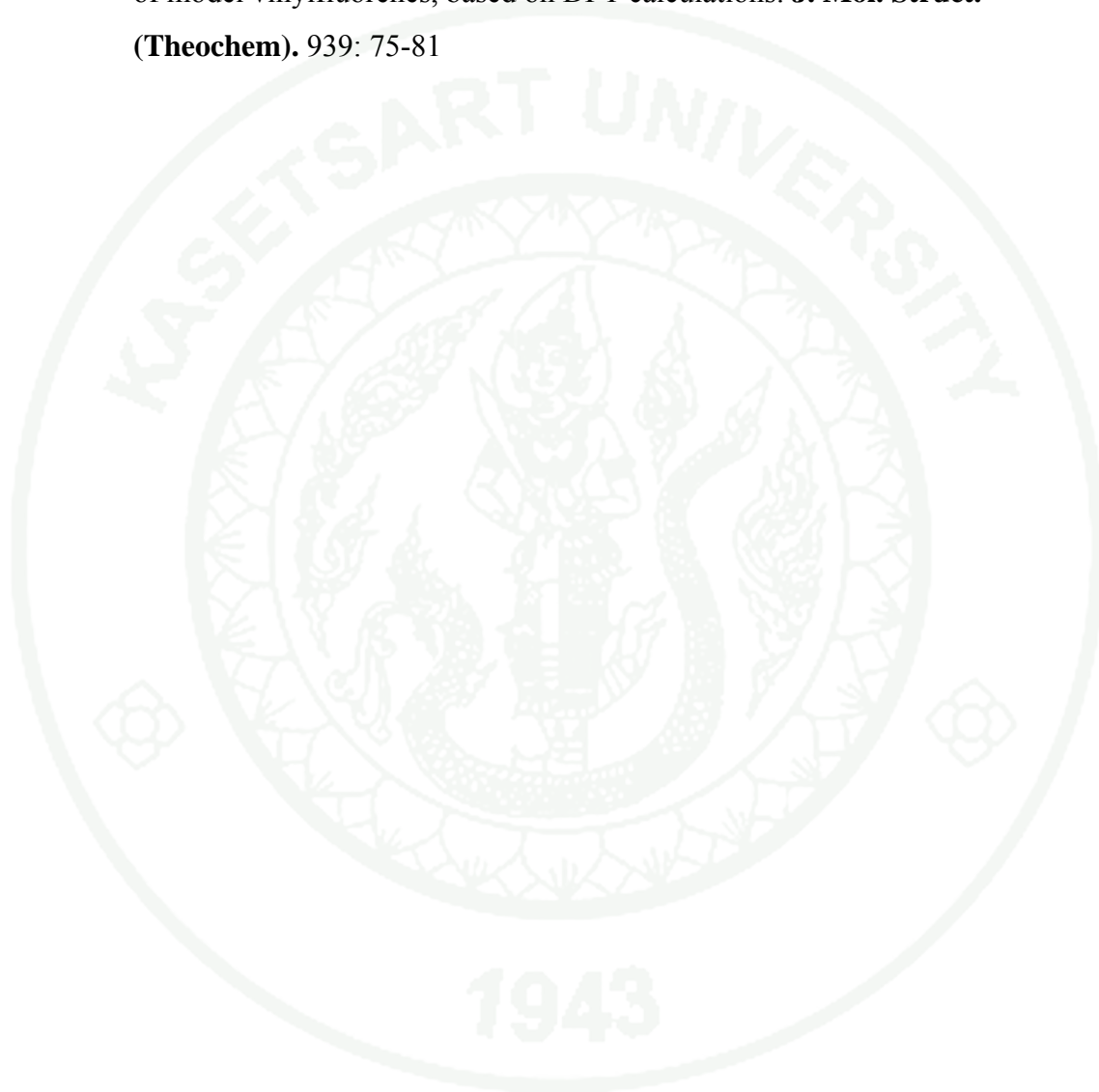
#### References

- [1] J.H. Burroughes, D.D.C. Bradley, A.R. Brown, R.N. Marks, K. Mackay, R.H. Friend, P.L. Burns, A.B. Holmes, *Nature* 347 (1990) 539.
- [2] C.K. Chiang, C.R. Fincher Jr., Y.W. Park, A.J. Heeger, H. Shirakawa, E.J. Louis, S.C. Gau, A.G. MacDiarmid, *Phys. Rev. Lett.* 39 (1977) 1098.
- [3] B. Becker, H. Spreitzer, K. Ibrom, W. Kreuder, *Macromolecules* 32 (1999) 4925.
- [4] M. Grell, D.D.C. Bradley, M. Inbasekaran, E.P. Woo, *Adv. Mater.* 9 (1997) 798.
- [5] Q. Pei, Y. Yang, *J. Am. Chem. Soc.* 118 (1996) 7416.
- [6] M. Ranger, D. Rondeau, M. Leclerc, *Macromolecules* 30 (1997) 7686.
- [7] K. Nomura, H. Morimoto, Y. Imanishi, Z. Rambani, Y. Geerts, *J. Polym. Sci., Part A* 39 (2001) 2463.
- [8] H.N. Cho, D.Y. Kim, J.K. Kim, C.Y. Kim, *Synthetic Met.* 91 (1997) 293.
- [9] K.A. Nguyen, J. Kennel, R.J. Pachter, *Chem. Phys.* 117 (2002) 7128.
- [10] S.H. Jin, H.J. Park, J.Y. Kim, K. Lee, S.P. Lee, D.K. Moon, H.J. Lee, Y.S. Gal, *Macromolecules* 35 (2002) 7532.
- [11] V.P. Barberis, J.A. Mikroyannidis, *Synthetic Met.* 156 (2006) 1408.
- [12] D. Anastopoulos, M. Fakis, P. Persephoinis, V. Giannetas, J. Mikroyannidis, *Chem. Phys. Lett.* 421 (2006) 205.
- [13] F. Costanzo, D. Tonelli, G. Scalmani, J. Cornil, *Polymer* 47 (2006) 6692.
- [14] L.D.A. Siebbeles, F.C. Grozema, M.P. Haas, J.M. Warman, *Radiat. Phys. Chem.* 72 (2005) 85.
- [15] S. Yang, P. Oleshevski, M. Kertesz, *Synthetic Met.* 141 (2004) 171.
- [16] P. Poolmee, M. Ehara, S. Hannongbua, H. Nakatsuji, *Polymer* 46 (2005) 6474.
- [17] I. Corral, L. Gonzalez, *Chem. Phys. Lett.* 446 (2007) 262.
- [18] M. Barbati, G. Granucci, M. Persico, H. Lischka, *Chem. Phys. Lett.* 401 (2005) 276.
- [19] L. Yang, Y. Liao, J.K. Feng, A.M. Ren, *J. Chem. Phys.* 109 (2005) 7774.
- [20] E. Badaeva, S. Tretiak, *Chem. Phys. Lett.* 450 (2008) 332.
- [21] J.S.K. Yu, W.C. Chen, C.H. Yu, *J. Phys. Chem. A* 107 (2003) 4268.
- [22] J.F. Wang, J.K. Feng, A.M. Ren, X.D. Liu, Y.G. Ma, P. Lu, H.X. Zhang, *Macromolecules* 37 (2004) 3451.
- [23] V. Lukes, A. Aquino, H. Lischka, *J. Phys. Chem. A* 109 (2005) 10232.
- [24] B. Saha, M. Ehara, H. Nakatsuji, *J. Phys. Chem. A* 111 (2007) 5473.
- [25] V. Lukes, A. Aquino, H. Lischka, H.F. Kauffmann, *J. Phys. Chem. B* 111 (2007) 7954.
- [26] K. Sriwichitkamol, S. Suramit, P. Poolmee, S. Hannongbua, *J. Theor. Comp. Chem.* 5 (2006) 595.
- [27] R. Chidthong, S. Hannongbua, A. Aquino, P. Wolschann, H. Lischka, *J. Comput. Chem.* 28 (2007) 1735.
- [28] L. Yang, Y. Liao, J.K. Feng, A.M. Ren, *J. Phys. Chem. A* 109 (2005) 7764.
- [29] Y. Jin, J. Ju, J. Kim, S. Lee, L.Y. Kim, S.H. Park, S. Son, S. Jin, K. Lee, H. Suh, *Macromolecules* 36 (2003) 6970.
- [30] I. Georgieva, N. Trendafilova, A. Aquino, H. Lischka, *J. Phys. Chem. A* 109 (2005) 11860.
- [31] G.R. Hutchison, Y.J. Zhao, B. Delley, A.J. Freeman, M.A. Ratner, T.J. Marks, *Phys. Rev. B* 68 (2003) 035204.
- [32] G. Brooks, P.J. Kelly, R. Car, *Synthetic Met.* 57 (1993) 4243.
- [33] S. Suramit, T. Kerdcharoen, T. Srihirin, S. Hannongbua, *Synthetic Met.* 155 (2005) 27.
- [34] P. Poolmee, S. Hannongbua, *J. Theor. Comp. Chem.* 3 (2004) 481.
- [35] C.P. Hsu, S. Hirata, M. Head-Gordon, *J. Phys. Chem. A* 105 (2001) 451.
- [36] L. Serrano-Andres, M. Merchán, *J. Mol. Struct. (THEOCHEM)* 729 (2005) 99.
- [37] M. Belletete, G. Durocher, S. Hamel, M. Cote, S. Wakim, M. Leclerc, *J. Chem. Phys.* 122 (2005) 104303.
- [38] G. Liu, W. Liu, B. Yao, H. Tian, Z. Xie, Y. Geng, F. Wang, *Macromolecules* 40 (2007) 1851.
- [39] E. Jansson, P.C. Jha, H. Ågren, *Chem. Phys.* 336 (2007) 91.
- [40] H. Meier, U. Stalmach, H. Kolshorn, *Acta Polym.* 48 (1997) 379.
- [41] M.J. Frisch, G.W. Trucks, H.B. Schlegel, G.E. Scuseria, M.A. Robb, J.R. Cheeseman, J.A. Montgomery Jr., T. Vreven, K.N. Kudin, J.C. Burant, J.M. Millam, S.S. Iyengar, J. Tomasi, V. Barone, B. Mennucci, M. Cossi, G. Scalmani, N. Rega, G.A. Petersson, H. Nakatsuji, M. Hada, M. Ehara, K. Toyota, R. Fukuda, J. Hasegawa, M. Ishida, T. Nakajima, Y. Honda, O. Kitao, H. Nakai, M. Klene, X. Li, J.E. Knox, H.P. Hratchian, J.B. Cross, V. Bakken, C. Adamo, J. Jaramillo, R. Gomperts, R.E. Stratmann, O. Yazyev, A.J. Austin, R. Cammi, C. Pomelli, J.W. Ochterski, P.Y. Ayala, K. Morokuma, G.A. Voth, P. Salvador, J.J. Dannenberg, V.G. Zakrzewski, S. Dapprich, A.D. Daniels, M.C. Strain, O. Farkas, D.K. Malick, A.D. Rabuck, K. Raghavachari, J.B. Foresman, J. V. Ortiz, Q. Cui, A.G. Baboul, S. Clifford, J. Cioslowski, B.B. Stefanov, G. Liu, A. Liashenko, P. Piskorz, I. Komaromi, R.L. Martin, D.J. Fox, T. Keith, M.A. Al-Laham, C.Y. Peng, A. Nanayakkara, M. Challacombe, P.M.W. Gill, B. Johnson, W. Chen, M.W. Wong, C. Gonzalez, J.A. Pople, Gaussian, Inc., Wallingford CT, 2004.
- [42] R. Ahlrichs, M. Bär, M. Häser, H. Horn, C. Kölmel, *Chem. Phys. Lett.* 162 (1989) 165.
- [43] B.H. Branden, C.J. Joachain, *Physics of Atoms and Molecules*, Longman Group Limited, London, 1983.
- [44] X.H. Zhou, Y. Zhang, Y.Q. Xie, Y. Cao, J. Pei, *Macromolecules* 39 (2006) 3830.



**Publication II**

Meeto, W., S. Suramitr, V. Lukeš, P. Wolschann and S. Hannongbua. 2010. Effects of the CN and NH<sub>2</sub> substitutions on the geometrical and optical properties of model vinylfluorenes, based on DFT calculations. **J. Mol. Struct. (Theochem)**. 939: 75-81





Contents lists available at ScienceDirect

Journal of Molecular Structure: THEOCHEM

journal homepage: [www.elsevier.com/locate/theochem](http://www.elsevier.com/locate/theochem)

## Effects of the CN and NH<sub>2</sub> substitutions on the geometrical and optical properties of model vinylfluorenes, based on DFT calculations

Wichanee Meeto<sup>a</sup>, Songwut Suramitr<sup>a</sup>, Vladimír Lukeš<sup>b</sup>, Peter Wolschann<sup>c</sup>, Supa Hannongbua<sup>a,\*</sup>

<sup>a</sup> Department of Chemistry, Faculty of Science, and Center of Nanotechnology, Kasetsart University, Bangkok 10900, Thailand

<sup>b</sup> Department of Chemical Physics, Slovak University of Technology, Radlinského 9, SK-81 237 Bratislava, Slovakia

<sup>c</sup> Institute for Theoretical Chemistry, University of Vienna, Währingerstrasse 17, A-1090 Wien, Austria

### ARTICLE INFO

#### Article history:

Received 16 July 2009

Received in revised form 21 September 2009

Accepted 21 September 2009

Available online 6 October 2009

#### Keywords:

Bifluorenevinylene

Density functional theory

Torsional potential

Vertical excitation energy

Conducting polymer

Substitutional effect

### ABSTRACT

A systematic study on the structural and photo-physical properties of model bifluorenevinylene compounds based on the density functional theory (DFT) and its time-dependent (TD-DFT) version is presented. The main aim of this work is to investigate the influence of substitution on bifluorenevinylene using strong electron acceptor CN or electron donor NH<sub>2</sub> groups on: (a) the optimal geometry, (b) torsional potentials and (c) photo-physical properties. Our results indicate that the substitution on the vinylene bridge, leads to the twisting of molecular fragment on the side of added group and are in good overall agreement with experiment. In the case of the amino mono-substituted bifluorenevinylene, the amino group leads to non-planarity at the non-substituted portion of the molecule. The chemical modification also have a pronounced impact on the electronic properties. The shape of the potential energy curves evaluated for the lowest vertically excited states is heavily dependent on the molecular conformation. Finally, we discuss how the structural and electronic information presented here can be useful in designing of novel optical materials as well as understanding of excitation–relaxation phenomena which may occur in various time-dependent optical experiments.

© 2009 Elsevier B.V. All rights reserved.

### 1. Introduction

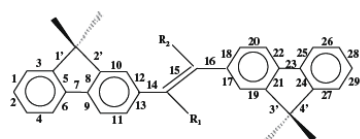
Polyfluorenes, with their excellent photoluminescence quantum characteristics, excellent solubility in common organic solvents, can be used as blue-shift emitters [1,2]. Additionally, their thermal and chemical stability can be modified and improved by adding of different alkyl substituents at the 9-th position of the fluorene ring [3]. However, the polyfluorenes systems containing simple connected fluorene units tend to aggregate in the condensed phase and provide less effective performance. Fortunately, these problems can be limited with the modification of their molecular structure, such as the polyfluorene-2,7-vinylenes (PFVs) [4]. Moreover, the various electron-donating or electron-accepting groups can be added to the vinylene bridge located within the aromatic molecular chain which subtly alters the intermolecular steric interactions which can be used to effectively tune the optical spectra from blue to the infrared region without the necessity to perturb the planarity of aromatic units [5,6].

Theoretical quantum studies of  $\pi$ -conjugated oligomers or polymers can provide a fundamental understanding of the physical process occurring, and make a considerable contribution to the design of novel optoelectronic materials. These include theoretical

studies done using semiempirical, *ab initio* and density functional theory (DFT) methods, focusing on the electronic properties based on the ground-state equilibrium geometries [7–10]. Among them, the DFT approach and its time-dependent (TD) extension [11] for the excited states have been successfully demonstrated in investigations of optical and electronic properties of moderate to large organic conjugated oligomers [12]. These results are often used in cooperation with the experimental data to characterize the structural, electronic and optical properties of conjugated polymers and represent primary information to aid in our understanding of phenomena connected with conformation relaxation processes occurring during the electronic excitation and/or de-excitation [13]. Bifluorenevinylene derivatives are the focus of this research investigation, being shortest computationally efficient representation of oligo- and poly-vinylfluorenes which are of significant scientific interest.

The main aim of this work is the investigation of the direct influence of substitution using strong electron acceptor CN or electron donor NH<sub>2</sub> groups on the optimal geometry, torsional potentials and photo-physical properties. We do this by modifying the electronic structure of these model systems by the symmetric or asymmetric addition of the representative electron-accepting cyano and electron-donating amino groups on vinyl positions (see Fig. 1). We focus on the *all-trans* conformations and the electronic ground-state torsional potential curves in this investigation. The

\* Corresponding author. Tel.: +66 2 562555x2140; fax: +66 2 5793955.  
E-mail address: [fsicph@ku.ac.th](mailto:fsicph@ku.ac.th) (S. Hannongbua).



Molecule	R <sub>1</sub>	R <sub>2</sub>
F <sub>2</sub> V	H	H
F <sub>2</sub> V-(CN) <sub>2</sub>	CN	CN
F <sub>2</sub> V-(NH <sub>2</sub> ) <sub>2</sub>	NH <sub>2</sub>	NH <sub>2</sub>
F <sub>2</sub> V-CN	CN	H
F <sub>2</sub> V-NH <sub>2</sub>	NH <sub>2</sub>	H
F <sub>2</sub> V-CN-NH <sub>2</sub>	CN	NH <sub>2</sub>

Fig. 1. Schematic structure, bond and dihedral angle numbering of studied systems in *all-trans* conformation.

corresponding vertical excitation characteristics of these molecules are calculated using (TD)-DFT method. Finally, the physical origin of the lowest electronic transitions will be explained using molecular orbital analysis.

## 2. Methodology

The geometries and torsion potential of studied dimers F<sub>2</sub>V, F<sub>2</sub>V-(CN)<sub>2</sub>, F<sub>2</sub>V-(NH<sub>2</sub>)<sub>2</sub>, F<sub>2</sub>V-CN, F<sub>2</sub>V-NH<sub>2</sub> and F<sub>2</sub>V-CN-NH<sub>2</sub> (formula and abbreviations are given in Fig. 1) are optimized by the DFT method using the Becke three parameter hybrid (B3LYP) [14] functional in conjunction with the 6-31G(d) basis set [15]. The torsion potentials were calculated for the fixed angles from the

Table 1

The B3LYP/6-31G(d) optimal dihedral angles (in deg) and BLA parameters (in Å) for *all-trans* conformations.

Molecule	Θ <sub>1</sub>	Θ <sub>2</sub>	BLA
F <sub>2</sub> V	0	0	0.224
F <sub>2</sub> V-(CN) <sub>2</sub>	38	−38	0.218
F <sub>2</sub> V-(NH <sub>2</sub> ) <sub>2</sub>	45	−45	0.236
F <sub>2</sub> V-CN	28	−7	0.212
F <sub>2</sub> V-NH <sub>2</sub>	36	−31	0.227
F <sub>2</sub> V-CN-NH <sub>2</sub>	52	−44	0.223

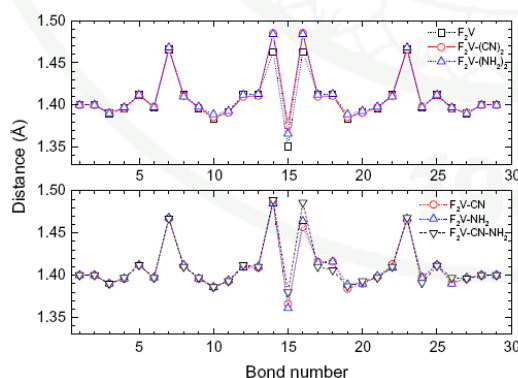


Fig. 2. Computed B3LYP/6-31G(d) bond lengths of the molecules under study in *all-trans* conformation. For notation see Fig. 1.

Table 2  
The lowest excitation energies in eV and oscillator strengths (values in parentheses) for the optimal *all-trans* geometries. The values written in italics stand for the excitation contributions in percentage involved in each calculated transition (H denotes HOMO and L is LUMO).

Molecule	S <sub>1</sub>	S <sub>2</sub>	S <sub>3</sub>	S <sub>4</sub>	S <sub>5</sub>	S <sub>6</sub>	S <sub>7</sub>
F <sub>2</sub> V	3.23 (1.870) 99%: H → L	3.98 (0.000) 60%: H-1 → L 38%: H → L+1	4.18 (0.000) 50%: H → L+3 36%: H-2 → L	4.19 (0.006) 68%: H → L+2 32%: H-3 → L	4.41 (0.00) 43%: H → L+2 57%: H-4 → L	4.44 (0.019) 33%: H-2 → L 67%: H-5 → L	4.44 (0.000) 60%: H-3 → L 40%: H-6 → L
F <sub>2</sub> V-(CN) <sub>2</sub>	2.82 (0.907) 99%: H → L	3.22 (0.000) 97%: H-1 → L 3%: H → L+1	3.64 (0.009) 70%: H-2 → L 30%: H-3 → L	3.67 (0.000) 75%: H-3 → L 25%: H-4 → L	3.67 (0.000) 68%: H-4 → L 32%: H-5 → L	3.88 (0.000) 73%: H-5 → L 27%: H-6 → L	4.29 (0.336) 72%: H-6 → L 28%: H-7 → L
F <sub>2</sub> V-(NH <sub>2</sub> ) <sub>2</sub>	2.90 (0.586) 99%: H → L	3.30 (0.000) 97%: H → L+1 3%: H-1 → L	3.53 (0.009) 94%: H → L+2 6%: H-2 → L	3.61 (0.000) 92%: H → L+3 8%: H-3 → L	4.21 (0.016) 91%: H → L+4 9%: H-4 → L	4.24 (0.000) 90%: H → L+5 10%: H-5 → L	4.41 (0.713) 93%: H-2 → L+1 7%: H → L+1
F <sub>2</sub> V-CN	3.08 (1.424) 99%: H → L	3.72 (0.096) 91%: H-1 → L 9%: H → L+1	4.08 (0.002) 98%: H-2 → L 2%: H-3 → L	4.08 (0.016) 62%: H-3 → L 38%: H-4 → L	4.22 (0.007) 42%: H-4 → L 58%: H-5 → L	4.26 (0.006) 44%: H-5 → L 56%: H-6 → L	4.39 (0.063) 75%: H → L+1 25%: H-6 → L
F <sub>2</sub> V-NH <sub>2</sub>	3.29 (1.099) 99%: H → L	3.86 (0.251) 87%: H → L+1 13%: H-1 → L	4.03 (0.013) 67%: H-1 → L 33%: H-2 → L	4.08 (0.021) 69%: H → L+3 31%: H-3 → L	4.40 (0.079) 83%: H-1 → L 17%: H-2 → L	4.54 (0.023) 39%: H → L+6 61%: H-4 → L	4.58 (0.027) 41%: H → L+5 59%: H-4 → L
F <sub>2</sub> V-CN-NH <sub>2</sub>	3.53 (0.824) 98%: H → L	4.01 (0.165) 73%: H → L+1 27%: H-1 → L	4.25 (0.006) 70%: H-1 → L 30%: H-2 → L	4.29 (0.085) 67%: H → L+1 33%: H-3 → L	4.38 (0.010) 61%: H → L+3 39%: H-4 → L	4.41 (0.131) 70%: H-2 → L 30%: H-5 → L	4.63 (0.015) 70%: H-4 → L 30%: H-6 → L

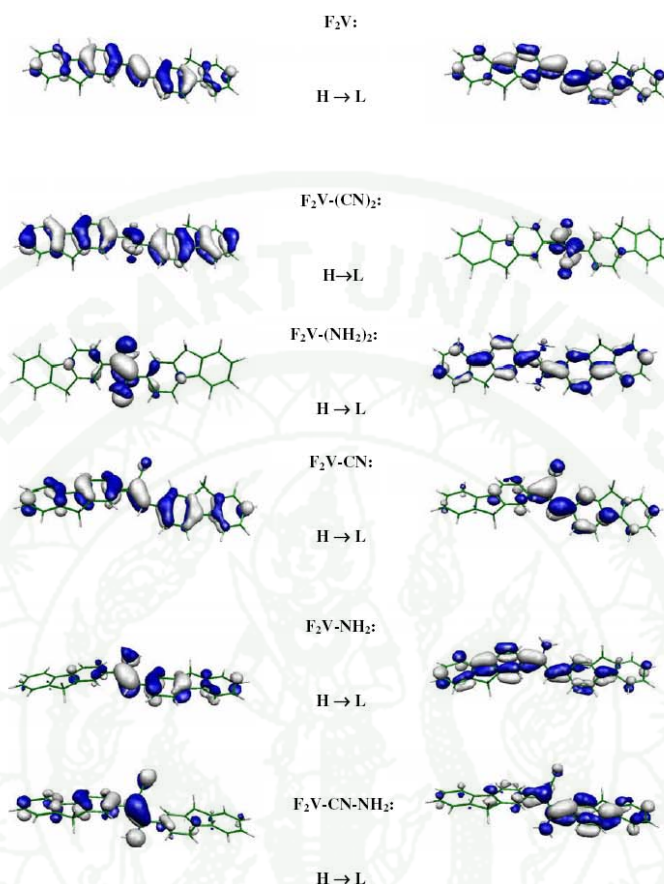


Fig. 3. Plots of the B3LYP/6-31G(d) molecular orbitals contributing significantly to the lowest energy transitions of studied molecules in *all-trans* conformation. H denotes HOMO and L is LUMO.

interval  $0^\circ$  to  $180^\circ$  using a  $10^\circ$  step size. In the case of asymmetric molecules, dihedral angles for both sides were investigated due to the different steric effects. Singlet vertical excitation energies are calculated from the optimized geometries using the TD-B3LYP method. All calculations are performed using the Gaussian 03 program package [16]. Due to the computational cost reduction, the alkyl groups at 9-th position on fluorene ring were replaced by hydrogen atoms. This is because reports suggest that substituents at the 9-th position play an important role in the thermal stability and solubility but do not affect the electronic structure and optical property of fluorene-based polymer [17,18]. All minima were confirmed as such through normal mode analysis, displaying no imaginary vibration frequencies.

### 3. Results and discussion

Comparison of the optimized ground-state  $1^1A$  geometries in terms of bond lengths and torsional angles can help us to understand the structural and energetic differences observed between

the different systems. Schematic visualization of the molecular structure of the bifluorenevinylene skeleton studied here are given in Fig. 1. The data presented in Table 1 show the energy profile for the dihedral angles  $\theta_1$  (between the bond nos. 12, 14 and 15) and  $\theta_2$  (between the bond nos. 15, 16 and 17) between fluorene unit and the vinylene bridge on the substitution. The B3LYP/6-31G(d) calculation indicates the structure of  $F_2V$  molecule is completely planar. Substitution at the vinylene bridge leads to the perturbation of planarity due to the steric hindrance and the effect of electronegativity from nitrogen atoms in the vicinity of the newly added substituents. In the case of mono-substituted molecules, the presence of CN substituents increases the angle  $\theta_1$  to the value of  $30^\circ$  while the torsion for  $NH_2$  group is higher,  $35^\circ$ . Interestingly, the second angle  $\theta_2$  is evidently non-planar only for molecule  $F_2V-NH_2$ . The symmetric bi-substitution is responsible for a torsion angle increase of  $\sim 10^\circ$  with respect to the mono-substituted systems. The most distorted structure is obtained for the asymmetric  $F_2V-CN-NH_2$  molecule, where the torsion on the side of cyano group results in a dihedral angle of  $52^\circ$ .



The computed bond lengths for the molecules studied here are presented in Fig. 2. In all cases the smallest C–C bond distances are located in the central part of the fluorene rings (see bond nos. 3, 10, 19 and 27) and double bond on vinylene bridge (see bond no. 15). The largest bond lengths are found for the inter-ring distances (bond nos. 7 and 23) which have a larger single bond character than the next bonds in the fluorene unit. The single bond nos. 14 and 16 on vinylene bridge exhibit also the largest distances. The substitution of vinylene bridge affects only the bonds in the vicinity of added group, especially the bonds of vinylene bridge. The double bond no. 15 as well as the neighbouring single bond nos. 14 and 16 are elongated while the bonds on rigid fluorene rings are very slightly shortened. Our calculations indicate that the differences in bond length changes for CN and NH<sub>2</sub> substitutions are significant only for bond no. 15. The CN substitution elongates it at 0.03 Å while the amino group changes it only 0.02 Å with respect to the F<sub>2</sub>V molecule. Similar changes in bond lengths are observed for the mono-substituted NH<sub>2</sub> and CN compounds. However, in this case the bonds on the side of the substituted part are affected. The asymmetric substitution of F<sub>2</sub>V–CN–NH<sub>2</sub> molecule leads to the formation of electronic system where NH<sub>2</sub> acts as an electron donor to the aromatic system and the fluorene atoms as electron acceptor. In comparison with previously discussed molecules the bonds on the side of CN group and located on fluorene rings (bond nos. 17, 18, 24 and 26) are more influenced than in the F<sub>2</sub>V–CN and F<sub>2</sub>V–(CN)<sub>2</sub> molecules.

Bond length changes in aromatic systems can be efficiently described using the bond length alternation (BLA) definition [19]. The BLA values for a given molecular fragment is defined as the difference in length between single and double bonds between non-hydrogen atoms. The positive sign of BLA for example indicates that the molecular unit has an aromatic character. The BLA value for central vinylene bridge may be evaluated using equation 1,

$$\text{BLA} = (d_{14} + d_{16}) - 2d_{15}$$

where  $d$  symbols denote the bond lengths determined in Fig. 1.

Brédas et al. [20] studied the relationship between band gap and bond length alternation of conjugated polymers and their results indicate that in aromatic-based conjugated polymers, the energy gap decreases as a function of increasing quinoid character of polymer backbone. As can be seen from data in Table 1, the mono-substitution with electron-withdrawing CN group leads to decrease of the BLA value by 0.006 Å with respect to the F<sub>2</sub>V molecule. The next presence of CN group has an additive influence on the BLA decrease. The presence of CN groups leads to increasing quinoid character. Consequently, the lowest excitation energies of F<sub>2</sub>V–CN and F<sub>2</sub>V–(CN)<sub>2</sub> are decreased when compared to the original compound. On the other hand, a small increase of BLA value is obtained for amino derivatives F<sub>2</sub>V–NH<sub>2</sub> and F<sub>2</sub>V–(NH<sub>2</sub>)<sub>2</sub>. For the push–pull system of F<sub>2</sub>V–CN–NH<sub>2</sub>, the resulting influence of both groups has a compensatory effect since the BLA value is similar to the non-substituted F<sub>2</sub>V molecule.

The structural changes in the central part of the molecule, induced by the strong electron-withdrawing cyano or donating amino groups, are also reflected in the vertically excited electronic states, reflecting the balance between the perturbation of conjugation due to the distortion of the planar scaffold and the electronic effects of the substituents. The first seven vertical excitation energies with non-negligible oscillator strengths are summarized in Table 2. The lowest excitation energy for non-substituted molecule F<sub>2</sub>V is 3.23 eV, compared to 3.08 eV [21] for tetrahydrofuran, suggesting the model systems employed and the level of theory employed is sufficiently accurate to gain useful insights.

The mono- or symmetric bi-substitutions lead to a bathochromic energy shift. Only in the case of F<sub>2</sub>V–NH<sub>2</sub> molecule, the lowest excitation is blue-shifted by 0.06 eV. The global hypsochromic shift of excitation energies is indicated for the F<sub>2</sub>V–CN–NH<sub>2</sub> system. The

lowest excitation energy is higher about 0.20 eV with respect to the F<sub>2</sub>V. It seems that the torsion of molecular chains has more dominant influence of the photo-physical properties than the global push–pull effects of used substituents. Finally, in all cases, the substitution of vinylene bridge leads to a decrease in the oscillator strength for the lowest singlet excitation transition (S<sub>1</sub>) and to the increase of the oscillator strengths for the next optical transitions.

In order to understand the physical origin of optical transitions for the selected excitation energies, it is useful to examine the (highest) occupied (HOMO) and lowest unoccupied molecular orbitals (LUMO). As reported in Table 2, the lowest energy electronic excitation is from the HOMO to the LUMO for all molecules and displays  $\pi\pi^*$  character. However, the electronic distribution observed for the next transitions, as different as given by the molecular orbitals, are very different for the different substitutions. As presented in Fig. 3, the HOMO orbital of F<sub>2</sub>V molecule is located mostly on the double bond of vinylene bridge (bond no. 15) and neighbouring bonds on fluorene units perpendicular oriented with respect to the chain (see bond nos. 12, 13, and 17, 18). The LUMO orbital is spread over the single bonds of vinylene bridge (bond nos. 14 and 16) and bonds on the fluorene units which are parallel with the molecular chain (see bond nos. 10, 11 and 19, 20). The presence of electron-withdrawing cyano group in F<sub>2</sub>V–CN and F<sub>2</sub>V–(CN)<sub>2</sub> molecules increases the electron delocalization in HOMO over the fluorene units. On the other hand, the electron-donating amino groups in F<sub>2</sub>V–NH<sub>2</sub>

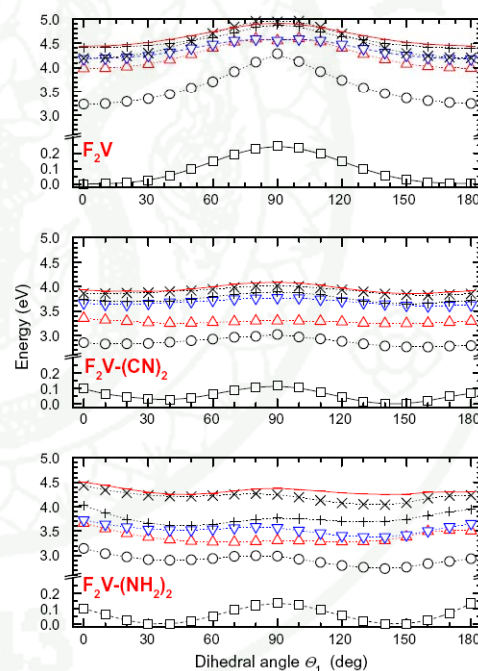


Fig. 4. One-dimensional dependence of the electronic ground-state and vertically excited energies of studied symmetric systems on the torsion calculated at the B3LYP/6-31G(d) theoretical level. The ground-state energy minimum is taken as energy reference (see also Table 3). The open square denote electronic ground-state and the next symbols indicate the first six excited states (S<sub>1</sub>, ○; S<sub>2</sub>, △; S<sub>3</sub>, ▽; S<sub>4</sub>, +; S<sub>5</sub>, ×; S<sub>6</sub>, –).



and  $F_2V-(NH_2)_2$  molecules is responsible for the electron delocalization over the vinylene bond no. 15.

The opposite situation is observed in the LUMOs for both types of derivatives. With respect to this fact, we can deduce that the optical transition for cyano derivatives is oriented from the fluorene units to the CN chromophore while for the amino derivatives it is spread from the central part to the fluorene units. This character is also reflected for the higher vertical excitations. The transi-

tions from lower occupied orbitals to the LUMO orbital play important role for the CN derivatives. The transitions from HOMO to the next unoccupied orbitals occur for the amino derivatives. In the case of the  $F_2V-CN-NH_2$  molecule, the presence of the strong push-pull systems leads to the combined effect with strongly determined direction of optical transition. This electron transition starts from the fluorene unit and neighbouring  $NH_2$  group and goes to the CN group and opposite fluorene unit.

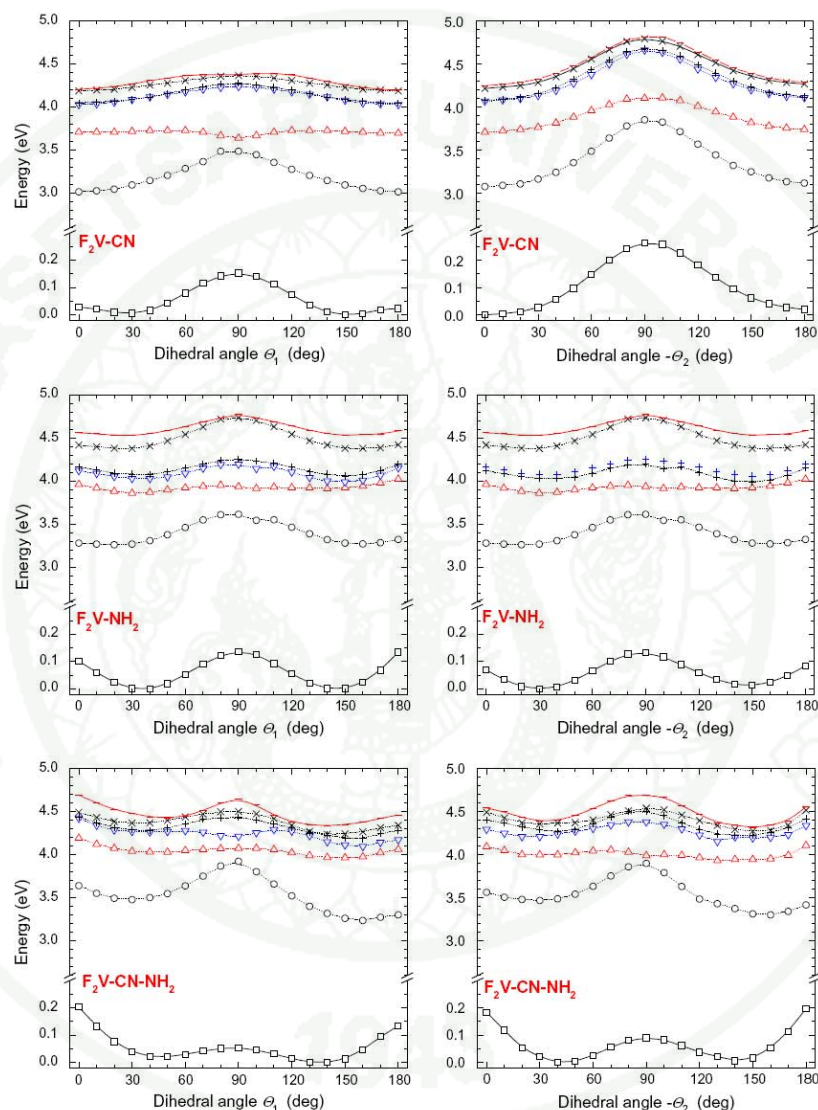


Fig. 5. One-dimensional dependence of the electronic ground-state and vertically excited energies of studied asymmetric systems on the torsion calculated at the B3LYP/6-31G(d) theoretical level. The ground-state energy minimum is taken as energy reference (see also Table 3). The open square denote electronic ground-state and the next symbols indicate the first six excited states ( $S_1$ ,  $\circ$ ;  $S_2$ ,  $\Delta$ ;  $S_3$ ,  $\nabla$ ;  $S_4$ ,  $+$ ;  $S_5$ ,  $\times$ ;  $S_6$ ,  $-$ ).

The electronic ground-state torsional potentials of the fluorene unit around the common single bond were also investigated using the B3LYP/6-31G(d) method with the results being depicted in Figs. 4 and 5 and the geometrical and energetic values in Table 3. As can be seen in Fig. 4, the non-substituted molecule  $F_2V$  has two planar minima and the barrier for perpendicular arrangement ( $\Delta E = 0.245$  eV or  $5.65$  kcal mol $^{-1}$ ). We note that the similar shape of potential and barrier location with  $\Delta E = 0.22$  eV ( $5.0$  kcal mol $^{-1}$ ) were obtained for the torsion of phenylene ring around the vinylene single bond at the B3LYP/cc-pVDZ theoretical level [22]. The presence of cyano or amino groups on the vinylene bridge leads to structures that are more stable to a non-planar conformation. The obtained potential curves exhibit two non-planar minima corresponding to the most stable *trans* or *cis* conformations and two first-order saddle points. The most stable conformation of  $F_2V-(NH_2)_2$  molecule is at  $45^\circ$  while the  $F_2V-(CN)_2$  molecule prefers *trans* conformation ( $144^\circ$ ). The mutual comparison of the energy barriers with respect to the  $F_2V$  molecule shows that the vinylene bridge substitution decreases the barrier at perpendicular arrangement. The cyano substitution decreases the barrier relative to  $F_2V$  by  $0.092$  eV (for  $F_2V-CN$ ) and by  $0.128$  eV (for  $F_2V-(CN)_2$ ). Although the amino substitution leads to the higher decrease of the perpendicular barrier relative to  $F_2V$  ( $0.108$  eV for  $F_2V-NH_2$  and  $0.169$  eV for  $F_2V-(NH_2)_2$ ), the torsion at the planar arrangements is more restricted. The electronic ground-state potential curves for mono-substituted molecules around the second dihedral

angle  $\Theta_2$  have different shape. For the  $F_2V-CN$  molecule, the shape is similar to the potential curve of non-substituted  $F_2V$  molecule. A different situation occurs for the  $F_2V-NH_2$  molecule in that the second evaluated curve copies the shape of the dependence around the first dihedral angle. It seems that the strong electron donor amino group is able directly to affect through the double bond no. 15 the torsional motion on the opposite molecular side. The modification of the torsional potential with the amino or cyano groups is also observed for mixed  $F_2V-CN-NH_2$  molecule. As can be seen in Fig. 5, the torsional potential profile for the  $\Theta_1$  and  $\Theta_2$  dihedral angles are two-times lower in energy for the perpendicular arrangement compared to the planar arrangement. In addition, the potential curve for the torsion around the angle  $\Theta_1$  (at the side of CN substitution) exhibits more stable conformation at  $132^\circ$ . The energy difference with respect to the second minimum at  $52^\circ$  is  $0.021$  eV. This is a different situation to that presented for  $F_2V-CN$  and  $F_2V-NH_2$ . It appears that these features have a different impact on the excitation–relaxation phenomena which occur in various time-dependent optical experiments.

The excited-state potential energy curves calculated at the TD-B3LYP/6-31G(d) level based on ground-state optimized geometries are also shown in Figs. 4 and 5. The curve for the lowest excited state of  $S_1$  with dominant oscillator strengths for  $F_2V$  exhibits the energy minimum for a planar geometry and a maximum for the perpendicular one. The energy difference between these points is ca  $1.06$  eV. In the case of  $F_2V-CN$  and  $F_2V-NH_2$ , the  $S_1$  state practically reflects the curve for the  $F_2V$  molecule, but the energy differences between the perpendicular and planar arrangements are approximately two-times lower. The symmetric bi-substitution decreases very effectively the sensitivity of the evaluated potential curves on the torsion. Moreover, in all investigated molecules, the lowest  $S_1$  state does not cross the next higher states. The potential energy curves for the next higher excited states of  $F_2V$  molecule are quite closely spaced to each other and show multiple intersections (around  $70$ – $120^\circ$ ). On the other hand, the substitution can cause the small separation of crossing region of potential curves between the next lowest excited states.

#### 4. Conclusions

The (TD)-B3LYP method has been used for the systematic theoretical investigation of the photo-physical properties of substituted model bifluorenevinylene compounds. The substitutions of the vinylene unit by strong electron-accepting CN and/or electron-donating  $NH_2$  groups were considered. Our calculations indicate that the non-substituted  $F_2V$  compound is planar and that substitution leads to the twisting of the molecular fragment on the side of substitution. In the case of the  $F_2V-NH_2$  molecule, the amino group is also responsible for the non-planarity on the non-substitute side. Additionally, the chemical modification of vinylene bridge affects the electronic ground-state torsional potentials of the fluorene unit around the single bond. The non-substituted molecule  $F_2V$  has two planar minima and the barrier for perpendicular arrangement. The presence of cyano or amino groups on vinylene bridge is responsible for the restriction of the torsional motion at the barriers located for planar and perpendicular arrangements. The energy barrier highs are also dependent on the substitution.

The TD-DFT torsional potential energy curves in the vertically excited states were also investigated in this work. From our calculations, we do not find any indication of state crossings of the  $S_1$  state with higher ones for all investigated systems. The symmetric bi-substitution markedly decreases the potential curves on the torsion. The potential energy curves for the next higher excited states of  $F_2V$  molecule are quite closely spaced to each other and show multiple intersections (around  $70$ – $120^\circ$ ). On the other hand, the substitution can modulate the separation of crossing region of

**Table 3**  
Relative energies  $\Delta E$  and dihedral angles  $\Theta_1$  and  $\Theta_2$  of external points for torsional dependencies with respect to the most stable structure. The angles are in degrees and energies in eV or kcal mol $^{-1}$  (values in parentheses). See also Figs. 4 and 5.

Molecule	$\Theta_1$	$\Theta_2$	$\Delta E$
$F_2V$	0	0	0.000 (0.00)
	90	0	0.245 (5.65)
	180	0	0.003 (0.07)
$F_2V-(CN)_2$	0	–46	0.099 (2.28)
	38	–38	0.000 (0.00)
	90	–29	0.117 (2.70)
	144	–37	0.001 (0.02)
	180	–45	0.069 (1.59)
$F_2V-(NH_2)_2$	0	–57	0.224 (5.17)
	45	–45	0.000 (0.00)
	90	–39	0.076 (1.75)
	128	–37	0.038 (0.88)
	180	–45	0.298 (6.88)
$F_2V-CN$	0	0	0.029 (0.67)
	28	–7	0.001 (0.02)
	90	0	0.153 (3.53)
	148	–7	0.000 (0.00)
	180	–1	0.024 (0.55)
	25	–90	0.293 (6.76)
	29	–180	0.049 (1.13)
$F_2V-NH_2$	0	–31	0.102 (2.35)
	36	–31	0.000 (0.00)
	90	–28	0.137 (3.16)
	146	–24	0.002 (0.05)
	180	–38	0.134 (3.09)
	36	0	0.070 (1.61)
	35	–90	0.132 (3.04)
	35	–148	0.013 (0.30)
	39	–180	0.085 (1.96)
$F_2V-CN-NH_2$	0	–31	0.205 (4.73)
	52	–44	0.021 (0.50)
	90	–28	0.056 (1.29)
	132	–43	0.000 (0.00)
	180	–38	0.124 (2.65)
	57	0	0.184 (4.24)
	42	–90	0.091 (2.10)
	43	–133	0.024 (0.57)
	58	–180	0.198 (4.57)

potential curves between the next lowest excited states. The absence of the intersections of excited states around the stable structures and relative well separation of the lowest excited state around the minima enable us to perform the molecular dynamics studies of investigated molecules based on an adiabatic approach. These results show that theoretical studies can help us to understand the relationship between the torsional broadening of absorption spectra, chemical structure and time-dependent optical phenomena, having implications for the design and synthesis of novel optical materials.

#### Acknowledgements

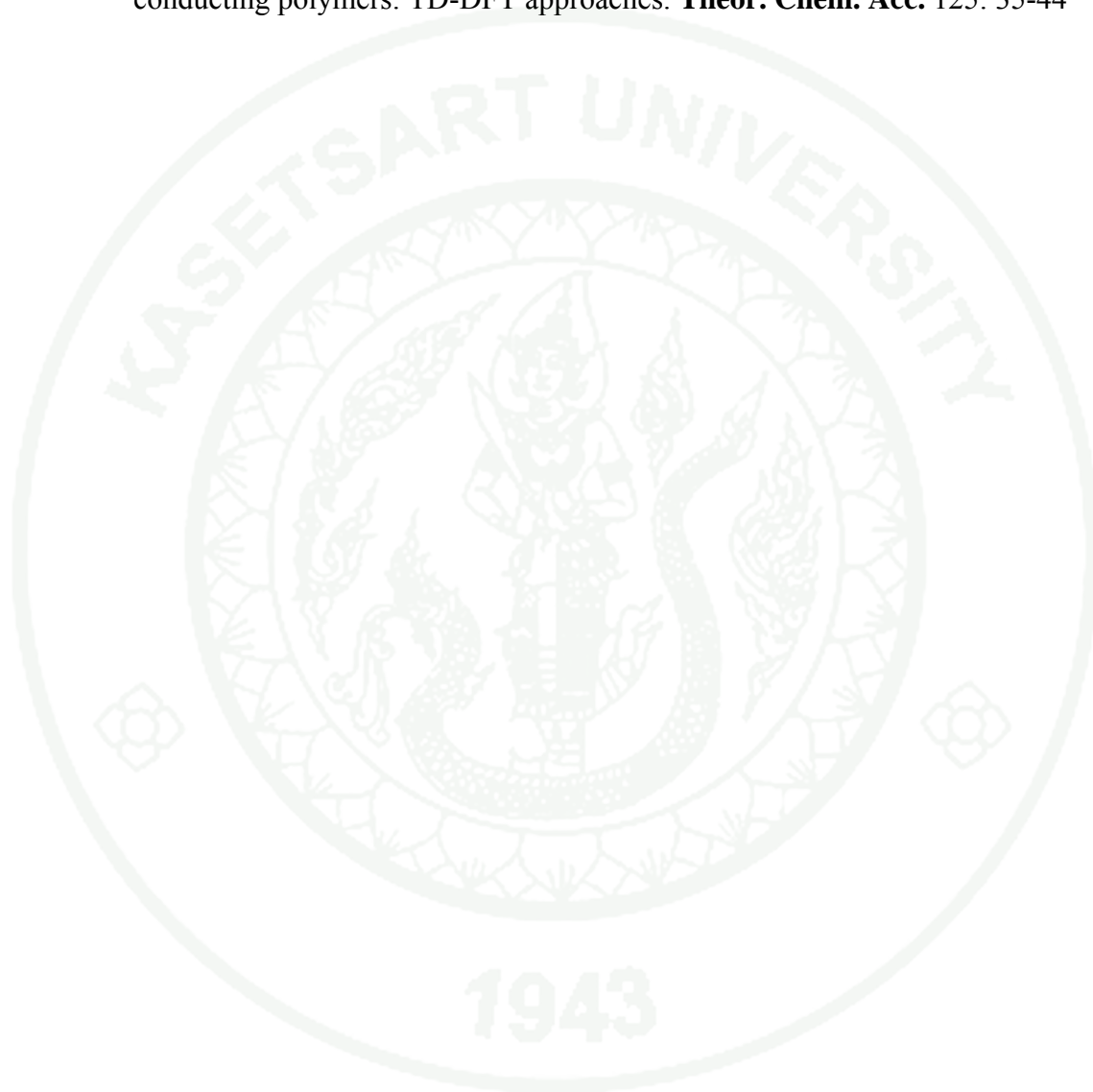
The authors thank Prof. Harald Kauffmann for valuable comments and discussion. This work was supported by the Thailand Research Fund (RTA5080005 to S.H. and MRG5180287 to S.S.). W.M. is grateful to Thai Graduate Institute of Science and Technology (TGIST), the Austrian Science Fund within the framework of the Special Research Program F16, Advanced Light Sources (ADLIS), and Bilateral Research Cooperation (BRC) from Faculty of Science, Kasetsart University for scholarships and supporting. The National Center of Excellence in Petroleum, Petrochemical Technology and Advanced Materials is gratefully acknowledged for research supporting and facilities. The calculations were performed in part on the Schrödinger III cluster of the University of Vienna. Thanks are also due to Dr. Matthew Paul Gleeson for helpful comments and reading of the manuscript.

#### References

- [1] M. Ranger, D. Rondeau, M. Leclerc, *Macromolecules* 30 (1997) 7686.
- [2] V.P. Barberis, J.A. Microyannidis, *Synth. Met.* 156 (2006) 1408.
- [3] C. Chi, C. Im, V. Enkelmann, A. Ziegler, G. Lieser, G. Wegner, *Chem. Eur. J.* 11 (2005) 6833.
- [4] S.H. Jin, H.J. Park, J.Y. Kim, K. Lee, S.P. Lee, D.K. Moon, H.J. Lee, Y.S. Gal, *Macromolecules* 35 (2002) 7532.
- [5] Y. Jin, J.Y. Kim, S. Song, Y. Xia, J. Kim, H.Y. Woo, K. Lee, H. Suh, *Polymer* 49 (2008) 467.
- [6] L. Zhang, Q. Zhang, H. Ren, H. Yan, J. Zhang, H. Zhang, J. Gu, *Sol. Energy Mater. Sol. Cells* 92 (2008) 581.
- [7] V. Lukes, A. Aquino, H. Lischka, *J. Phys. Chem. A* 109 (2005) 10232.
- [8] W. Meeto, S. Suramitr, S. Vannarat, S. Hannongbua, *Chem. Phys.* 349 (2008) 1.
- [9] S. Suramitr, T. Kerdcharoen, T. Srihirin, S. Hannongbua, *Synth. Met.* 155 (2005) 27.
- [10] Y. Yang, J.K. Feng, Y. Liao, A.M. Ren, *Polymer* 46 (2005) 9955.
- [11] F. Furche, R. Ahlrichs, *J. Chem. Phys.* 117 (2002) 7433.
- [12] J. Gierschner, J. Cornil, H.J. Egelhaaf, *Adv. Mater.* 19 (2007) 173.
- [13] S. Tretiak, A. Saxena, R.L. Martin, A.R. Bishop, *Phys. Rev. Lett.* 89 (2002) 97402.
- [14] A.D. Becke, *J. Chem. Phys.* 98 (1993) 5648.
- [15] P.M.W. Gill, B.G. Johnson, J.A. Pople, M.J. Frisch, *Chem. Phys. Lett.* 197 (1992) 499.
- [16] M.J. Frisch, G.W. Trucks, H.B. Schlegel, G.E. Scuseria, M.A. Robb, J.R. Cheeseman, J.A. Montgomery Jr., T. Vreven, K.N. Kudin, J.C. Burant, J.M. Millam, S.S. Iyengar, J. Tomasi, V. Barone, B. Mennucci, M. Cossi, G. Scalmani, N. Rega, G.A. Petersson, H. Nakatsuji, M. Hada, M. Ehara, K. Toyota, R. Fukuda, J. Hasegawa, M. Ishida, T. Nakajima, Y. Honda, O. Kitao, H. Nakai, M. Klene, X. Li, J.E. Knox, H.P. Hratchian, J.B. Cross, V. Bakken, C. Adamo, J. Jaramillo, R. Gomperts, R.E. Stratmann, O. Yazyev, A.J. Austin, R. Cammi, C. Pomelli, J.W. Ochterski, P.Y. Ayala, K. Morokuma, G.A. Voth, P. Salvador, J.J. Dannenberg, V.G. Zakrzewski, S. Dapprich, A.D. Daniels, M.C. Strain, O. Farkas, D.K. Malick, A.D. Rabuck, K. Raghavachari, J.B. Foresman, J.V. Ortiz, Q. Cui, A.G. Baboul, S. Clifford, J. Cioslowski, B.B. Stefanov, G. Liu, A. Liashenko, P. Piskorz, I. Komaromi, R.L. Martin, D.J. Fox, T. Keith, M.A. Al-Laham, C.Y. Peng, A. Nanayakkara, M. Challacombe, P.M.W. Gill, B. Johnson, W. Chen, M.W. Wong, C. Gonzalez, J.A. Pople, 567 revision B.05. Gaussian, Inc., Pittsburgh, 2003.
- [17] P. Poolmee, M. Ehara, S. Hannongbua, H. Nakatsuji, *Polymer* 46 (2005) 6474.
- [18] K. Sriwichitkamol, S. Suramitr, P. Poolmee, S. Hannongbua, *J. Theor. Comput. Chem.* 5 (2006) 595.
- [19] D. Jacquemin, E.A. Perpète, H. Chermette, I. Ciofini, C. Adamo, *Chem. Phys.* 332 (2007) 79.
- [20] J.L. Brédas, *J. Chem. Phys.* 82 (1985) 3808.
- [21] Q. Liu, W. Liu, B. Yao, H. Tian, Z. Xie, Y. Geng, F. Wang, *Macromolecules* 40 (2007) 1851.
- [22] S.P. Kwasniewski, L. Claes, J.P. Franco, M.S. Deleuze, *J. Chem. Phys.* 118 (2003) 7823.

**Publication III**

Suramitr, S., W. Meeto, P. Wolschann and S. Hannongbua. 2010. Understanding on absorption and fluorescence electronic transitions of carbazole-based conducting polymers: TD-DFT approaches. **Theor. Chem. Acc.** 125: 35-44





## Understanding on absorption and fluorescence electronic transitions of carbazole-based conducting polymers: TD-DFT approaches

Songwut Suramitr · Wichanee Meeto ·  
 Peter Wolschann · Supa Hannongbua

Received: 7 May 2009 / Accepted: 5 October 2009 / Published online: 30 October 2009  
 © Springer-Verlag 2009

**Abstract** The electronic excitation transitions of carbazole-based oligomers,  $(\text{Cz-co-Cz})_N$ ,  $(\text{Cz-co-Fl})_N$  and  $(\text{Cz-co-Th})_N$  ( $N = 2-4$ ) were investigated using density functional theory (DFT) and time-dependent (TD) DFT methods. Our results show that the calculated ground state geometries favor a more aromatic, planer structure, while the electronically excited geometries favor a quinoidic type structure. Absorption and fluorescence energies have been obtained from TD-B3LYP/SVP calculations performed on the  $S_1$  optimized geometries and are in excellent agreement with experimental data. The experimental fluorescence excitation energies for  $(\text{Cz-co-Cz})_4$ ,  $(\text{Cz-co-Fl})_4$  and  $(\text{Cz-co-Th})_4$  (2.76, 2.63, and 2.25 eV, respectively) correspond closely with the predicted  $S_1$  transitions (2.84, 3.91 and 2.43 eV, respectively). We also report the predicted radiative lifetimes 0.52, 0.47, and 0.99 ns for  $(\text{Cz-co-Cz})_N$ ,  $(\text{Cz-co-Fl})_N$  and  $(\text{Cz-co-Th})_N$ , discuss the origin of the small stoke shift of the carbazole based oligomers and the magnitude of bathochromic shifts. We conclude by discussing the benefits of theoretical calculations, which can provide critical structural and electronic understanding of

excitation–relaxation phenomena that can be exploited in design of novel optical materials.

**Keywords** Carbazole-based · Density functional theory · TDDFT · Radiative lifetimes

### 1 Introduction

Conducting polymers as light-emitting diodes, field effect transistors, charge storage devices, photodiodes, sensors, etc. [1, 2] are currently of interest. In the last year, novel well-defined 2,7-carbazole-based (Cz) polymers were synthesized by Leclerc et al. [2–7]. 2,7-Carbazole-based polymers and derivatives with thiophene, pyrrole, phenylene, and fluorene subunits have been synthesised [8–10], are currently of both industrial and academic interest because of their wide-ranging potential in electronic devices. These novel polymeric materials are stable in air and soluble in many usual organic solvents. Interestingly, the absorption and fluorescence spectra of these materials exhibit significant differences [11–13]. It is found that the existence of multi-components in the fluorescence decay profiles of such polymers in the solid state is caused by several distinct intermolecular  $\pi$ – $\pi^*$  interactions. However, these interactions are not strong enough to provoke the appearance of distinct fluorescence bands or even to increase the bandwidths of the emission bands in solution. Fundamental understanding on structural and energetic properties of this kind of copolymers could lead to beneficial knowledge for the design of novel copolymers. Therefore, it is of interest to compare the absorption and fluorescence transitions of 2,7-carbazole-based polymers and its dependence on the structural and the electronic properties. We are also interested in exploring the

S. Suramitr · W. Meeto · S. Hannongbua  
 Department of Chemistry, Faculty of Science,  
 Kasetsart University, Bangkok 10900, Thailand  
 e-mail: fscisph@ku.ac.th

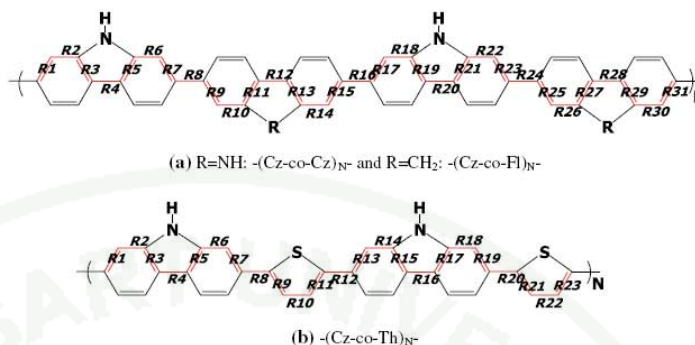
S. Suramitr (✉) · W. Meeto · S. Hannongbua  
 The Center of Nanoscience, Kasetsart University,  
 Bangkok, 10900, Thailand  
 e-mail: fsciswsm@ku.ac.th

P. Wolschann  
 Institute for Theoretical Chemistry, University of Vienna,  
 Währinger Straße 17, 1090 Vienna, Austria

 Springer



**Fig. 1** Structures and numbering schemes of **a** (Cz-co-Cz)<sub>N</sub> and (Cz-co-Fl)<sub>N</sub> and **b** (Cz-co-Th)<sub>N</sub> oligomers



excitation mechanism since this will affect the pattern of the emission bands.

In previous studies of carbazole-based molecules [11–13], calculations were performed using DFT as well as (TD-DFT) with the B3LYP functional and three basis sets: 6-31G, 6-31G(d) and 6-311G(d,p). However, only ground state conformational analysis and calculations of the vertical excitation energies were carried out. From these calculations, it was reported that the optimized ground state geometries of oligomers with six-membered heterocyclic rings copolymers are nonplanar, whereas planar copolymer structures were found for with five-membered heterocyclic ring a results of the subtle balance between minimizing steric repulsion and maximizing electronic conjugation [14].

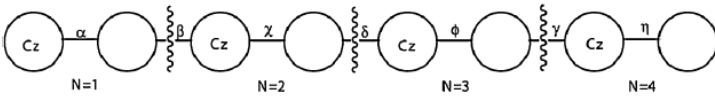
To increase our understanding of this important polymer class, we have performed calculations on the excited state properties of carbazole-based homopolymers and copolymers with fluorene and thiophene substituents (formulas are given in Fig. 1). In this study, we put particular emphasis on understanding the ground and low-lying excited states of the carbazole-homopolymer (Cz-co-Cz)<sub>N</sub>, carbazole-co-fluorene (Cz-co-Fl)<sub>N</sub> and carbazole-co-thiophene (Cz-co-Th)<sub>N</sub> oligomers, which are explored by theoretical studies. The transitions associated with the absorption and fluorescence spectra of carbazole-based oligomers are explored. The fluorescence energies and radiative lifetimes are also analyzed in an attempt to gain better, more general understanding of the behavior of such systems.

## 2 Computational details

All QM calculations were performed using TURBOMOLE version 5.7 [15]. All geometry optimizations were performed using TURBOMOLE's JOBEX program with generalized internal coordinates and the corresponding

STATPT module [16]. The ground state and the lowest singlet excited-state geometries of the carbazole-based oligomers were optimized by DFT and TDDFT, respectively, using the B3LYP [17–21] functional for the carbazole homopolymer (Cz-co-Cz)<sub>N</sub>, the carbazole-co-fluorene (Cz-co-Fl)<sub>N</sub> and the carbazole-co-thiophene (Cz-co-Th)<sub>N</sub> oligomers (Fig. 1). The default *m*<sup>3</sup> numerical quadrature grid [22] was employed in all DFT calculations. The geometries of carbazole-based analogs were optimized without symmetry constraints using redundant internal coordinates and were considered converged if the gradient was less than 10<sup>−4</sup> au. In all optimizations, the criterion for convergence was set to 10<sup>−8</sup> for the energy and 10<sup>−7</sup> for the density. To calculate excitation energies and analytic excited-state gradients, the TD-DFT method was used. Modules DSCF [22], GRAD, and ESCF [23] have been used. Sufficiently converged results were obtained with the valence-double-zeta quality with polarization functions SVP basis sets in close agreement with many previous studies; the conclusions are thus not expected to vary upon further basis set extensions [11–13]. In order to consider solvent effects on excitation energies, we adopted the conductor-like screening model (COSMO) [24] with a dielectric constant of  $\epsilon = 4.8$  to simulate the chloroform solvent and optimized atomic radii (C, 2.00 Å; N, 1.83 Å; O, 1.72 Å; H, 1.30 Å) for the construction of the molecular cavity were used for the calculations of all molecules.

For each oligomer in Fig. 1, the chain lengths studied varied from dimers to tetramers (*N* = 1, 2, 3 and 4). The first five singlet–singlet electronic transitions (*S*<sub>0</sub> → *S*<sub>*n*</sub>) were calculated for (Cz-co-Cz)<sub>N</sub>, (Cz-co-Fl)<sub>N</sub>, and (Cz-co-Th)<sub>N</sub> oligomers using the B3LYP/SVP and TD-B3LYP/SVP methods, respectively. Based on the optimized geometries of the oligomers, the electronic absorption and fluorescence spectra were calculated at the DFT and TD-DFT levels. The absorption and fluorescence excitation energies were obtained from the ground state and the

**Table 1** Bond torsional angles of oligomers in ground ( $S_0$ ) and lowest excited state ( $S_1$ ) (in brackets) for the (Cz-co-Cz) $_N$ , (Cz-co-Fl) $_N$  and (Cz-co-Th) $_N$  molecules optimized using B3LYP/SVP and TD-B3LYP/SVP (in parenthesis) methods


Oligomers	Bond torsional angles (°)						
	$\alpha$	$\beta$	$\chi$	$\delta$	$\phi$	$\gamma$	$\eta$
<b>(Cz-co-Cz)<math>_N</math></b>							
$N = 1$	140.51 (170.24)						
$N = 2$	141.54 (155.15)	141.15 (163.88)	141.56 (155.03)				
$N = 3$	141.94 (147.13)	142.79 (155.54)	142.80 (160.24)	142.76 (155.39)	142.00 (146.68)		
$N = 4$	141.99 (146.06)	141.58 (152.82)	142.25 (159.91)	143.44 (154.50)	141.88 (155.69)	141.77 (148.60)	141.91 (143.88)
<b>(Cz-co-Fl)<math>_N</math></b>							
$N = 1$	142.14 (170.71)						
$N = 2$	142.20 (156.46)	142.19 (167.58)	142.30 (155.39)				
$N = 3$	142.53 (146.86)	143.38 (157.03)	142.40 (164.52)	143.21 (157.34)	142.42 (148.24)		
$N = 4$	142.69 (156.46)	142.60 (167.58)	142.44 (155.39)	141.78 (167.58)	142.66 (156.46)	142.59 (167.58)	143.04 (155.39)
<b>(Cz-co-Th)<math>_N</math></b>							
$N = 1$	21.06 (0.01)						
$N = 2$	27.23 (0.02)	27.41 (0.00)	27.00 (0.00)				
$N = 3$	24.19 (0.02)	24.52 (0.04)	25.67 (0.02)	24.72 (0.00)	25.61 (0.03)		
$N = 4$	26.82 (0.00)	25.78 (0.01)	27.81 (0.01)	26.14 (0.00)	27.53 (0.01)	25.49 (0.00)	26.04 (0.02)

All torsional angles are given in degrees.  $N$  represents the number of the oligomer units

lowest singlet excited-state optimized geometries. The fluorescence electronic transitions were calculated as the vertical de-excitation based on the optimized geometry of the lowest excited state.

### 3 Results and discussion

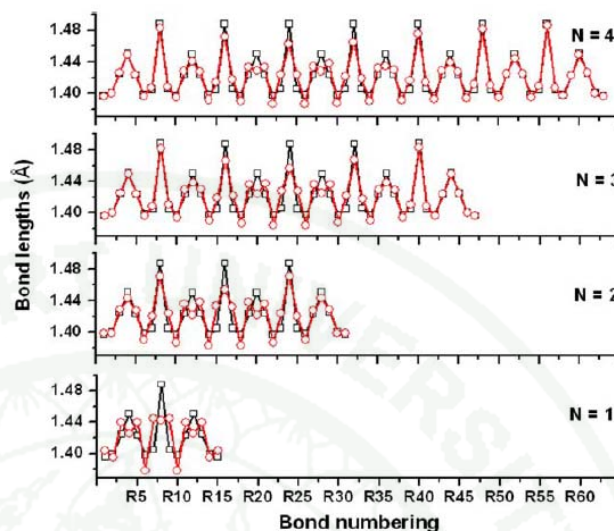
#### 3.1 Ground and excited states structural properties

The chain length dependence on the oligomer torsional angles ( $\theta$ ), both at ground and excited state has been

investigated for the carbazole-based oligomers using our ground state optimized geometries. The torsion angles of the oligomers are given in Table 1 for the ground ( $S_0$ ) and the lowest excited state ( $S_1$ ) for the (Cz-co-Cz) $_N$ , (Cz-co-Fl) $_N$  and (Cz-co-Th) $_N$  molecules.

The optimized structures of carbazole-based oligomers in the ground states are generally more distorted than the structures in excited states. We found twisted conformations with torsional angles ( $\alpha$ ,  $\beta$ ,  $\chi$ ,  $\delta$ ,  $\phi$ ,  $\gamma$  and  $\eta$ ) around 140° for both Cz-co-Cz-co-Cz and Cz-co-Fl-co-Cz. For Cz-co-Th-co-Cz, the torsional angles are around 30°, which means that the *syn* or *cis* structure of the copolymerized

**Fig. 2** Computed bond lengths of ground state and excited state of homocarbazole oligomers  $(\text{Cz-co-Cz})_N$ . The open square denote electronic ground state and the open circle indicate the first excited state. Calculated at the B3LYP/SVP level of theory



heterocycles ring (thiophene) is energetically more favorable than the “trans” conformations [11, 12].

These ground state torsional angles appear independent the number of oligomer subunits used in the calculations. Only in the case of  $(\text{Cz-co-Th})_N$  is the monomer more planar than the oligomers. On the contrary, the excited state-torsion angles are more planar than the ground state geometries with torsional angles around  $180^\circ$  or  $0^\circ$ , respectively. The differences in the bond torsional angles between the ground and lowest singlet excited state can be explained by considering the bond length changes. The structures of the ground state and the lowest singlet excited-state optimized oligomers geometries are given in Figs. 2 and 3, where the changes bond lengths for copolymer derivatives and carbazole-based oligomer can be compared. The bond numbering schemes of  $(\text{Cz-co-Cz})_N$ ,  $(\text{Cz-co-Fl})_N$  and  $(\text{Cz-co-Th})_N$  oligomers are depicted in Fig. 1. In Fig. 2, the conjugated carbon–carbon bonds are illustrated for the ground state ( $S_0$ ) and singlet excitations ( $S_1$ ) for  $(\text{Cz-co-Cz})_N$  oligomers, dimer to octamer.

From Fig. 2, it is found that the carbon–carbon bonds which lie parallel to the polymer chain (i.e. bond numbering R2, R4, R6, R8, R10, R12 and R14) become shorter while those that lie at angles other than  $180^\circ$  become longer. The carbon–carbon bonds are found to alternate in length between a single and double bond. In the lowest excited states, the double bond lengths increase, whereas the single bond length decreases with the changes being localized toward the centre of the oligomers. For example, the geometric changes in  $(\text{Cz-co-Cz})_1$ ,  $(\text{Cz-co-Cz})_2$ ,

$(\text{Cz-co-Cz})_3$  and  $(\text{Cz-co-Cz})_4$  due to excitation affect the central units only. It should be noted that the spatial extent of the geometry deformations is not constant; the deformations continue to extend over the entire chain when the length increases, at least up to  $(\text{Cz-co-Cz})_{N=4}$  and this can be understood in terms of the degree of charge delocalization. For longer chains, the amount of charge per monomer unit is lower and thus the geometry change is smaller. The geometry change, as obtained from DFT calculations, are found in all the  $(\text{Cz-co-Cz})_N$  oligomer chains. This suggests that the center rings in the larger carbazole-based oligomers have more quinoidic character than the terminal rings [12, 13]. Therefore, the central rings in the larger oligomers were selected to confirm the trends of the C–C bond alternation along the backbone of the  $(\text{Cz-co-Cz})_3$ ,  $(\text{Cz-co-Fl})_3$  and  $(\text{Cz-co-Th})_3$  as shown in Fig. 3. We monitor the changes in bond length of these aromatic systems using the bond length alternation (BLA) [25]. The BLA values for selected molecular fragment can be defined as the differences in lengths between single bonds ( $d_{\text{single}}$ ) and double bonds ( $d_{\text{double}}$ ) of carbon–carbon atoms (Eq. 1). A positive BLA value indicates that the molecular unit has an aromatic (quinoidic) character [26–28].

$$\text{BLA} = \sum \frac{(d_{\text{single}} - d_{\text{double}})}{N}, \quad (1)$$

The BLA associated with the carbon–carbon conjugated bond for the ground and singlet excitations states for the central rings of  $(\text{Cz-co-Cz})_3$ ,  $(\text{Cz-co-Fl})_3$  and  $(\text{Cz-co-Th})_3$  oligomer was estimated. We find that the BLA changes



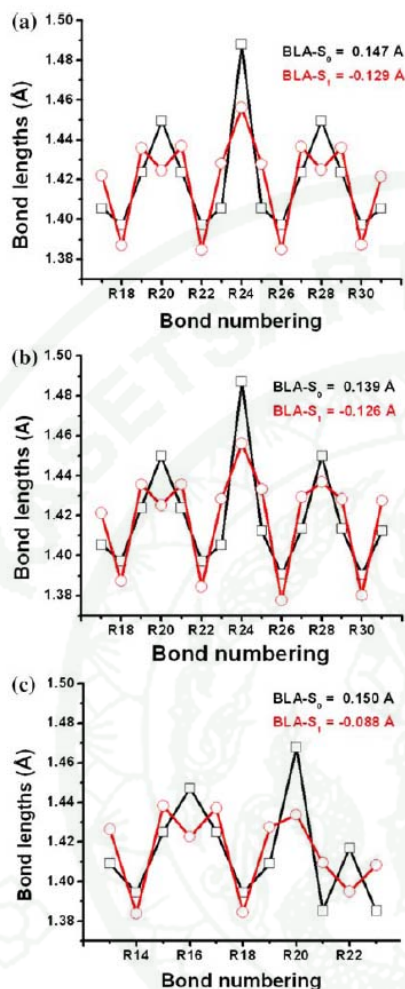


**Fig. 3** The bond length alternating (BLA) of the central rings of the oligomers of (a)  $(Cz-co-Cz)_3$ , (b)  $(Cz-co-Fl)_3$  and (c)  $(Cz-co-Th)_3$  as shown. The open square denote electronic ground state and the open circle indicate the first excited state. Calculated using TD-DFT at the B3LYP/SVP level of theory

significantly in the excited states compared to the ground states, in the case of  $(Cz-co-Cz)_3$  and  $(Cz-co-Fl)_3$ , decreasing from 0.147, 0.139 Å in  $S_0$  to  $-0.129$ ,  $-0.125$  Å in  $S_1$ , respectively. In both, the ground and singlet states, the BLA differences are between 0.014 and 0.019 Å, whereas in the case of  $(Cz-co-Th)_3$ , the BLA decreases from 0.150 Å in  $S_0$  to  $-0.088$  Å in  $S_1$ . These

results indicate that the thiophene unit leads to a decrease in the BLA value by 0.063 Å with respect to the  $(Cz-co-Cz)_3$  and  $(Cz-co-Fl)_3$  oligomers. In addition, the center of the quinoidic structures is located at the linking bonds between the copolymer units such as R8, as seen clearly in Fig. 1. Chidthong et al. [29] and Wichanee et al. [13] suggest that the elongation of the molecular chain leads to minor changes in the inter-ring distances of oligomers, the largest change localized at the terminal ring. In addition to, it was found that the inter-ring bond distances do not display appreciable variations with the oligomer size. Moreover, the bond-changing pattern is varied systematically when the molecular chain is elongated. These behaviors have been also found in the case of carbazole-based homopolymer and copolymer oligomers.

### 3.2 Absorption and fluorescence transitions

The absorption and fluorescence excitation energies calculated by the TD-B3LYP/SVP method are reported in Table 2. The excitations energies with highest oscillator strength ( $\pi-\pi^*$  transition) of each polymer calculated by TD-B3LYP/SVP method and were extrapolated by linear regression. There is a good linear relation ( $r^2 = 0.99$ ) between the lowest excitations and the inverse chain length. A comparison the extrapolated energy of the absorption and fluorescence excitation with the experimental results and other computed values is shown in Table 2. From these results, it was found that the excitation energies of these materials are lower than the experimental data, 0.34, 0.31, and 0.18 eV (absorption) and 0.33, 0.51, and 0.69 eV (fluorescence) for its carbazole-based,  $(Cz-co-Cz)_N$ ,  $(Cz-co-Fl)_N$  and  $(Cz-co-Th)_N$ , respectively. Comil et al. [30, 31] have shown that this can result from the overestimation of long-range electron correlation effects in the TD-DFT methods. Previous works [30–33] have shown that the high accuracy of DFT functionals such as TPSS functional is more suitable for calculation of conjugated oligomers. However, for small molecules, the impact of inductive and/or mesomeric effects induced by substituents appears to be well reproduced; however, the agreement with the correspondingly experimental values deteriorates when the chain size is increased. Our results confirm previous reports that a proper extrapolation procedure recommends the use of a rather large number of oligomers to improve the accuracy of the fit, and an accurate fitting function [30, 31, 34–37]. In fact, in order to obtain more accurate excitation energy for an infinite oligomer, one needs to use higher order polynomials. Jansson et al. studied the chain length dependence of singlet and triplet excited states of oligofluorene and used an empirical relationship proposed by Meier et al. [35, 36]. They discussed in detail the concept of “effective conjugation length”

**Table 2** The calculation absorption ( $E_{\text{abs}}$ ), fluorescence energies ( $E_{\text{flu}}$ ) and fluorescence lifetimes of carbazole-based polymers

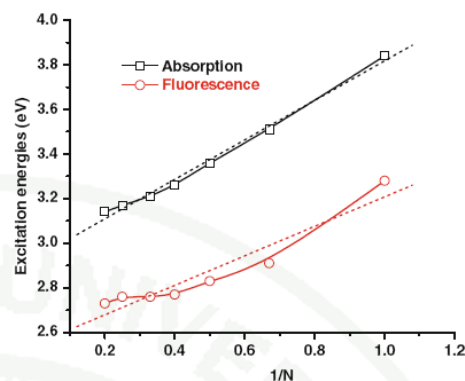
Oligomers	Absorption	Fluorescence	
	$E_{\text{abs}}$ (eV)	$E_{\text{flu}}$ (eV)	Lifetime (ns)
<b>(Cz-co-Cz)<sub>N</sub></b>			
$N = 1.0$	3.84	3.28 (1.484)	1.44
$N = 1.5$	3.51	2.91 (2.482)	1.10
$N = 2.0$	3.36	2.83 (3.222)	0.89
$N = 2.5$	3.26	2.77 (3.933)	0.76
$N = 3.0$	3.21	2.76 (4.561)	0.66
$N = 4.0$	3.17	2.76 (5.814)	0.52
$N = \infty$	2.91	2.51	
Expt.	3.25 <sup>a</sup>	2.84 <sup>a</sup>	
<b>(Cz-co-Fl)<sub>N</sub></b>			
$N = 1.0$	3.80	3.23 (1.517)	1.46
$N = 2.0$	3.32	2.77 (3.242)	0.93
$N = 3.0$	3.18	2.68 (4.537)	0.71
$N = 4.0$	3.14	2.63 (7.076)	0.47
$N = \infty$	2.89	2.40	
Expt.	3.20 <sup>a</sup>	2.91 <sup>a</sup>	
<b>(Cz-co-Th)<sub>N</sub></b>			
$N = 1.0$	3.87	3.59 (0.862)	2.07
$N = 2.0$	3.14	2.57 (2.318)	1.50
$N = 3.0$	2.87	2.34 (3.517)	1.20
$N = 4.0$	2.81	2.25 (4.598)	0.99
$N = \infty$	2.42	1.74	
Expt.	2.60 <sup>b</sup>	2.43 <sup>b</sup>	

Values in parentheses are oscillator strengths

<sup>a</sup> Ref. [6]<sup>b</sup> Ref. [7]

(ECL), defined as the conjugation length at which the wavelength of the absorption maximum in the series of oligomers is not more than 1 nm above the lower limit, which is given by the infinitely long polymer chain [30, 35–37]. From this definition, the ECL largely differs for the various oligomer series. Given these issues, we focus on ECL for estimate the excitation energies of these systems in the following section.

We estimate the ECL for all selected oligomers based on the convergence of the calculated excited energies of the first dipole-allowed excited states with the increasing chain length (Fig. 4). The ECL was estimated by the convergence of excitation energies with the chain length within a threshold of 0.05 eV, based on the obtained linearity between the excitation energy and reciprocal chain length. Apart from the selected carbazole-based oligomers, well-studied oligomers, such as (Cz-co-Cz)<sub>N</sub>, (Cz-co-Fl)<sub>N</sub> and (Cz-co-Th)<sub>N</sub> oligomers are also reexamined with TDDFT for further validating the theory and for comparison. These results will be discussed only briefly.

**Fig. 4** First singlet excitation energies as calculated by TDDFT for absorption and fluorescence energies in poly(2,7-carbazole) oligomers, as a function of  $1/N$ 

We present their absorption and fluorescence energies in Table 2 by applying the ECLs for the absorption and fluorescence energies for compounds (Cz-co-Cz)<sub>N</sub>, (Cz-co-Fl)<sub>N</sub> and (Cz-co-Th)<sub>N</sub> oligomers. The ECL value at which a convergence of the optical properties, absorption and emission properties is reached corresponds to  $N = 4$  for (Cz-co-Cz)<sub>N</sub>, (Cz-co-Fl)<sub>N</sub> and (Cz-co-Th)<sub>N</sub> oligomers. Comparison of the results between experiment and absorption spectrum calculations of are shown in Fig. 5 and indicate that the estimated excitation energies, at ECLs  $N = 4$ , are in good agreement with the optical properties. We therefore conclude that this procedure can be used to reliably estimate the excitation energies of such polymers.

We next look at the details of the electronic transitions of each carbazole-based tetramer ( $N = 4$ ) at TD-B3LYP/SVP level (Table 3) which can be used to describe the possible excitations of all carbazole-based molecules. From the absorption transitions, it was found that for (Cz-co-Cz)<sub>4</sub>, (Cz-co-Fl)<sub>4</sub> and (Cz-co-Th)<sub>4</sub> molecules, the  $S_0 \rightarrow S_1$  excitation primarily corresponds to the promotion of an electron from the highest occupied molecular orbital (HOMO) to the lowest unoccupied molecular orbital (LUMO) ( $H \rightarrow L$ ) (in Fig. 6) as indicated by large oscillator strengths ( $f$ ) of : 6.112, 6.169 and 4.277, respectively. The isosurface plot of the HOMO and LUMO (Fig. 6) indicate an exchange of the double and single bonds as is typical for a  $\pi \rightarrow \pi^*$  transition in conjugated polymers. On the other hand, the  $S_2$ ,  $S_3$  and  $S_4$  electronic transitions of each compound possess very small oscillator strengths. The fluorescence energies and the radiative lifetimes of (Cz-co-Cz)<sub>4</sub>, (Cz-co-Fl)<sub>4</sub> and (Cz-co-Th)<sub>4</sub> computed with the TD-B3LYP/SVP method using  $S_1$  state optimized geometries are collected in Table 3. The fluorescence energies were



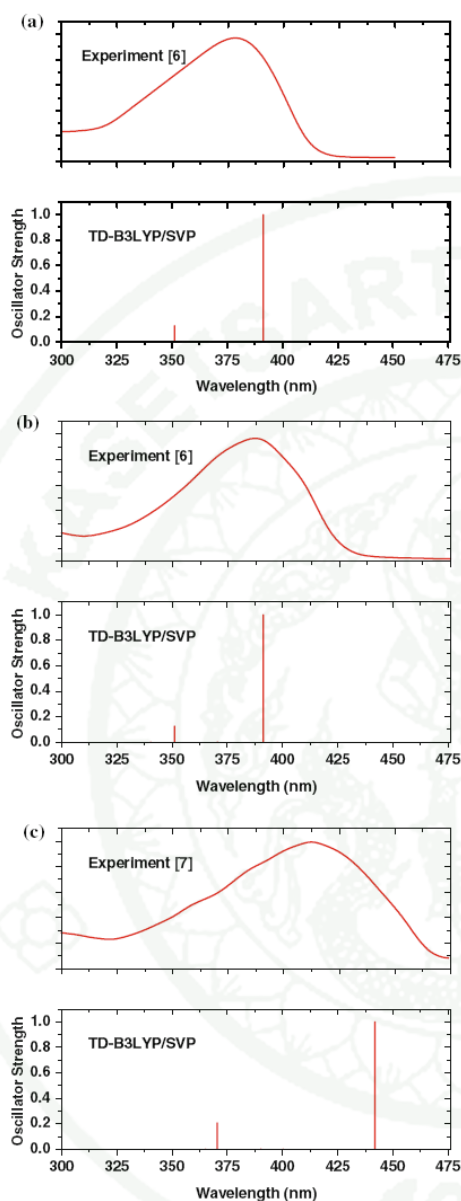


Fig. 5 Absorption spectra [6, 7] and TD-B3LYP/SVP calculations of (Cz-co-Cz)<sub>4</sub>, (Cz-co-Fl)<sub>4</sub> and (Cz-co-Th)<sub>4</sub> oligomers

also investigated. From Table 2, it is clear that the fluorescence energies of (Cz-co-Th)<sub>N</sub> and (Cz-co-Fl)<sub>N</sub> molecules are red-shifted from the excitation energies of (Cz-co-Cz)<sub>N</sub> with values of 2.76, 2.63 and 2.25 eV for (Cz-co-Cz)<sub>N</sub>, (Cz-co-Fl)<sub>N</sub> and (Cz-co-Th)<sub>N</sub>, respectively. These energies are in good agreement with experimental values [6, 7].

The differences in absorption and fluorescence energies should also lead to different Stokes shifts. We therefore evaluate the Stokes-shift as the differences  $\Delta E = E_{\text{abs}} - E_{\text{flu}}$ . The TD-B3LYP/SVP values exhibit Stokes shift of about 0.3 eV for (Cz-co-Fl)<sub>N</sub> and are lower than those for (Cz-co-Cz)<sub>N</sub> and (Cz-co-Th)<sub>N</sub> by about 0.6 eV. This result demonstrates that the (Cz-co-Fl)<sub>N</sub> structure is more relaxed than those of (Cz-co-Cz)<sub>N</sub> and (Cz-co-Th)<sub>N</sub> upon excitation. These results also show that the electronic excitation leads to the formation of a quinoide-type structure.

Using the computed structures, we can also relate the differences in the bond lengths between the ground (GS) and lowest singlet excited state (ES) to the molecular orbital nodal patterns. Because the lowest singlet state corresponds to an excitation from the HOMO to the LUMO in all of the oligomers considered here (Fig. 5), the bond-length variations were explored further in terms of the changes to the HOMO and LUMO. By comparing Fig. 5, we can see that the HOMO has nodes across the *R1*, *R3*, *R5*, *R7*, *R9*, *R11* and *R13* bonds in all molecules, but the LUMO is bonding in these regions. Therefore, one would expect a contraction of these bonds. The data reported in Fig. 2 and Fig. 3 do in fact show this given the bonds are in fact considerably shorter in the excited state. However, the bond length will increase when the bonding changes to antibonding. The dihedral angle (Table 1) between the two adjacent units shortened from 140° to 170° in (Cz-co-Cz)<sub>N</sub> and (Cz-co-Fl)<sub>N</sub> molecules. Whereas the dihedral angle of (Cz-co-Th)<sub>N</sub> shortened from 28° to nearly 0°. It is obvious that the excited structure has a strong coplanar tendency in all molecules. It is indicated that is, the conjugation is better in the excited structure. In this result, it can see that geometry of excited state is more planar than ground state.

Finally, to investigate the effects of the structural relaxation upon excitation, radiative lifetimes were investigated. Based on the fluorescence energy and oscillator strength, the radiative lifetimes have been computed for spontaneous emission using the Einstein transition probabilities according to the formula (in au) [29, 38, 39].

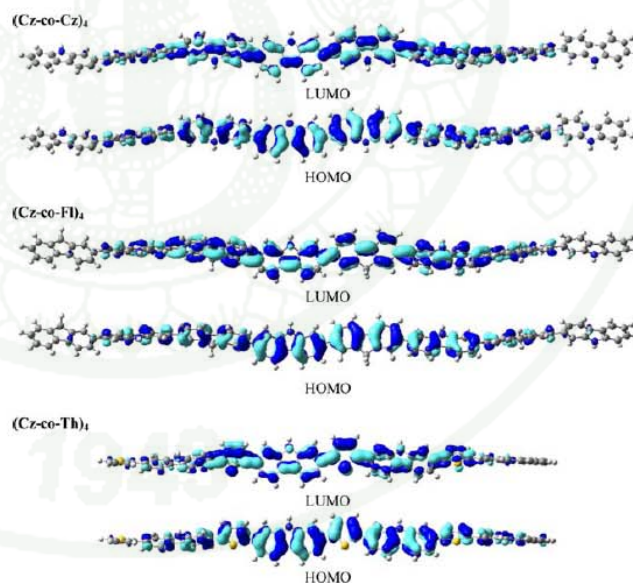
$$\tau = \frac{c^3}{2(E_{\text{flu}})^2 f} \quad (2)$$

In Eq. 2, *c* is the velocity of light, *E<sub>flu</sub>* is the transition energy and *f* is the oscillator strength. The computed lifetimes, *τ*, for the carbazole-based oligomers are depicted

**Table 3** Excitation energies ( $E_{\text{ex}}$ (eV)), oscillator strengths ( $f$ ), and wave function compositions for the lowest singlet electronic states of (Cz-co-Cz)<sub>4</sub>, (Cz-co-Fl)<sub>4</sub> and (Cz-co-Th)<sub>4</sub> molecules computed by TD-B3LYP/SVP

Electronic transitions	$E_{\text{ex}}$	$f$	Wave function composition
(Cz-co-Cz) <sub>4</sub>			
Absorption			
$S_0 \rightarrow S_1$	3.17	6.112	H $\rightarrow$ L(61.8%), H-1 $\rightarrow$ L+1(25.1%)
$S_0 \rightarrow S_2$	3.34	0.002	H-1 $\rightarrow$ L(45.8%), H $\rightarrow$ L+1(45.8%)
$S_0 \rightarrow S_3$	3.51	0.773	H-1 $\rightarrow$ L+1(46.5%), H $\rightarrow$ L+2(31.8%)
$S_0 \rightarrow S_4$	3.54	0.008	H-1 $\rightarrow$ L+1(47.4%), H $\rightarrow$ L+1(46.8%)
Fluorescence			
$S_1 \rightarrow S_0$	2.76	5.814	H $\rightarrow$ L(65.3%), H-1 $\rightarrow$ L+1(17.8%)
(Cz-co-Fl) <sub>4</sub>			
Absorption			
$S_0 \rightarrow S_1$	3.14	6.169	H $\rightarrow$ L(61.4%), H-1 $\rightarrow$ L+1(25.8%)
$S_0 \rightarrow S_2$	3.31	0.011	H-1 $\rightarrow$ L(46.4%), H $\rightarrow$ L+1(45.4%)
$S_0 \rightarrow S_3$	3.50	0.039	H $\rightarrow$ L+1(46.9%), H-1 $\rightarrow$ L(46.3%)
$S_0 \rightarrow S_4$	3.51	0.731	H $\rightarrow$ L+1(47.1%), H-2 $\rightarrow$ L(30.6%)
Fluorescence			
$S_1 \rightarrow S_0$	2.63	7.076	H $\rightarrow$ L(59.9%), H + 1 $\rightarrow$ L + 1(28.7%)
(Cz-co-Th) <sub>4</sub>			
Absorption			
$S_0 \rightarrow S_1$	2.81	4.277	H $\rightarrow$ L(65.0%), H-1 $\rightarrow$ L+1(18.4%)
$S_0 \rightarrow S_2$	3.10	0.000	H $\rightarrow$ L+1(47.9%), H-1 $\rightarrow$ L (45.3%)
$S_0 \rightarrow S_3$	3.18	0.012	H-1 $\rightarrow$ L+1(50.0%), H $\rightarrow$ L+1(47.0%)
$S_3 \rightarrow S_4$	3.35	0.886	H-1 $\rightarrow$ L+1(63.3%), H $\rightarrow$ L (19.1%)
Fluorescence			
$S_1 \rightarrow S_0$	2.25	4.598	H $\rightarrow$ L(65.7%), H-1 $\rightarrow$ L+1(13.3%)

**Fig. 6** HOMO and LUMO of (Cz-co-Cz)<sub>4</sub>, (Cz-co-Fl)<sub>4</sub> and (Cz-co-Th)<sub>4</sub> oligomers. Depicted are two isosurfaces of equal values but opposite sign



in Table 2. The lifetime of carbazole-based oligomers at  $N = 4$  amounts to 0.52, 0.47, and 0.99 ns for (Cz-co-Cz) $_N$ , (Cz-co-Fl) $_N$  and (Cz-co-Th) $_N$ , respectively. Among the carbazole-based molecules, the (Cz-co-Fl) $_N$  shows the lowest lifetime, which is close to that of (Cz-co-Cz) $_N$ . For the purpose of comparison, the results of a chemically similar system were used. The radiative lifetimes of poly(*N*-octyl-2,7-carbazole) and poly(*N*-octyl-2,7-carbazole-alt-9,9-dioctyl-2,7-fluorene) in THF solution are 0.51 and 0.45 ns [28] which is in good agreement with the predicted lifetimes of (Cz-co-Cz) $_N$  (0.52 ns) and (Cz-co-Fl) $_N$  (0.47 ns), respectively. Similar results have been reported for several other polymers (thin films) [40–44] and it can be concluded that their low radiative lifetime can produce useful fluorescent emission [40–44].

#### 4 Conclusions

Absorption and fluorescence properties of (Cz-co-Cz) $_N$ , (Cz-co-Fl) $_N$  and (Cz-co-Th) $_N$ , are presented herein. The optimized ground state and the first singlet excited electronic state have been obtained using B3LYP and TD-B3LYP, methods, respectively, in conjunction with the SVP basis set. A chloroform solvent effect on excitation has been assessed using the COSMO implicit solvent model.

The estimated excitation energies of the absorption and fluorescence excitation based on ECLs  $N = 4$  are in good agreement with the optical properties of (Cz-co-Cz) $_N$ , (Cz-co-Fl) $_N$  and (Cz-co-Th) $_N$  polymers, 3.17, 3.14 and 2.81 eV (absorption) and 2.76, 2.63 and 2.25 eV (fluorescence), respectively. Compared to experimental fluorescence excitation energies available for (Cz-co-Cz) $_N$ , (Cz-co-Fl) $_N$  and (Cz-co-Th) $_N$ , it can be seen that TD-B3LYP/SVP calculations give good predictions of the excitation energies for the  $S_1$  transition (2.84, 2.91 and 2.43 eV, respectively). This suggests that the procedure used herein is reliable method for the estimation of excitation energies of such polymers.

Moreover, we find that the geometry of excited states is more planar than that of the ground states. The excitation to the  $S_1$  state causes significant changes in the predicted geometry which is in agreement with the small Stokes shifts observed experimentally. Furthermore, the radiative lifetime of carbazole-based oligomers at  $N = 4$  amounts to 0.52, 0.47 and 0.99 ns for (Cz-co-Cz) $_N$ , (Cz-co-Fl) $_N$  and (Cz-co-Th) $_N$ , respectively, which is in agreement with the experiment lifetimes of (Cz-co-Cz) $_N$  (0.51 ns) and (Cz-co-Fl) $_N$  (0.45 ns), respectively. It is shown that the existence of multi-components in the fluorescence decay profiles of polymers is caused by several distinct intermolecular  $\pi$ – $\pi^*$  interactions. We therefore conclude that homopolymers and copolymers derived from *N*-substituted-2,7-carbazoles

appear to be very promising materials for the future development of light-emitting diodes, electrochromic windows, photovoltaic cells, photorefractive materials.

**Acknowledgments** Supporting from the Thailand Research Fund (RTA5080005 to SH and MRG5180287 to SS), and the National Center of Excellence in Petroleum, Petrochemical Technology, Center of Nanotechnology Kasetsart University, Kasetsart University Research and Development Institute (KURDI), National Nanotechnology Center (NANOTEC) and Laboratory of Computational and Applied Chemistry (LCAC) are gratefully acknowledged. The calculations were performed in part on the Schrödinger III cluster of the University of Vienna. Thanks are also due to Matthew Paul Gleeson for helpful comments and reading of the manuscript.

#### References

- Burroughes JH, Bradley DDC, Brown AR, Marks RN, Friend RH, Burn PL, Holmes AB (1990) Light-emitting diodes based on conjugated polymers. *Nature* 347:339–341
- Morin JF, Beaupre S, Leclerc M, Levesque I, D'Iorio M (2002) Blue light-emitting devices from new conjugated poly(*N*-substituted-2,7-carbazole) derivatives. *Appl Phys Lett* 80(3):341–343
- Morin JF, Leclerc M (2001) Syntheses of conjugated polymers derived from *N*-alkyl-2,7-carbazoles. *Macromolecules* 34(14):4680–4682
- Zotti G, Schiavon G, Zecchin S, Morin JF, Leclerc M (2002) Electrochemical, conductive, and magnetic properties of 2,7-carbazole-based conjugated polymers. *Macromolecules* 35(6):2122–2128
- Morin JF, Boudreault PL, Leclerc M (2003) Blue-light-emitting conjugated polymers derived from 2,7-carbazoles. *Macromol Rapid Commun* 23:1032–1036
- Bouchard J, Belletete M, Durocher G, Leclerc M (2003) Solvatochromic properties of 2,7-carbazole-based conjugated polymers. *Macromolecules* 36:4624–4630
- Morin JF, Leclerc M (2002) 2,7-Carbazole-based conjugated polymers for blue, green, and red light emission. *Macromolecules* 35(22):8413–8417
- Belletete M, Bedard M, Leclerc M, Durocher G (2004) Absorption and emission properties of carbazole-based dyads studied from experimental and theoretical investigations. *Synth Met* 146(1):99–108
- Belletete M, Bedard M, Leclerc M, Durocher G (2004) Ground and excited state properties of carbazole-based dyads: correlation with their respective absorption and fluorescence spectra. *J Mol Struct (THEOCHEM)* 679(1–2):9–15
- Belletete M, Bedard M, Bouchard J, Leclerc M, Durocher G (2004) Spectroscopic and photophysical properties of carbazole-based triads. *J Can J Chem* 82:1280–1288
- Suramitr S, Hannongbua S, Wolschann P (2007) Conformational analysis and electronic transition of carbazole-based oligomers as explained by density functional theory. *J Mol Struct (THEOCHEM)* 807(1–3):109–119
- Marcon V, Van der Vegt N, Wegner G, Raos G (2006) Modeling of molecular packing and conformation in oligofluorenes. *J Phys Chem B* 110(11):5253–5261
- Meeto W, Suramitr S, Vannarat S, Hannongbua S (2008) Structural and electronic properties of poly(fluorine-vinylene) copolymer and its derivatives: Time-dependent density functional theory investigation. *Chem Phys* 349(1–3):1–8
- Jespersen KG, Beenken WJD, Zaushitsyn Y, Yartsev A, Andersson M, Pullerits T, Sundström V (2004) The electronic states



- of polyfluorene copolymers with alternating donor–acceptor units. *J Chem Phys* 121:12613–12617
15. Ahlrichs R, Bär M, Häser M, Horn H, Kölmel C (1989) Electronic structure calculations on workstation computers: the program system turbomole. *Chem Phys Lett* 162(3):165–169
  16. von Arnim M, Ahlrichs R (1999) Geometry optimization in generalized natural internal coordinates. *J Chem Phys* 111(20):9183–9190
  17. Dirac PAM (1929) Quantum mechanics of many-electron systems. *Proc R Soc Lond A* 123:714–733
  18. Slater JC (1951) A simplification of the Hartree–Fock method. *Phys Rev* 81:385–390
  19. Vosko SH, Wilk L, Nusair M (1980) Accurate spin-dependent electron liquid correlation energies for local spin density calculations: a critical analysis. *Can J Phys* 58(8):1200–1211
  20. Becke AD (1988) Density-functional exchange-energy approximation with correct asymptotic behavior. *Phys Rev A* 38(6):3098–3100
  21. Kohn W, Becke AD, Parr RG (1996) Density functional theory of electronic structure. *J Chem Phys* 100(31):12974–12980
  22. Treutler O, Ahlrichs R (1995) Efficient molecular numerical integration schemes. *J Chem Phys* 102(1):346–354
  23. Bauernschmitt R, Ahlrichs R (1996) Treatment of electronic excitations within the adiabatic approximation of time dependent density functional theory. *Chem Phys Lett* 256(4–5):454–464
  24. Klamt A, Schuurmann G (1993) COSMO: a new approach to dielectric screening in solvents with explicit expressions for the screening energy and its gradient. *J Chem Soc Perkin Trans* 2:799–805
  25. Jacquemin D, Perpète EA, Chermette H, Ciofini I, Adamo C (2007) Comparison of theoretical approaches for computing the bond length alternation of polymethineimine. *Chem Phys* 332(1):79–85
  26. Liu Q, Liu W, Yao B, Tian H, Xie Z, Geng Y, Wang F (2007) Synthesis and chain-length dependent properties of monodisperse oligo(9, 9-di-n-octylfluorene-2,7-vinylene)s. *Macromolecules* 40(6):1851–1857
  27. Yang L, Ren AM, Feng JK, Wang JF (2005) Theoretical investigation of optical and electronic property modulations of  $\pi$ -conjugated polymers based on the electron-rich 3, 6-dimethoxy-fluorene unit. *J Org Chem* 70(8):3009–3020
  28. Wang JF, Feng JK, Ren AM, Liu XD, Ma YG, Lu P, Zhang HX (2004) Theoretical studies of the absorption and emission properties of the fluorene-based conjugated polymers. *Macromolecules* 37(9):3451–3458
  29. Chidithong R, Hannongbua S, Aquino A, Wolschann P, Lischka H (2007) Excited state properties, fluorescence energies, and lifetime of a poly(fluorene-pyridine) copolymer, based on TD-DFT investigation. *J Comput Chem* 28(10):1735–1742
  30. Cornil J, Gueli I, Dkhissi A, Sancho-García JC, Hennebicq E, Calbert JP, Lemaire V, Beljonne D (2003) Electronic and optical properties of polyfluorene and fluorene-based copolymers: a quantum-chemical characterization. *J Chem Phys* 118:6615–6623
  31. Gierschner J, Cornil J, Egelhaaf HJ (2007) Optical bandgaps of  $\pi$ -conjugated organic materials at the polymer limit: experiment and theory. *Adv Mater* 19:173–191
  32. Sancho-García JC (2006) Assessing a new nonempirical density functional: difficulties in treating  $\pi$ -conjugation effects. *J Chem Phys* 124:124112/1–124112/10
  33. Sancho-García JC (2007) Treatment of singlet–triplet splitting of a set of phenylene ethylenes organic molecules by TD-DFT. *Chem Phys Lett* 439:236–242
  34. Jansson E, Chandra Jha P, Ågren H (2007) Chain length dependence of singlet and triplet excited states of oligofluorenes: a density functional study. *Chem Phys* 336(2–3):91–98
  35. Meier H, Stalmach U, Kolshorn H (1997) Effective conjugation length and UV/vis spectra of oligomers. *Acta Polymer* 48:379–384
  36. Oelkrug D, Tompert A, Egelhaaf HJ, Hanack M, Steinhuber E, Hohlloch M, Meier H, Stalmach U (1996) Towards highly luminescent phenylene vinylene films. *Synth Met* 83(3):231–237
  37. Peach GMJ, Tellgren EI, Saek P, Helgaker T, Tozer DJ (2007) Structural and electronic properties of polyacetylene and polyyne from hybrid and coulomb-attenuated density functionals. *J Phys Chem A* 111(46):11930–11935
  38. Luke V, Aquino A, Lischka H, Kauffmann HF (2007) Dependence of optical properties of oligo-*para*-phenylenes on torsional modes and chain length. *J Phys Chem B* 111(28):7954–7962
  39. Beenken WJD, Lischka H (2005) Spectral broadening and diffusion by torsional motion in biphenyl. *J Chem Phys* 123:144311–144319
  40. Tirapattur S, Belletete M, Drolet N, Leclerc M, Durocher G (2003) Steady-state and time-resolved studies of 2,7-carbazole-based conjugated polymers in solution and as thin films: determination of their solid state fluorescence quantum efficiencies. *Chem Phys Lett* 370(5–6):799–804
  41. Jenekhe SA, Lu L, Alam MM (2001) New conjugated polymers with donor–acceptor architectures: Synthesis and photophysics of carbazole-quinoline and phenothiazine-quinoline copolymers and oligomers exhibiting large intramolecular charge transfer. *Macromolecules* 34(21):7315–7324
  42. Schenning APH, Tsipis AC, Meskers SCJ, Beljonne D, Meijer EW, Brdas JL (2002) Electronic structure and optical properties of mixed phenylene vinylene/phenylene ethynylene conjugated oligomers. *Chem Mater* 14(3):1362–1368
  43. Pålsson LO, Wang C, Russell DL, Monkman AP, Bryce MR, Rumbles G, Samuel DW (2002) Photophysics of a fluorene copolymer in solution and films. *Chem Phys* 279(2–3):229–237
  44. Sun RG, Wang YZ, Wang DK, Zheng QB, Kyllö EM, Gustafson TL, Wang F, Epstein AJ (2000) High PL quantum efficiency of poly(phenylene vinylene) systems through exciton confinement. *Synth Met* 111–112:595–602

## CURRICULUM VITAE

**NAME** : Miss. Wichanee Meeto

**BIRTH DATE** : Sep 22, 1979

**BIRTH PLACE** : Chainat, THAILAND

**NATIONALITY** : Thai

[illegible]

: 2002 Chiang Mai Univ. B. Sc. (Chemistry)

: 2005      Kasetsart Univ.      M. Sc. (Chemistry)

**SCHOLARSHIP** : Postgraduate Education and Research Program in Petroleum and Petrochemical Technology (MUA-ADB) 2005-2007  
Thailand Graduate Institute of Science and Technology (TGIST) 2005-2007

## PRESENTATION :

Meeto, W., S. Suramitr, P. Poolmee, K. Sriwichitkamol, and S. Hannongbua. **Effect of conjugation length on structural and electronic properties of conjugated polymeric compounds:** The abstract of 31<sup>st</sup> Congress on Science and Technology of Thailand (STT 2005), Suranaree University of Technology, Nakhon Ratchasima, Thailand, 18-20 October 2005.

Meeto, W., S. Suramitr, and S. Hannongbua. **Quantum Chemical Calculations on Structural and Electronic Properties of Poly (fluorenevinylene):** International Conference on Modeling in Chemical and Biological Engineering Sciences, Rama garden hotel, Bangkok, Thailand, 25-27 October 2006.

Suramitr, S., W. Meeto and S. Hannongbua. **Theoretical Investigation of Ground and Excited States Geometry of Conjugated Based on Carbazole Copolymers:** International Conference on Modeling in Chemical and Biological Engineering Sciences, Rama garden hotel, Bangkok, Thailand, 25-27 October 2006.



Meeto, W., S. Suramitr, and S. Hannongbua. **Electronic Properties of the Poly(fluorenevinylene) Derivatives: Time Dependent Density Functional Theory Calculations:** German-Thai Symposium on Nanoscience and Nanotechnology, The Tide Resort, Bangsean Beach, Chonburi, Thailand, 27-28 September 2007.

Meeto, W., S. Suramitr, S. Vannarat and S. Hannongbua. **Ground and Excited States Geometries of Fluorenevinylene Based Oligomers: Time Dependent Density Functional Theory Study:** The 11<sup>th</sup> Annual National Symposium on Computational Science and Engineering (ANSCSE11), Prince of Songkla University (PSU), Phuket Campus, Thailand, 28-30 March 2007.

#### **PUBLICATION :**

Meeto, W., S. Suramitr, S. Vannarat and S. Hannongbua. 2008. Structural and electronic properties of poly(fluorene–vinylene) copolymer and its derivatives: Time-dependent density functional theory investigation. **Chem. Phys.** 349: 1-8.

Meeto, W., S. Suramitr, V. Lukeš, P. Wolschann and S. Hannongbua. 2010. Effects of the CN and NH<sub>2</sub> substitutions on the geometrical and optical properties of model vinylfluorenes, based on DFT calculations. **J. Mol. Struct. (Theochem).** 939: 75-81

Suramitr, S., W. Meeto, P. Wolschann and S. Hannongbua. 2010. Understanding on absorption and fluorescence electronic transitions of carbazole-based conducting polymers: TD-DFT approaches. **Theor. Chem. Acc.** 125: 35-44